SPATIAL VARIATION IN MODELLED HYDRODYNAMIC CHARACTERISTICS ASSOCIATED WITH VALLEY CONFINEMENT IN THE KROM RIVER WETLAND: IMPLICATIONS FOR THE INITIATION OF EROSIONAL GULLIES

A thesis submitted in fulfilment of the academic requirements for the degree of

MASTER OF SCIENCE

DEPARTMENT OF GEOGRAPHY, RHODES UNIVERSITY

By

PHILIPPA KIRSTEN SCHLEGEL

2017

Supervisor: W.N. Ellery

Co-supervisor: M.C. Grenfell

Krom River wetland in the Kompanjiesdrif basin, looking down the valley

ABSTRACT

Gully erosion is a significant and widespread feature of southern African wetlands, including the wetlands of the Krom River, Eastern Cape. Gully erosion in wetlands is consistently being viewed as a major contributing factor to wetland degradation and eventual collapse. Many gullies exist in the Krom River and Working for Wetlands has spent large sums of money to stabilise head-cuts with the expectation that further erosion would be halted and possibly avoided altogether. Observations in the Krom River wetlands have revealed that most gullies in the wetland are initiated where the width of the trunk valley has been reduced as a consequence of deposition by tributary alluvial fans that impinge on the trunk valley and reduce its width. The aim of this study was to examine variation in hydrodynamic characteristics for a range of discharges, as flow in the broad Kompanjiesdrif basin (~250 meters wide) is confined in a downstream direction to a width of less than 50 meters by a combination of a large impinging left bank tributary alluvial fan that coincides with a resistant bedrock lithology. The study was done by collecting topographical survey data using a Differential Global Positioning System in order to create a Digital Terrain Model with a suitable resolution. Flow was recorded using a Marsh-McBirney Model 2000 Flo-Mate as well as recording the flood extent for each flow condition; this was used in the calibration process of the model. Vegetation measurements were conducted in order to calculate a roughness value across the valley floor. A two-dimensional raster based flood inundation model, CAESAR-Lisflood and a one-dimensional hydraulic analysis model, HEC-RAS, were then used to simulate different parameters associated with variation in discharge, including flow velocity, water depth and stream power, thereby creating a better understanding of the hydraulic characteristics that may promote the formation of gullies in the wetland. Based on these hydraulic analyses it is evident that the effect of impinging alluvial fans on hydraulic characteristics such as flow velocity, water depth and stream power, may lead to the initiation of gullies within the Krom River wetland. This work improves understanding of the collapse of palmiet wetlands in steep-sided valleys within the Cape Fold Mountains of South Africa, and can aid in wetland management.

PREFACE

The research described in this thesis was carried out at the Department of Geography, Rhodes University, Grahamstown, from January 2015 to December 2016, under the supervision of Professor W.N. Ellery, and co-supervision of Dr. M.C. Grenfell.

This study represents the original work by the author. Where use has been made of the work of others it is duly acknowledged in the text.

Name: Philippa Kirsten Schlegel

Student Number: G14S7180

Signed:

ACKNOWLEDGMENTS

I would like to thank the following people and organisations for their generosity and support, without which, this research would not have been possible:

Firstly, my supervisor, Professor W.N. Ellery, is sincerely thanked for his inspiration and his never ending amount of curiosity and questions about the natural world, for giving his time so generously, and for his words of encouragement. My co-supervisor, Dr. M.C. Grenfell, is thanked for answering my many questions on hydrodynamic modelling; and for his kindness and encouraging words.

The National Research Foundation, for funding me for the duration of my research.

The landowner of the Kompanjiesdrif basin, who allowed access to the wetland.

Mr. Dlamini, from the South African weather station, and Mr. Volschenk, from Department of Water and Sanitation, for assisting me in gathering weather data for catchment K90A and flow records for the Krom River.

Those who helped me collect data in the field; Nicholaus Huchzermeyer, Juliette Lagesse, Simon Pulley, Amy Barclay, Ryan Silbernagl, Chloe Wallace, Shaun McNamara and Matt Hermon, thank you for persevering and exploring the depths of the palmiet wetland with me.

My parents, for their unfaltering love, kindness and support. Thank you for always believing in me and my abilities.

Nicholaus Huchzermeyer, for your kind words, strength and love when it was most needed.

TABLE OF CONTENTS

LIST OF FIGURES

LIST OF TABLES

CHAPTER ONE: GENERAL INTRODUCTION

1.1 BACKGROUND

Soil erosion, in the form of gullies, is a worldwide phenomenon and has been identified as a key cause of land and water systems degradation (Wasson *et al*., 2002; de Vente *et al*., 2005; Valentin *et al*., 2005). Gullies are commonly defined as deep erosional channel-like features associated with incision by flowing water (either surface or subsurface), into a pre-existing land surface (Kirkby & Bracken, 2009). Gully erosion is a severe global problem due to its destruction of fertile land and the production of large quantities of sediment that affect reservoir capacity, and water quality. According to Valentin *et al*. (2005), gully erosion is difficult to study and understand due to the complex nature of gully formation, the multiple factors and processes involved, and the problem of accurately predicting spatial and temporal gully initiation. Although, most research has shown that gully erosion is generally triggered or accelerated by a change in land use or poor land management (Eitel *et al.,* 2002; Bork, 2004; Avni, 2005; Mieth & Bork, 2005; Valentin *et al.,* 2005; Nyssen *et al.,* 2006), there are other factors such as extreme climate events, geomorphic thresholds and antecedent landscape memory that must also be understood in order to appreciate the mechanisms behind gully initiation and its continuation in the landscape (Schumm & Hadley, 1961; Patton & Schumm, 1975; Schumm, 1979; Fryirs & Brierley, 2010; Wohl, 2013).

Wetland erosion in the form of gullies is an extensive problem across the globe and is consistently being viewed as a major contributing factor to degradation and the ultimate collapse of these ecologically and economically valuable ecosystems (Ellery *et al*., 2009). There is some debate as to the causes of gully initiation in wetlands. However, studies have largely attributed gully formation to anthropogenic factors (Eitel *et al.,* 2002; Bork, 2004; Avni, 2005; Mieth & Bork, 2005; Valentin *et al.,* 2005; Nyssen *et al.,* 2006). It is believed that anthropogenic activities such as poor land management and over-utilisation such as over-grazing of livestock, incorrect farming practices, deforestation, wetland drainage using artificial drains and encroachment by invasive alien plant species, have significantly contributed to gully erosion within wetlands (Ellery *et al.,* 2009). This has been illustrated by research from all over the world (Zimbabwe (Lizias and Felix 2013); Northern Ireland (Cooper *et al.,* 1991); United Kingdom (Lane, 2001); China (Liu *et al.,* 2004); South Africa (McCarthy *et al.,* 2007) such that land use change is expected to have a greater effect on gully development (Valentin *et al*., 2005). Yet, gully development has been observed in wetlands across a range of land use settings stretching from heavily modified land in communal catchments to near pristine environments within nature reserves (Ellery *et al.,* 2009). In fact several studies have suggested that

gully erosion may be a natural phenomenon caused by geomorphic thresholds and climate variations (Schumm & Hadley, 1961; Patton & Schumm, 1975; Schumm, 1979; Ellery *et al.,* 2009; Ngetar, 2011).

Schumm (1973) recognised that the geomorphic characteristics of a catchment are fundamental to understanding the spatial and temporal variations in gully development. It was discovered that, in semi-arid Western America, discontinuous gullies frequently initiate where there is a local over-steepening of valley floor topography. A similar deduction was drawn by Ellery *et al*., (2009), from a number of studies conducted around South Africa. They noted that many gullies were initiated where the slope of the wetland was steep in relation to the size (area). This was found to occur irrespective of the land cover or land use of the surrounding catchment. Further, Ngetar (2011) observed in the Craigieburn wetland in Mpumalanga, South Africa, that some of the erosion gullies that have formed within the wetland have been caused by localised over-steepening of certain sections of the valley floor above a threshold gradient, such that gully erosion was not solely due to anthropogenic activities. These localised steep sections were viewed to lead to increased flow velocity and stream power, which triggers gully erosion. Further evidence for non-anthropogenic origin of gully formation is that gullies pre-date commercial farming practices and settlements in some areas (McCabe & Dardis, 1989; Fryirs & Brierley, 1998).

Major geomorphic events that have had a significant influence on wetland formation and their subsequent erosion in southern Africa include the multiple uplift events and sea level changes that have occurred over the geological history of the subcontinent. Southern Africa's relatively high elevation is unusual on a global scale given the lack of mountain building associated with collision of tectonic plates. Compared to areas of similar geology, such as western Australia, northern Canada, northern Asia and eastern South America, which lie only a few hundred meters above sea level, the southern African subcontinent is characterised by a comparatively high elevation due to two tectonic uplift events, one in the Miocene (20 Million years ago) and the second in the late Pliocene (5 Million years ago). Uplift was most pronounced on the eastern side of the subcontinent such that the continent tilts gently downwards from east to west. These events have elevated the subcontinent to a mean land surface altitude of approximately 1 000 m.a.s.l (Marker & Holmes, 2005; McCarthy & Rubidge, 2005; McCarthy *et al.,* 2007; Lewis, 2008; Marker & Holmes, 2010). These uplift events resulted in a drop in the ultimate base level of rivers flowing to the sea such that the subcontinent has entered a period of long-term erosion. The consequence of this geologic memory on the landscape is that the eastern side of southern Africa is characterised by steeper slopes and steep channel gradients, with a greater predisposition to erode.

South Africa being semi-arid has higher rates of evaporation than precipitation, resulting in most large wetlands forming part of river systems. It is crucial to understand river characteristics in order to understand wetland origin, functioning, dynamics and their persistence in the landscape, and use this to guide wetland management. Most wetland degradation has been a consequence of gully erosion and one of the challenges has been to understand why gully erosion is such a persistent feature of the region. In South Africa, an estimated 50 percent of the wetlands have been lost and this trend of degradation is continuing (Kotze and Breen, 1994; and Department of Environmental Affairs and Tourism, 2006). Wetlands across South Africa are of high importance due to their fulfillment of vital hydrological and biogeochemical functions, while also supporting high biodiversity including a disproportionate frequency of rare and endangered species (Cowan, 1995; McCarthy & Hancox, 2000; Tooth & McCarthy, 2007; Rebelo, 2012). A loss in these key environments has many detrimental effects that negatively affect human wellbeing, such as increased flooding risk or decreased water quality in streams. Furthermore, degradation of wetlands results in sediment buildup that shortens the lifespan of downstream reservoirs. Sedimentation in South Africa has cost water treatment approximately two billion Rand (Hoffman & Ashwell, 2001) and it is estimated that the annual loss of soil is ~2.5 tonnes per hectare, which exceeds the rate of soil regeneration in the country. In addition to the loss of ecosystem services associated with the collapse of wetlands, there is widespread and pervasive loss of key habitats of natural importance.

Like so many other rivers in South Africa, the Krom River and its accompanying wetlands have shown ongoing degradation, predominantly in the form of extensive gully erosion. This is a threat to the greater Mandela Bay Metropole because the Churchill Dam on the Krom River is the main source of water for the area. A rehabilitation program began in the mid-1990s with the intention of controlling erosion in the wetlands. The main method to achieve this has been to build stabilising weirs. Tens of millions of Rands have been spent by Working for Wetlands with the aim to halt further erosional gullies in the Krom River. However, erosion has persisted. This has opened a window of opportunity to examine the specific hydraulic features and landscape characteristics of a basin with an un-channeled wetland in order to improve the understanding of the factors leading to persistent erosion. A large wetland "basin" in the Krom River wetland, the Kompanjiesdrif basin, has been chosen for this study as it is threatened by gully erosion, with the erosional nick point of the gully at the toe of the basin having been stabilised by two large weirs.

In the Kompanjiesdrif basin two large tributary alluvial fans (one at the head of the wetland and the other at the toe of the wetland) enter from the left bank (Figure 1). Another two smaller alluvial fans enter from the left bank in the middle of the wetland (Figure 1). Observations in the Kompanjiesdrif

basin have revealed that most gullies in the wetland are initiated where the width of the trunk valley has been reduced as a consequence of deposition by tributary alluvial fans, Figure 1. In addition, it is thought that the distribution of gullies has been associated with the localised steepening of slopes at the distal end of the alluvial fans. Hermon (2016) showed that the original wetland surface at the point at which an alluvial fan enters the valley was steeper by an order of magnitude than the bed of gullies found in the area. As such, areas of local aggradation, where tributary alluvial fans enter the system, are thought to be important as potential sites of gully initiation and propagation.

Hydrodynamic model simulations are a useful and valuable tool in scientific research as a means of increasing scientific understanding. Modelling can be used to simulate a number of key mechanisms that drive hydrological processes and feedback systems. Hydrodynamic models are a useful tool in that a modification of reality can be artificially created in accordance to physical laws, such that the modeller has full control of input parameters. A number of deliberate scenarios can be created within physical constraints to understand a system and the possible outcome of a specified change to that system. There has been very little research related to hydrodynamic factors that may be associated with gully formation in wetlands. This research would be useful to reveal the relative importance of factors that may contribute to erosion in wetlands.

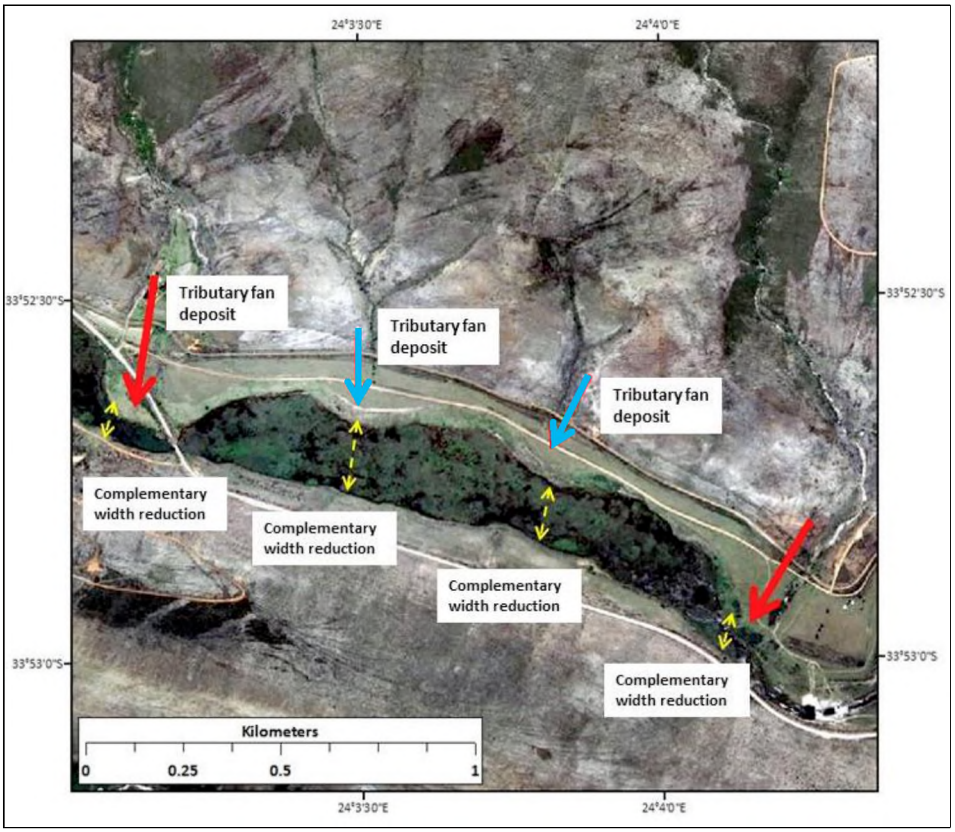

Figure 1: Aerial photograph of the tributary alluvial fan deposits reducing the width of the trunk valley of the Kompanjiesdrif basin wetland

1.2.1 AIM

Given this background, the aim of this research was to examine spatial variation in hydrodynamic characteristics for a range of discharges in the Kompanjiesdrif basin of the Krom River wetland complex, given variation in longitudinal slope and wetland width associated with impingement of tributary alluvial fans. Hydrodynamic modelling was used in order to improve understanding of the hydraulic features that may cause wetland erosion, and thereby improve restoration approaches.

1.2.2 RESEARCH QUESTION

The specific research question explored is:

How does surface water flow, for a given discharge, vary from a non-confined to a confined reach in respect of hydraulic characteristics such as velocity, water depth and stream power; and what implications may this have for the initiation of gully erosion?

1.2.3 RESEARCH OBJECTIVES

In order to achieve the aim of the study the following objectives were identified using the Kompanjiesdrif basin as a case study:

1. Determine the current hydraulic properties of the Kompanjiesdrif basin in terms of peak discharge, measured discharge, flood extent and hydraulic properties of the vegetated wetland surface.

2. Model surface flow through the non-confined to the confined reach using Caesar-LISFLOOD (two-dimensional software) and HEC-RAS (one-dimensional software).

3. Develop a conceptual model of the effect of natural valley confinement on wetland erosion, and use this to explore the implications of this research for wetland erosion and restoration.

CHAPTER TWO: LITERATURE REVIEW

2.1 TURBULENT GEOLOGICAL HISTORY OF THE CAPE FOLD BELT

This section, based on an appraisal of the following pivotal texts: Truswell (1977), Buckle (1978) and McCarthy and Rubidge (2005), covers the deposition of the Cape Supergroup sediments (~500 Million years Before Present), the creation of the Cape Fold Mountains by collision of the Falkland Plateau with Africa (~330 Million years Before Present), and the two uplift events that have shaped the modern structure of the subcontinents landscape.

During the Cambrian-Ordovician period, beginning around 510 Million years ago and ending around 350-330 Million years ago, the sediments that would ultimately form the impressive Cape Fold Belt were laid down. Gondwana, by 500 Million years ago, had consolidated and the Pan African belts were being eroded, exposing the rocks deep beneath the surface, such as the Cape Granites. At this time Gondwana was slowly sliding northwards. This northward drift created tension that was concentrated along the Pan African belts. The Pan African belt running along what is now the southern Cape responded by stretching and thinning, initiating a large rift valley. The rift valley separated the supercontinent from the Falkland Plateau (Truswell, 1977; Buckle, 1978; McCarthy & Rubidge, 2005). Rapid flooding of the rift valley created the Agulhas Sea. The sediments that were deposited on the floor of the Agulhas Sea accumulated and consolidated into an 8 kilometre thick layer, known as the Cape Supergroup. The Cape Supergroup can be subdivided into three broad units of differing age, environment of formation and fossil content. These were deposited over a period from the Ordovician to the Carboniferous, approximately 500 to 330 Million years ago. The basal sequence of the Cape Supergroup is the Table Mountain Group. This sequence was deposited by numerous sandy, braided rivers. Somewhere between the Ordovician and the Silurian Periods the Cederberg Formation was deposited in shallow bays and glacial lakes. About 400 Million years ago in the early Devonian Period, Gondwana experienced further extension accompanied by rapid subsistence which deepened the Agulhas Sea. This brought about the deposition of the mudstones of the Bokkeveld Group. Approximately 370 to 330 Million years ago the more sand-rich Witteberg Group was deposited on top of the Bokkeveld Group. These sediments were deposited in a multitude of settings ranging from rivers, fresh and brackish lakes, to deltas. The Witteberg Group marks the end of the depositions and aggradation in the Agulhas Sea. During the Carboniferous to the early Permian period (~330 to ~280 Million years ago), a subduction zone developed along the southern margin of Gondwana and as a result the rift valley began to close. Simultaneously, the Falkland Plateau began to drift back towards Africa. With the closing of the rift valley the

consolidated Cape Supergroup sediments were folded into a series of parallel folds. These folds run predominantly from east to west and stretch from the south-western and southern coastlines of South Africa for 850 kilometres from the Cederberg as far east as Port Elizabeth.

The modern structure of the subcontinent landscape has been a consequence of a series of events that has occurred since the splitting of Gondwana. Africa due to its central position, stood much higher than the surrounding proto-continents. It is thought that prior to break up, the central plateau of the African proto-continent, (what is known as the Bloemfontein-Kimberley region) had an elevation of approximately 1 800 meters above present sea level (m.a.s.l) and about 2 350 m.a.s.l in the highest portions of the Lesotho Mountains (Partridge & Maud, 1987). During the Jurassic period (~140 Million years ago), the disintegration of the supercontinent resulted in extensive eruptions of lava (~2 km thick) which covered large areas of the central plateau of southern Africa. The remnants of these lava flows form today's Drakensberg Mountains. Fifty million years later (~90 Million years ago) the proto-continents of the former supercontinent had separated and were shifting towards their present locations (McCarthy, 2009). This was the beginning of a period of denudation.

This continental erosion cycle abruptly ended at the beginning of the Miocene approximately 18 Million years ago. This was due to a modest uplift event along the Transvaal-Griqualand axis (Figure 2), stretching across South Africa, concentrated in the eastern region of the subcontinent. As illustrated by Figure 2, the subcontinent was lifted by about 250 to 300 meters in the eastern section, and by about 100 meters in the western region. The Miocene uplift was epeirogenic, non-faulting and non-volcanic in nature (Partridge & Maud, 1987; Maud, 2012). The Miocene uplift caused rivers to incise to a new base level, in some cases up 100 to 120 meters into the existing African erosion surface. This incision initiated another cycle of erosion, known as the Post-African I Surface. Another epeirogenic uplift event occurred in the early Pliocene (5 Million years ago). This uplift event was again concentrated in the eastern region of the subcontinent but was much larger than that of the Miocene (Figure 2). Along the eastern region the uplift was between 600 to 900 meters. The southern and western sections of the subcontinent experienced uplift of between 100 to 200 meters. This resulted in an accumulated uplift of the two events of approximately 1 000 meters. It was the cumulative effect of these two uplift events that resulted in the present day topography of southern Africa. Drainage systems along the eastern coast entered a crucial stage of incision. A new cycle termed the Post African II Surface was initiated at this time. Additionally, river systems were rejuvenated during the Pliocene due to the more humid climate. This cycle of erosion ended just 3 million years after it began as a consequence of climate and glacio-eustatic sea-level

fluctuations related to the growth and decline of ice-sheets in the high latitudes after 2.6 Million years ago (Maud, 2012).

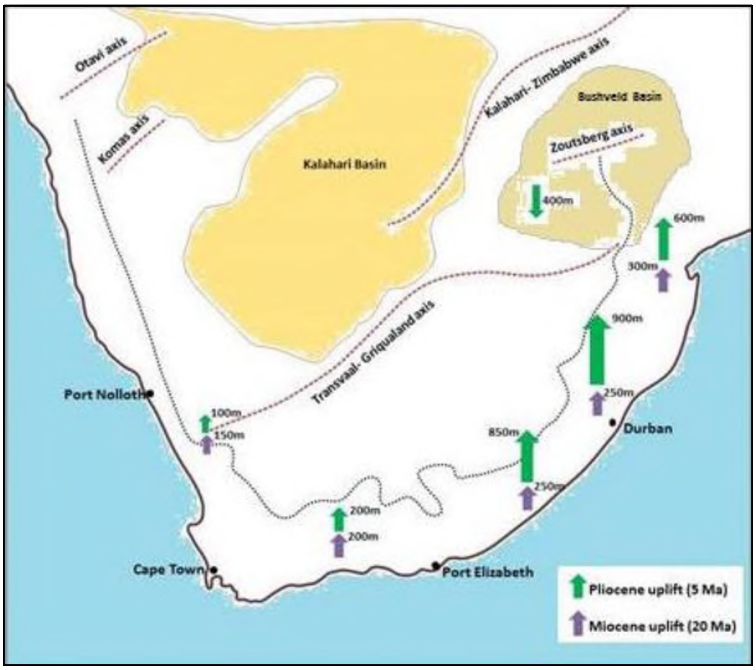

Figure 2: A map of southern Africa depicting the uplift events of the Miocene and Pliocene with the interior axes. Adapted from Partridge (1988)

The turbulent history of southern Africa has made a subcontinent with unique macro-topography, asymmetrical drainage systems and a landscape dominated by erosion. The present pattern and form of fluvial systems is a consequence of the imprint of landscape memory, base level changes and climate fluctuations. This deep-time knowledge of the subcontinent is important to wetland origin, function and management. Wetlands form at the border between terrestrial and aquatic environments; and between ground water and surface water systems. Wetlands in the subcontinent are an anomaly and vary from their counterparts in the temperate or humid Northern Hemisphere. However, wetlands occur in southern Africa across a broad range of settings from flat coastal plains in KwaZulu-Natal, to headwaters forming along the Great Escarpment, in hyper-arid to arid settings in the Namib Desert and Karoo environment to the cool and wet southern coast of the subcontinent. As mentioned before the southern African subcontinent is ancient, with no major tectonic activity or mountain-building episodes in recent times. In addition, the continent is situated at a relatively high and unusual mean elevation, associated with a low annual rainfall, approximately one-half of the global average for continental areas, and high potential evapotranspiration due to high mean annual temperatures. The combination of these factors make wetland and peat formation in the subcontinent an anomaly (Ellery *et al.,* 2009). As a consequence, the majority of the wetlands found

in southern Africa exist where there are locally positive (near-) surface water balances for all or part of the year (Tooth & McCarthy, 2007). This means that most wetlands in southern Africa are intrinsically linked to fluvial systems and the fluvial geomorphological history.

In spite of this turbulent geological history, today the Krom River wetlands exist in a mountainous landscape with broad sections, such as the Kompanjiesdrif basin (Figure 3), that have a near-horizontal cross-section of over 250 meters and a longitudinal slope of approximately 1 percent. This is a remarkable outcome in an intensely folded mountainous landscape where the dominant lithology is resistant quartzite.

Figure 3: Photograph showing the broad Kompanjiesdrif basin boarded by the intensely folded Suuranys Mountains of the Cape Fold Belt

2.2 FLUVIAL SYSTEMS AND WETLANDS

2.2.1 RIVER LONGITUDINAL PROFILES

An important aspect of river geometry is the longitudinal profile. A longitudinal profile illustrates how a river's gradient changes as it flows from its source to its mouth. A graded longitudinal profile is schematised as a logarithmic curve with a concave-upward shape, as depicted by the thick black line in Figure 4. However, it must be noted that in reality a river's longitudinal profile is hardly ever the perfect concave-upward profile depicted in the textbook illustration in Figure 4, so the idea of a graded profile is, essentially, theoretical. The long profile shows how, in the upper stage of a river's course, the river's gradient is steep and is characterised by fast flowing headwaters, incised streams,

narrow V-shaped valleys and dominated by large sediment being transported (cobbles and boulders), as shown by section A in Figure 4. The river profile gradually flattens out as the river creates a gradient on the stream bed that represents the appropriate one for the given discharge and sediment supply. Streams are able to alter their gradient by erosion and deposition, given that the ability of a stream to move sediment is dictated by stream power, which is related to velocity and discharge. If the slope on the bed of the stream is too high for the stream power and sediment, erosion will occur, thereby lowering the slope on the bed of the stream. Conversely, where the slope of the stream bed is too low for the stream power, deposition occurs in order to increase the slope of the stream bed. Given that streams exhibit feedback, they work to build a slope along their entire length that is appropriate for the available discharge and stream power such that continuity of flow is maintained along their length. Discharge typically increases downstream due to tributaries adding water, such that streams develop a logarithmic profile down their entire length.

Given this the middle reaches of streams are characterised by a gradually decreasing gradient, broader and wider valleys, as shown by section B in Figure 4. The lower section of the rivers longitudinal profile is shallow ending at the same elevation as sea level, which comprises the base level for all streams. The lower reaches of a river are characterised by wide cross-sectional area, low velocities, low friction and high discharges, as shown by section C in Figure 4. This creates the stylised concave-upwards logarithmic longitudinal river profile from the headwaters down to the mouths at the sea (Dollar *et al.,* 2006). A concave-upward longitudinal profile is for the most part determined by the ultimate base level which is the level of the sea. Drainage systems cannot erode their bed below this base level. However, it is important to consider that sea level fluctuates and as such, adjustments are made along river longitudinal profiles.

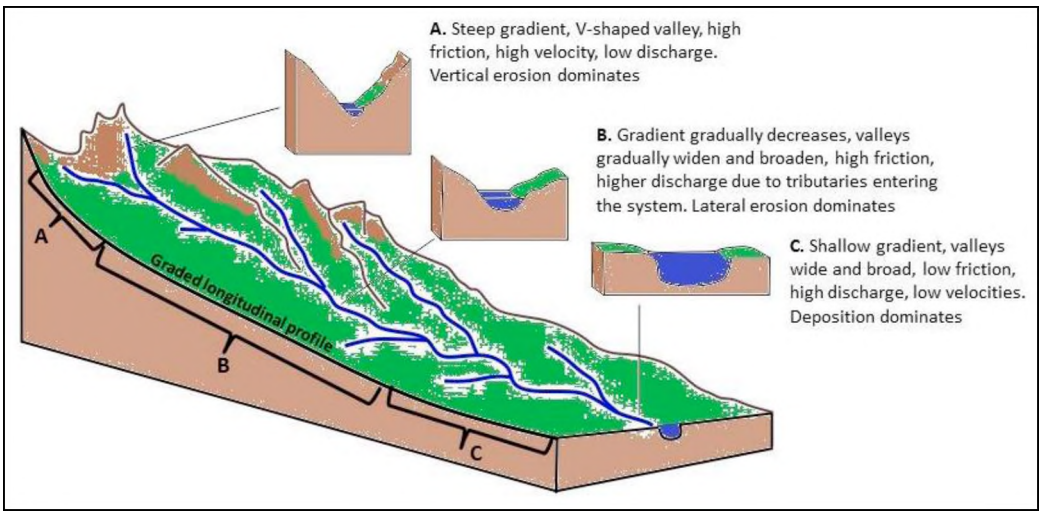

Figure 4: Diagram illustrating a graded river profile, stream processes and reach characteristics, adapted from Brierley and Fryirs (2005)

A specific fluvial system's longitudinal profile is the product of the long-term development and change of the landscape (Fryirs & Brierley, 2012a). A combination of tectonic uplift and down-wearing by the river create the profile. The longitudinal profile can also be thought of as a manifestation of the distribution of potential energy along the length of the drainage system, balanced by the resisting forces provided by the bank and bedload material; i.e. the steeper the slope and lower resistant force, the greater the potential energy. However, the stylised concave-upward longitudinal profile is rarely followed by all rivers (Rowntree, 2010). A number of South African rivers demonstrate this (Holmes *et al.,* 2016). Maud (2012), states that the longitudinal profiles of the rivers draining the eastern face of the Great Escarpment have been greatly influenced by the uplifts of the Miocene and Pliocene. Furthermore, varying lithology also has an impact on a river's profile, such that a more resistant lithology will create steps down the length of the longitudinal profile (Tooth *et al.,* 2002). The landscapes template coupled with varying lithologies occur as discontinuities at points of river rejuvenation along the longitudinal profile and therefore change the overall classic graded profile.

A graded river is defined as a river in which channel slope adjusts over timeframes of a year to enable available discharge and the dominant channel characteristics to have sufficient energy to entrain and transport the sediment load produced by the catchment (Fryirs & Brierley, 2012b). This adjustment means that the fluvial system acts as unified sections with feedbacks (cybernetic), where a change in one part will cause change in other parts. The key variables that will initiate compensating adjustments within the system are discharge, velocity, channel geometry, stream gradient, sediment load and base level. The adjustments of compensation are to restore the equilibrium between the energy, load and capacity of the channel. A channel will be in equilibrium if its channel geometry and gradient are roughly balanced to entrain and transport the available load of water and sediment such that neither deposition nor erosion will take place. When this circumstance is reached a river is called graded (Ellery *et al.*, 2009). As this is an ideal situation most streams are in constant adjustment whereby erosion and deposition occurs to varying degrees along different reaches of the system.

In South Africa wetlands are anomalies if one considers climate (rainfall and potential evapotranspiration) which generally results in a negative water balance with the potential evapotranspiration exceeding rainfall (Garden, 2008; Ellery *et al.,* 2009; Joubert & Ellery, 2013; Job, 2014). The combination of a negative water balance and a predominantly erosional landscape means that there should not be many wetlands in the region. This is especially true if one accepts that the origin of wetlands requires a positive water balance (Mitsch & Gosselink, 2007). Nevertheless, a

wide variety and a large number of wetlands have been identified within the southern African landscape. When one considers the macro-scale climate and geomorphology of this region, most wetlands will be closely linked to either or a combination of the drainage network and ground-water for their the primary water source (Tooth, 2000; Tooth & McCarthy, 2007; Ellery *et al.,* 2009). Secondly, a wetland must be situated in a local region where incision of the drainage network has been momentarily halted (Ellery *et al.,* 2009). The development of wetlands along a river profile is therefore likely to coincide with areas of temporary or permanent sediment deposition. This is especially so for floodplain or valley-bottom wetlands which form the largest and most extensive wetlands on the subcontinent. Sedimentation occurs along the longitudinal profile where, for example, a local resistant lithology forms a local base level in a catchment where more easily eroded rocks dominate the catchment. As sediment accumulates upstream of such a local base level, slope is reduced in the upstream direction of the node of deposition, but simultaneously steepened in the downstream direction. Another example occurs when steep, sediment-laden tributaries deposit large amounts of sediment along the trunk stream (Garden, 2008), creating an alluvial fan at the base of the tributary. The aggradation caused by the alluvial fan changes the longitudinal profile of that section of the main channel. A reduction in the gradient upstream of the alluvial fan creates an area of deposition, an environment conducive to wetland formation (Haigh, 2009).

Due to the close relationship of wetlands to fluvial systems on the subcontinent, understanding fluvial systems is essential part for developing conceptual models on the origin, preservation and protection of wetlands. A number of such conceptual models exist relating to the formation of wetlands in drylands, including those of Tooth *et al.* (2002); Tooth *et al*. (2004); Edwards (2009); Grenfell *et al*. (2010); Ellery *et al*. (2012); Joubert & Ellery (2013).

2.2.2 FLUVIAL SYSTEMS ADJUSTMENTS: GEOMORPHIC THRESHOLDS

Cyclic or dynamic equilibrium based understandings of landform development both suggest that modifications to landscape evolution are as a consequence of external forces such as tectonics, climate or human induced landscape changes (Schumm, 1973). This is certainly the case as much research can attest. However, within a fluvial system there may be adjustments made that cannot be adequately explained by external forces over long periods of time, such as channel aggradation and avulsion in the Okavango Delta (McCarthy *et al.,* 1986), slope failures (Korup *et al.,* 2006) and the modern periods of gullying (Schumm, 1973). Furthermore, it has been observed that not all systems in a region respond to an external stress in the same way, and in some cases systems have not responded at all. Schumm (1973, 1979) suggests that two additional factors should be

considered: geomorphic thresholds and dynamic responses of geomorphic systems. He suggests that inherent instabilities may occur naturally in a system which should be recognised.

Natural thresholds have been observed in many aspects of fluvial systems. The most recognised are the threshold velocities that are required for entrainment and transport of varying sizes of sediment. With an increase in velocity, threshold velocities are crossed at which entrainment and transport begins. The opposite may occur when velocities decrease and threshold velocity is met and entrainment and transport of sediment of a certain size ceases or deposition occurs. Brunet (1968) cited in Schumm (1973), calls these 'thresholds of manifestation' and 'thresholds of extinction' and are the most commonly documented thresholds. When a third variable is introduced to the system a 'threshold of reversal' may occur. An example of this is found in a study done by Langbein & Schumm (1958). A curve was created showing that sediment yield is directly related to annual precipitation and runoff, until a point where vegetation cover increases to a point where erosion is slowed, as illustrated in Figure 5. At this point there is a distinct change whereby with an increase in precipitation and runoff there is a decrease in sediment yield, because of increased vegetation cover. This is an example of an external variable progressively changing (rainfall), which in turn triggers an unexpected change within the system. Such responses to external factors are called extrinsic thresholds.

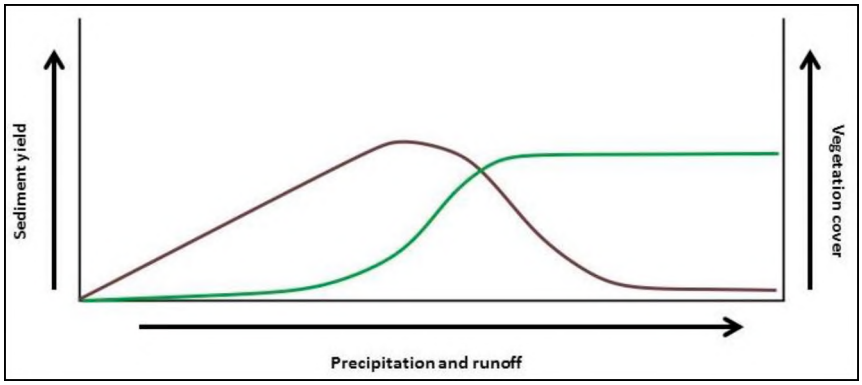

Figure 5: Graph depicting relationship between sediment yields (brown line) and vegetation cover (green line) in relation to precipitation and runoff, based on information from Langbein & Schumm (1958)

An intrinsic threshold can be encountered when the external factor stays constant, yet the progressive accumulative change within the system will render the system unstable and may cause it to fail (Schumm, 1973). For example, a cumulative increase in the slope of a valley as a consequence of gradual deposition of sediment, may eventually initiate incision as the slope threshold within the system is reached (Fryirs & Brierley, 2012a). In this way the threshold is internal to the system and is termed an intrinsic threshold. This type of threshold is deemed the geomorphic threshold by Schumm (1973). Thus a geomorphic threshold is one that is intrinsic within the system and the

resulting adjustments to that system are caused by modification to the morphology of the landscape over a period of time. In this way the inherent change within the system itself is most crucial, because until it has progressed to a critical state, adjustment or failure will not occur (Schumm, 1979).

This suggests that an external change is not always needed to reach a threshold and for a geomorphic change to occur. However, a progressive change to an external variable which causes a system to reach a threshold is also included in geomorphic thresholds. Thresholds can be the product of either cause or effect. For example, known thresholds of velocity, shear stress, and stream power above which sediment moves or banks fail, may be caused by various external factors. However, bank, channel and slope stability thresholds, can be internal, when the forces causing the failures are not clearly identified (Schumm, 1979).

Observations in both the field and experiments have been able to support the concept of geomorphic thresholds. Schumm & Hadley (1957) have demonstrated that gully development, especially those concentrated along valley floors, is a consequence of the local over-steepening of the valley surface. They observed that the initiation of gully erosion in these valleys tends to be found on localised steeper convex reaches of the valley floor. An expansion of this observation is that, given constant geology, climate and land-use, a valley has a critical slope at which failure (a geomorphic threshold), in this case the development of gullies, will occur. This suggests that at those reaches where the valley floor is steepest there is instability inherent to the system and is likely where failure will occur.

A similar study was conducted by Wohl (2013) in high energy, boulder-bed and bedrock dominated headwater mountain streams of the Front Range of the Rocky Mountains. Wohl (2013) observed that, although not as flashy as alluvial dominated systems, headwater mountain streams with resistant boundaries are also characterised by complex non-linear responses and both external and internal thresholds create spatially and temporally abrupt changes within the system.

2.3 HYDRAULIC FEATURES OF FLUVIAL SYSTEMS

This review examines the hydraulic literature relating to the flow of water within open channels. This appraisal mostly uses the pivotal engineering texts of Chow (1959), Henderson (1966), and Chow *et al.* (1988), together with ecological considerations of Rowntree & Wadeson (1999), Davis and Barmuta (1989), Gordon *et al.* (1992), Mitsch & Gosselink (2007) and Ellery *et al*. (2009).

Before examining the detail of flow hydraulics the cautionary suggestions of Simon (1981) are noted. Simon (1981) cautions that over the past century astounding advancements have been made in understanding fundamental laws of fluid mechanics. These laws have been bound by powerful mathematical calculations in an attempt to understand the workings of the world around us. However, the natural world still defies these mathematical scripts. The natural system by its very nature exhibits complex dynamics. As such, one must take heed of the fact that fluid mechanics and their associated mathematical scripts can only ever be a simplified version of the complex natural system.

Considering these cautionary observations, this review attempts to provide information for the practical description and simplifications of the dynamic, complex real world of flow hydraulics.

The hydraulics of fluvial systems has typically examined open channel flow. This is different to flow in pipes. The fundamental difference between the two types of flows is that open channel flow has a free deformable surface, while pipe flow does not. Open channel flow is considered to be much more difficult to calculate. This is due to the fact that open channel flow is influenced by many flow variables spanning both time and space dimensions. In open channel flow, depth of flow, discharge, gradient and the roughness elements are all independent (Chow, 1959). All of these factors may change along a cross section, or longitudinally down the channel, and change in time.

Within wetlands, flow hydraulics can be difficult to determine. Most wetlands are characterised by low velocities, low gradients, and highly variable roughness elements. In order to measure and describe flow hydraulic patterns in a wetland, it is necessary to understand a few concepts.

2.3.1 SURFACE WATER FLOW: VELOCITY, DEPTH AND TIME

The flow of water over the land surface is a complex and dynamic process, varying longitudinally, laterally, vertically and over time. The process begins when ponded water reaches a sufficient depth to overcome surface retention forces and begins to flow. Flow is usually categorised into two flow types: sheet flow and channel flow. Sheet flow, usually the first mechanism of surface water flow within a catchment, is discernable as a thin layer of water flowing over a wide surface. Channel flow is the outcome of sheet flow when changes in the catchment's land surface force the water to concentrate and flow in channels.

Flow velocity is the rate of movement of a fluid particle from one point in space to another over a given time (Chow, 1959; Henderson, 1966; Chow *et al.,* 1988; Gordon *et al.,* 1992; Rowntree & Wadeson, 1999). Hence, velocity is characterised as having both magnitude and direction. Velocity in

channels tends to increase with a decrease in wetted perimeter in relation to the cross-sectional area (hydraulic radius; (Figure 6 a), an increase in gradient (Figure 6 b), and when bed roughness decreases (Figure 6 c). On the other hand, velocity decreases when the opposite holds true, as shown on the right of Figure 6. Velocity also varies across the stream as well as with depth. These disparities are caused by variable frictional forces and turbulence.

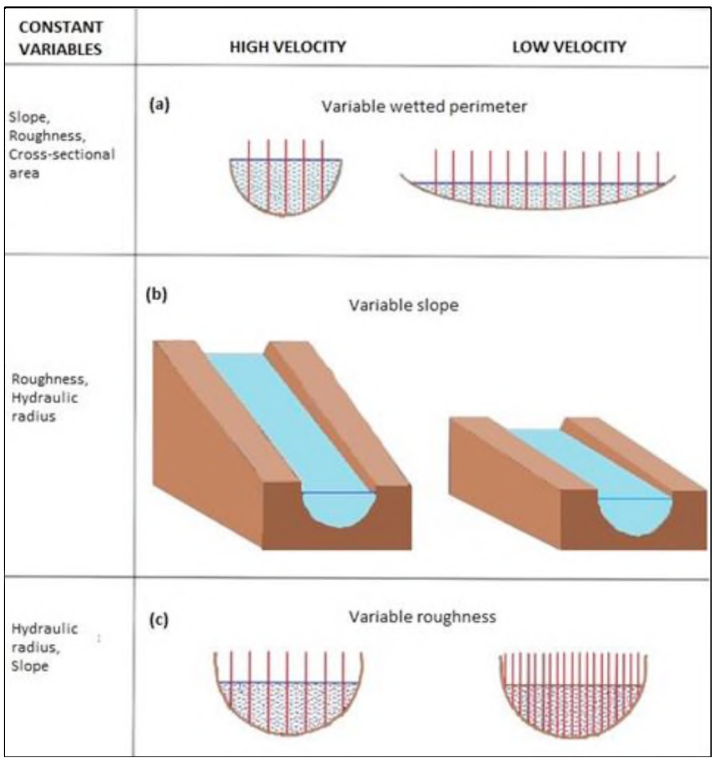

Figure 6: Schematic of the relationship between velocity and hydraulic variables, such as hydraulic radius (a), slope (b) and bed roughness (c) vegetation stems represented by vertical lines (Ellery *et al.,* 2009)

Velocity is an important hydraulic parameter of an open channel. It is influenced by channel gradient, depth, channel geometry, landscape features (confinement), and roughness elements. It varies in all three space dimensions and time. Velocity has a direct influence on the capacity of the channel to do work and as a consequence reflects erosion and deposition within the channel. Velocity is also a measureable component in hydrodynamic modelling.

2.3.2 CHANNEL-SHAPING: STREAM POWER

Fluvial processes are driven by two primary factors: factors that control the supply of sediment to the system and those that regulate the capacity for sediment transport or erosion of the channel. A hierarchical scale can be used to define these factors (Rowntree & Wadeson, 1999). The supply of sediment is, for the most part, dependent on the catchment's characteristics that control erosion occurring on the surrounding hillslopes, as well as any sediment accumulated in the system. The

capacity of the channel to entrain and transport sediment is mainly related to stream power. Stream power is defined as the ability of the water to perform work. Sediment transport is an important component of the soil erosion process, which is governed by a number of hydraulic parameters and is primarily a function of discharge, mean flow velocity, and slope gradient. A channels gradient is a product of the development of the rivers longitudinal profile over a long period of time. For a given stream section, discharge, on the other hand, is given and is a function of climatic and catchment characteristics that affects runoff.

Stream power per unit stream length is a function of discharge and gradient and is mathematically expressed as:

$$\omega_1 = \rho g Q S$$

where ω_1 is stream power per unit stream length in units of kg-m.s^3, ρ is water density, g is acceleration due to gravity, Q is flow discharge and S is the slope of the reach.

Sediment movement is dictated by the ability of water flow to first entrain and then transport it (Baker *et al.,* 2009). Sediment movement is retarded by the nature and composition of the stream bank and bed, which affect the ability of soil particles to resist detachment (Foster & Meyer, 1972). Surface water flow across a wetland has the capacity to carry sediment as a function of stream power.

A fundamental fluvial geomorphic principle is that, if capacity is greater than load, erosion will occur. Hence, sediment transport capacity and stream power play pivotal roles in the physical description of the soil erosion processes. '*Sediment transport capacity is defined as the maximum sediment load that a particular discharge can transport at a certain slope'* (Merten *et al.,* 2001). As such, transport capacity increases with an increase in one or more of the following: unit discharge, slope gradient, and mean flow velocity, since the energy exerted by a certain discharge on the bed increases with these variables (see Beasley *et al*., 1982; Everaert, 1991; Govers, 1992; and Zhang *et al*., 2009). Anthropogenic activities, such as clearing the channel or straightening it would also have an influence on stream power, as these activities would increase the gradient and velocity. Moreover, any changes to stream power at one point in the channels longitudinal profile can initiate changes in sediment transport and channel capacity elsewhere along the stream profile (Gordon *et al.,* 1992).

2.3.3 EROSION AND COUNTERACTING FORCES

Erosion, especially in the form of gullies, is a prominent feature across many environments across the globe. Gullies in river and wetland landscapes are dynamic features that can be the dominant force in landscape dissection, landscape connectivity and the production of sediment. Poesen *et al.,* (2003), estimated that ten to ninety percent of sediment production in some catchments is attributed to gully erosion. Headcut erosion is especially damaging to wetland environments. Headcuts are defined as a sudden near-vertical change in elevation or knickpoint at the leading edge of a gully that erodes the valley network by migrating upstream over time (Bull and Kirkby, 2002) and concentrate flow and add sediment to downstream gully channels. Due to the depositional nature of wetlands, the existence of gullies is potentially a driving force behind degradation and eventual collapse.

Whether gully erosion in wetland environments will occur is determined by the balance between forces of removal and forces of resistance (Ellery *et al.,* 2009). The forces of removal are related to to the eroding power (erosivity) of the water in motion and catchment characteristics, most notably the lack of vegetative cover and soil characteristics.

Factors counteracting or resisting the likelihood of erosion occurring within wetlands include, surface roughness ('n' in Manning's Equation), which in wetlands is primarily related to vegetation cover and soil properties. Surface roughness significantly affects flow velocity within wetlands. A key feature of wetlands is their varying, but typically high density of vegetation (Baker *et al.,* 2009). Kadlec (1990), observes that the role of vegetation within wetlands and its consequential effect on surface roughness is particularly complex. Flow velocity and direction can be significantly altered by the density, distribution, orientation and type of vegetation.

Kadlec (1990), demonstrates that traditional hydraulic equations, such as Manning's Equation, that include bottom-surface roughness, are often inadequate in explaining water flow within wetland systems. Spatial variabilities as well as varying vegetation densities across a wetland often exceed those densities described in these equations, which gives rise to errors when calculating flow within the wetland. In addition to variations in horizontal frictional resistance, water depth alters the resistance of vegetation (Baker *et al.,* 2009). It has been observed that, for example, in shallow water plant litter and herbaceous vegetation will often offer little resistance in comparison to shrubby or wooded wetlands. As water depth increases, the resistence provided by rushes, reeds and bushes also incrases initially, thereby having a greater effect on water movement (Baker *et al*., 2009). However, not all wetlands display this complexity in horizontal and vertical vegetation structure.

When water overtops the vegetation, frictional forces in the upper water column decline, leading to increased flow velocities and reduced modification of flow direction than if the vegetation was not fully submerged (Kadlec, 1990 and Baker *et al.,* 2009). Furthermore, nonlinearity introduced by tall, robust vegetation (such as palmiet) to change form from near-vertical over a height of three meters during low flows, to near horizontal over a height of one meter during high flows, makes modelling complex. This is particularly true as the horizontal form of palmiet during high flows offers considerable protection to the soil surface during high flows.

In addition, small-scale topographic features, that increase roughness and modify surface water velocities and flow direction, also play important roles. Wetland flows are typically at depths of 0.01 to 0.5 meters, as noted by Kadlec (1990). Microtopography makes it essential to re-assess notions of depth and velocity. It has been observed that the orientation of the microtopographic features relative to the prevailing local gradient may also play a role, as these features either create barriers and obstruct flow, or act as channels and promote water movement (Baker *et al*., 2009). This relates to the degree of connectedness, or lack thereof, between microtopographic features, and between other areas of surface water.

2.4 ESTIMATING PEAK DISCHARGES (Q)

As discussed in the previous section, hydrology is one of the most important factors in understanding the origin, function, preservation and even collapse of wetland ecosystems. In South Africa one of the most widespread mechanisms behind wetland degradation is gully formation, which often drains it of surface and subsurface flow (Ellery *et al*., 2009). Understanding the hydrology, especially the peak floods that occur within the wetland, is important in determining how often sediment might be mobilised and transported, thus influencing the vulnerability of the wetland to erosion. In South Africa streamflow data is captured and recorded using gauging weirs in most of the large river systems, but in smaller catchments these gauging weirs are infrequent and as a result data is scarce. Hence, estimates of flood characteristics (for example, peak discharges, run-off volume and shape of the hydrograph) are generally derived by mathematical equations and models.

In South Africa estimation of floods from small catchment areas is usually simulated using one of the following methods:

I. Empirical formulae

II. Rational Method

III. Unit hydrograph techniques

IV. Time area method

V. Kinematic method

For this research the Rational Formula Method was chosen and applied, because it is widely used in South Africa and around the world.

The deterministic rational formula (RF) approach to determine peak discharges (Q) involves analysis of all factors involved in flood prediction from converting rainfall inputs into runoff outputs. This method is used in calculating Q values for catchment areas of between 0.5 and 70 km². The Rational Method is a widely used model to calculate peak discharges. The formula was first created in 1851 by an Irish engineer, Mulvaney, but has been greatly improved since then.

The formula is:

$$Q_T = \frac{C_T \times I_T A}{3.6}$$

where, Q_T is peak flow in cubic meters per second for T-year return period, C_T is a runoff coefficient or dimensionless catchment characteristic that relates to the proportion of the rainfall that will run off from the catchment during a chosen design T-year return period storm. I_T is the average rainfall intensity over the catchment for a specific return period in mm/hr, A is the effective catchment area in kilometers squared and 3.6 is the conversion factor.

The Rational Method, although easy to use and quick to calculate, only simulates flood peaks and is sensitive to input design, rainfall intensity, and the selection of the runoff coefficient. The method assumes that the peak discharge occurs when the duration of the rainfall event is equal to the time of concentration of the catchment, and that the rainfall intensity does not vary and/or is uniformly distributed across the catchment. The runoff coefficient may be estimated as a function of Mean Annual Precipitation (MAP), catchment land cover, permeability of the soils, average slope of the catchment, vegetation cover and return period. The return period adjustment factor decreases the runoff coefficient for events with return periods of less than 50 years.

2.5 HYDRODYNAMIC MODELLING

In fluvial geomorphology numerical models have become an important tool for exploring and understanding how landscapes are shaped by water (Coulthard and van de Wiel, 2013). This has

resulted in an exponential increase in numerical codes and modelling software available both commercially and non-commercially in the last two decades. Modelling software have been developed for simulating processes ranging from reach-scale to catchment scale; and from a single flood event to time spans of thousands of years. All modelling programs have specific purposes as well as advantages and limitations (Coulthard and van de Wiel, 2013). A crucial challenge to new users lies in finding a code that is suitable for the purpose, and in understanding the key elements of how the code works (Grenfell, 2015).

All numerical models able to simulate processes within fluvial systems vary in complexity, realism and computational costs. There are a number of general focuses of fluvial modelling software. However, for this research study the interest lay in hydrodynamics, relating to surface water flow; as such only information pertaining to this will be discussed here.

Hydrodynamics is the study of the motion of liquids, and in particular, water. A hydrodynamic model is a tool capable of describing or representing the motion of water. Before the advent of widely available computer systems, a hydrodynamic model could be a physical model built to scale. However, virtually all hydrodynamic models in use today are computational numerical models. With the technological development of numerical models and advanced computational systems, hydrodynamic modelling has become part of the larger field of computational fluid dynamics (CFD). The common basis for these modelling activities is the numerical solution of the governing equations of conservation of momentum and mass in a fluid.

Hydrodynamic numerical modelling software can route water in two broad ways. Firstly, modelling software route water between cells aligned on a longitudinal profile such that water flows in one direction, such as one-dimensional models. The equations for modelling one-dimensional flow are derived from the conservation of mass and momentum equations between adjacent cross-sections (Bates *et al.,* 2005). Secondly, modelling software that route water between cells on a grid are either two-dimensional, quasi-three dimensional or three-dimensional. Both one-dimensional and two-dimensional software will be discussed here as these types of software were deemed sufficient to provide information of use in this research. One-dimensional allows water to be modelled simplistically longitudinally down the landscape. It assumes velocity flow is in one direction. Two-dimensional software allows water to be modelled in both longitudinal and lateral dimensions across the terrain, while velocity is presumed to be uniform in the vertical direction. Two-dimensional models are based on integration over the flow-depth to obtain depth averaged velocity values and are solved using an appropriate numerical approach such as a finite element model (Grenfell, 2015).

The base that most two-dimensional models are built on is a digital representation of the Earth's surface, such as a Digital Terrain Model or a Digital Elevation Model. In this digital format each cell is assigned a location that can be defined in the physical spatial coordinate realm. Cell properties such as elevation, bed characteristics (sediment size, porosity, roughness), and water levels, are defined from the physical coordinate system. According to Grenfell (2015), water routing software codes calculate fluxes of mass and momentum across the domain and through time based on physical laws that have been incorporated into the software and that may be represented by varying degrees of complexity.

Models are an effective and widely used tool in environmental planning and management. Policy makers and environmental managers frequently demand both qualitative and quantitative predictions of the future effects of current activities as well as the effect of future management activities. Numerical modelling incorporates the key mechanisms that drive hydrological processes, and the feedbacks that govern fluvial and wetland characteristics and dynamics, and ultimately their socio-ecological value. Kleinhans (2010) and Grenfell (2015) suggests that numerical modelling programs and the virtual systems they describe are useful tools due to the fact that they define the possibility for full control over boundary conditions and physical laws, to assess and weigh conflicting explanations, to clarify and explain key controls or necessary conditions, and in order to elicit a certain response from a system. Such activities normally necessitate insight that extends beyond the limits of field observation, or that is challenging to transfer from laboratory experiments.

A large number of varying hydrological models exists today, many of which can be used in, or adapted for, the use and simulation of hydrological processes within a wetland. Hydrological models vary in complexity from simple conceptual models to highly complex numerical models based on physics. McCartney & Acreman (2009) state, all models are a simplistic view of reality as it is not possible to represent all processes, physical and biological, as well as their feedback effects, governing water movement through a catchment or a wetland.

A common simplification used in hydrological modelling is 'lumping' or spatial averaging. This type of simplification simulates the system and its response to changing water fluxes mathematically using only depth and time (Blackie & Eels, 1985). Within these simulations the hydrological processes are represented as storage elements, each with defined capacities and outflow interactions. Due to the fact that processes are simulated conceptually, the parameters are adjusted until the model output is an acceptable estimate of observations (McCartney & Acreman, 2009). Observed and collected data is then used to calibrate the model.

The more complex models are based on our present understanding of the physics of hydrological processes. The descriptive equations for physically-based models are usually non-linear, partial differential equations that cannot be solved analytically. As a result, solutions must be found using approximate numerical methods. All of these types of models involve some form of simplification of the space and time coordinates into quantified points (McCartney & Acreman, 2009). Solutions are then generated for the points. McCartney & Acreman (2009) believe that model parameters should, in principle, be measurable in the field; but it may be necessary to calibrate the parameters.

The key advantage of physically-based more complex models is that they can be used to simulate changes across an area. Unfortunately, however, they require large amounts of input data and longer computational time and power.

2.5.1 DIMENSIONS

One-dimensional hydraulic analysis assumes that all water flows in the longitudinal direction, such that flow is perpendicular to cross-sections of the channel. One-dimensional software simulates flow in order to estimate the average velocity and water depth at each cross-section that represents the terrain (Bates *et al.,* 2005).

Two-dimensional hydraulic analysis allows water movement to be modelled in both the longitudinal and lateral directions, while velocity is presumed to be insignificant in the vertical direction. In contrast to one-dimensional models, two-dimensional models symbolise the terrain as a continuous surface through a finite element mesh created out of cells. Due to this continuous representation of the terrain, two-dimensional models are able to characterise lateral interactions of flow (Bates *et al.,* 2005).

Three-dimensional hydrodynamic modelling is unjustifiable in this study given the nature of the research question, also because of huge computational draw backs, especially at the reach scale. This is especially true when the parameters of interest, such as velocity direction and magnitude, inundation extent, and water depth can be predicted using one-dimensional or two-dimensional software (Bates & De Roo, 2000).

2.5.2 HEC-RAS ONE-DIMENSIONAL HYDRAULIC ANALYSIS

HEC-RAS is a hydraulic modelling software developed by the Hydrologic Engineering Center (HEC) of the U.S. Army Corps of Engineers. In 1964 the first software was released to the public called HEC-2. This was developed to assist hydraulic engineers to analyse channels and define floodplains. This

program quickly became popular and in the ensuing years many modifications and improvements have been made. Although HEC-2 was originally created to run on a mainframe computer, HEC-RAS can now be run on personal computers and work stations (Beavers, 1994).

In the early 1990's HEC released a Windows-compatible counterpart to HEC-2 as a consequence of the popularity and increased use of Windows-based personal computing software. This software was called the River Analysis System (RAS). HEC-RAS has a graphical user interface, to which are attached flow computation algorithms, many of which were derived from the HEC-2 model. HEC-RAS is a one-dimensional hydraulic analysis program and can be run in four modes: steady flow, unsteady flow analysis, and simulations can be done for sediment transport and water quality analysis. For this study the hydraulic analysis and will be explained in more depth below. The software is capable of modelling subcritical, supercritical, and mixed-flow regimes for streams consisting of a network of channels, a dendritic system, or a single river reach. The program output can be used in a multitude of ways to answer a host of questions related to river analysis. The HEC-RAS program results are usually employed in floodplain management and flood insurance studies in order to evaluate the effects of floodway encroachments. The HEC-RAS program can be downloaded at:

www.hec.usace.army.mil/software/hec-ras/hecras-hecras.html.

PLATFORM AND GOVERNING EQUATIONS

In a HEC-RAS steady state simulation, water surface profiles are computed from one cross-section to the next by solving a standard step iterative procedure to solve the energy equation. The energy equation is intended to calculate water surface profiles for steady gradually varied flow. The energy equation is shown below for two adjacent cross-sections XS1 and XS2:

$$Y_2 + Z_2 + \frac{a_2 V_2^2}{2g} = Y_1 + Z_1 + \frac{a_1 V_1^2}{2g} + h_e$$

where Y_1 and Y_2 are depths of water at adjacent cross-sections XS1 and XS2, Z_1 and Z_2 are the elevations of the main channel inverts, V_1 and V_2 are average velocities (total discharge/ total flow area), a_1 and a_2 are velocity weighting coefficients, g is the gravitational acceleration, and h_e is the energy head loss. The energy head loss is defined in the equation

$$h_e = LS_f + C\left|\frac{a_2 V_2^2}{2g} - \frac{a_1 V_1^2}{2g}\right|$$

where $\mathcal{L}$ is discharge weighted reach length, $\mathcal{S}_f$ is representative friction slope between XS1 and XS2, and $\mathcal{C}$ is an expansion or contraction loss coefficient. In order to calculate the representative friction slope HEC-RAS uses the average conveyance equation and the distance weighted reach length defined in the equations

$$\mathcal{S}_f = \left(\frac{\mathcal{Q}_1 + \mathcal{Q}_2}{\mathcal{K}_1 + \mathcal{K}_2}\right)^2$$

$$\mathcal{L} = \frac{\mathcal{L}_{lob}\mathcal{Q}_{lob} + \mathcal{L}_{ch}\mathcal{Q}_{ch} + \mathcal{L}_{rob}\mathcal{Q}_{rob}}{\mathcal{Q}_{lob} + \mathcal{Q}_{ch} + \mathcal{Q}_{rob}}$$

where $\mathcal{K}$ is conveyance, $\mathcal{L}_{lob}$,$\mathcal{L}_{ch}$ and $\mathcal{L}_{rob}$ are cross-sectional reach lengths for flow in the left over-bank, main channel, and right over-bank, respectively. $\mathcal{Q}_{lob}$, $\mathcal{Q}_{ch}$ and $\mathcal{Q}_{rob}$ are arithmetic averages of the flow between sections for the left over-bank, main channel, and right over-bank, respectively.

To determine total conveyance and the velocity coefficient for a cross-section, HEC-RAS subdivides flow in the main channel from the overbank components of flow. Conveyance is calculated for each subdivision using the equation

$$\mathcal{Q} = \mathcal{K}\mathcal{S}_f^{1/2}$$

$$\mathcal{K} = \frac{1.486}{n}\mathcal{A}\mathcal{R}^{2/3}$$

where $\mathcal{K}$ is conveyance for the subdivision, n is Manning's roughness coefficient for the subdivision, $\mathcal{A}$ is flow area for the subdivision, and $\mathcal{R}$ is hydraulic radius for each subdivision. The total conveyance for each subdivision is calculated as the sum of the conveyance from the left component of overbank flow, flow in the main channel, and the right component of overbank flow. Flow in the main channel is subdivided only when the Manning's roughness coefficient changes within the channel area. The composite main channel Manning's roughness coefficient is defined in the equation

$$n_c = \left[\frac{\sum_{i=1}^{N}\left(\mathcal{P}_i n_i^{1.5}\right)}{\mathcal{P}}\right]^{2/3}$$

where n_c is the composite or equivalent coefficient of roughness, $\mathcal{P}$ is the wetted perimeter of the whole main channel, $\mathcal{P}_i$ is the wetted perimeter of subdivision i, and n_i is the coefficient of roughness for subdivision i.

The limitations to running a simulation of steady flow calculations within HEC-RAS software is that the software assumes that the flow is steady, the flow is gradually varied, the flow is one-dimensional, and the slope of the channel is small. This can create erroneous results if one is modelling a very complex system.

2.5.3 CAESAR-LISFLOOD TWO-DIMENSIONAL HYDRODYNAMIC ANALYSIS

Hydrological modelling was also undertaken using two-dimensional modelling software, CAESAR-Lisflood 1.9b. The CAESAR-Lisflood is a reduced complexity model, this means that the two-dimensional depth-averaged form of the shallow water equation is not solved (it is not purely physics-based). CAESAR-Lisflood features conservation of mass but only partial conservation of momentum.

The CAESAR-Lisflood model is the product of the integration of the CAESAR landscape evolution model created by Coulthard *et al.* (2013), with the latest model version of Lisflood-FP a one-dimensional hydrodynamic flow model that is applied in the x- and y- directions to simulate two-dimensional flow as created by Bates *et al.* (2010). The CAESAR-Lisflood model, couples a landscape evolution model (LEM) with a simplified two-dimensional hydrodynamic model. This coupling produces faster results because it is based on a simple but stronger physical basis than the ones usually governing ordinary LEM models (van de Wiel *et al.,* 2007; Coulthard *et al.*, 2013). CAESAR-Lisflood 1.9b can be downloaded from:

http://code.google.com/p/CAESAR-Lisflood

PLATFORM AND GOVERNING EQUATIONS

CAESAR-Lisflood is a storage cell model, where a Digital Terrain Model (DTM) represents the landscape and water is stored at the raster cell locations. Water is routed over the landscape in the x- and y- directions (2D) from raster cell to cell using a simplification of the shallow water equations (Bates *et al.,* 2010). To calculate the flow (Q) between cells the model uses the equation

$$Q = \frac{q_i - g h_{flow} \Delta t \frac{\Delta(h + z)}{\Delta x}}{\left(1 + g h_{flow} \Delta t n^2 \backslash q_i / h_{flow}^{10/3}\right)}$$

where q_i is the flux between cells from the previous iteration ($m^2.s^{-1}$), g is acceleration due to gravity ($m.s^{-1}$), n is Manning's roughness coefficient, h is depth in meters, z is elevation (m), h_{flow} is the

maximum depth of flow between cells, x is grid cell width in meters and t is time in seconds. This equation establishes the discharge (Q) across all four boundaries of a cell. Then the cell water depth (h) is updated using the equation

$$\frac{\Delta h^{i,j}}{\Delta t} = \frac{Q_x^{i-1,j} - Q_x^{i,j} + Q_y^{i,j-1} - Q_y^{i,j}}{\Delta x^2}$$

where i and j are cell coordinates. The last part of the formulation is the time step (t) that is controlled by the shallow water Courant-Freidrichs-Lewy (CFL) condition, which requires that the wave does not spread across more than one cell per time step. This is represented by the equation

$$\Delta t_{max} = a \frac{\Delta x}{\sqrt{g h}}$$

where a is a coefficient typically defined between 0.3 and 0.7 (Bates *et al.,* 2010). The coefficient enhances the model's strength because the CFL condition is a necessary but (importantly) not a sufficient condition for stability in nonlinear systems.

CHAPTER THREE: DESCRIPTION OF THE STUDY AREA

3.1 LOCATION

The Krom River catchment is located in the southern part of the Eastern Cape Province of South Africa (Figure 7). The Krom River system arises in the easternmost section of an inter-montane valley within the Cape Fold Mountain Belt, which is an intensely folded mountain range with synclines and anticlines oriented in an east-west direction over a distance of over 1 000 km. Given that valleys are oriented east-west with mountain ranges to the north and south of major valleys, the region is characterised by a trellis drainage pattern (Lewis, 2008). Altitudes of the two mountain ranges that surround the Krom River, reach an elevation of 1 073 meters above sea level (m.a.s.l) in the Suuranys Mountains to the north and 1 251 m.a.s.l (Witelskop) in the Tsitsikamma Mountains to the south. The sides of the valley are steep with slopes between 20 % and 30 % on the north facing mountains and 25 % and 60 % on the south facing slopes (Kotze & Ellery, 2009). The Krom River is approximately 100 km in length from its upper reaches (550 m.a.s.l) to its estuary, near the town of St Francis Bay where it drains into the Indian Ocean. The Krom River spans five Quaternary catchments (K90A, B, C, D and E) with a drainage area of approximately 1 022 km². The Krom River system has two sizeable dams on it, namely the Churchill Dam and the Impofu Dam, which together form an important water resource for the Nelson Mandela Metropole (Figure 7).

The research study site is the Kompanjiesdrif basin, which is located in the upper catchment of the Krom River (sub-catchment K90A; Figure 7). The basin is located between latitudes 33° 52’ 41” S and 33° 52’ 53” S; and longitudes 24° 3’ 11” E and 24° 4’ 26” E. The Kompanjiesdrif basin wetland forms the bottom part of a wetland complex that has been dissected by the regional road R67. The wetland complex is approximately 6 km in length of which the Kompanjiesdrif basin is the lower 1.8 km. The Kompanjiesdrif basin has a drainage area of roughly 60 km². This is approximately 5.5 % of the total Krom River catchment and 25 % of sub-catchment K90A. Of the 60 km², the Krom River palmiet (*Prionium serratum*) wetland complex makes up 1.43 km² or 1.8 % of its catchment. Of this 1.43 km² the Kompanjiesdrif basin occupies about 0.3 km², making up 0.5 % of the wetland complex catchment.

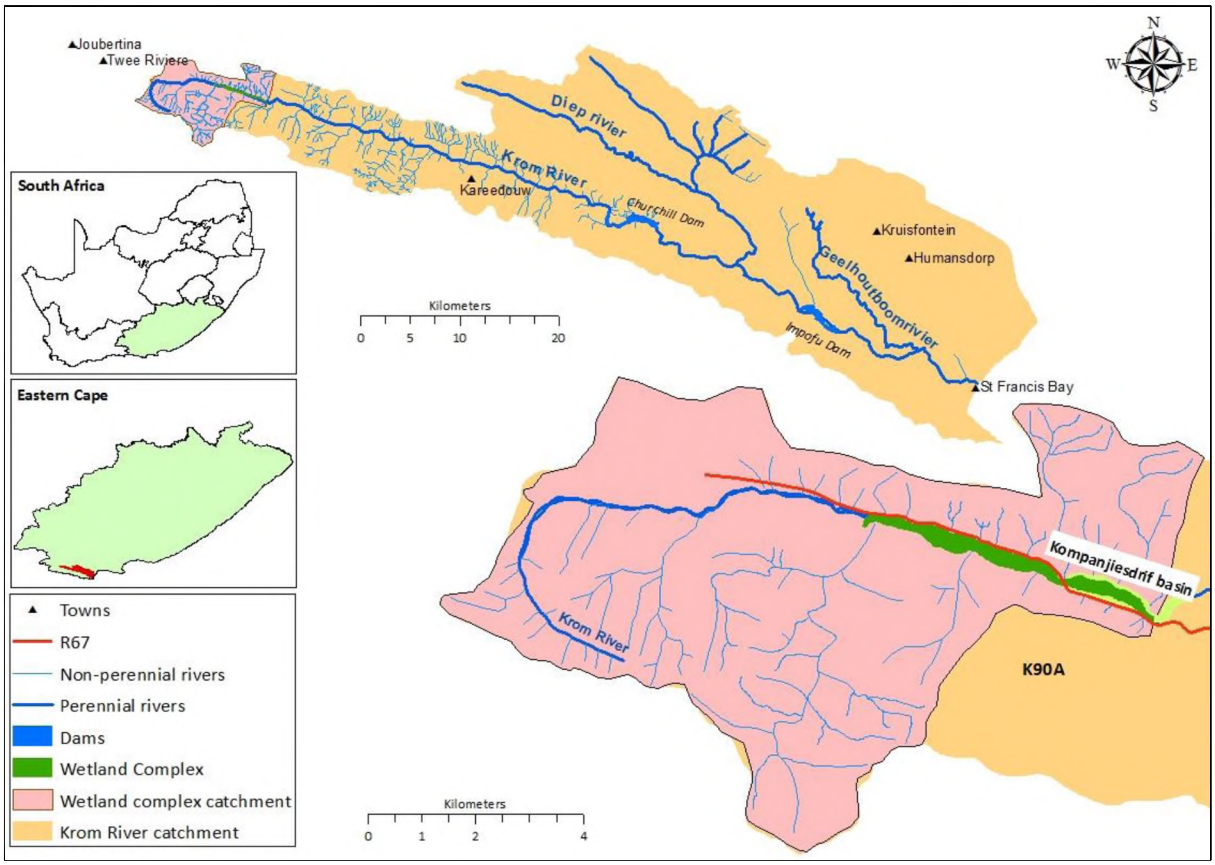

Figure 7: The catchment of the Krom River and the catchment of the Kompanjiesdrif basin in quaternary catchment (K90A) in the upper Krom River catchment

3.2 GEOLOGY, SOILS, TOPOGRAPHY AND GEOMORPHOLOGY

GEOLOGY

The high-lying ridges of the Tsitsikamma and Suuranys mountains, which are found to the south and north of the valley respectively, are formed by resistant quartzite lithologies of the Table Mountain Group. These ridges are divided as follows: at the base of the Krom River valley, sandstones and subordinate shales of the Baviaanskloof Formation occur, which are overlain by the more resistant quartzitic sandstones of the Skurweberg and Goudini Formations (Figure 8). Above this are shales of the Cederberg Formation which are capped by the quartzitic sandstones of the Peninsula Formation. These formations are part of the Table Mountain Group with the exception of the Gydo Formation, which forms the base of the stratigraphically younger Bokkeveld Group.

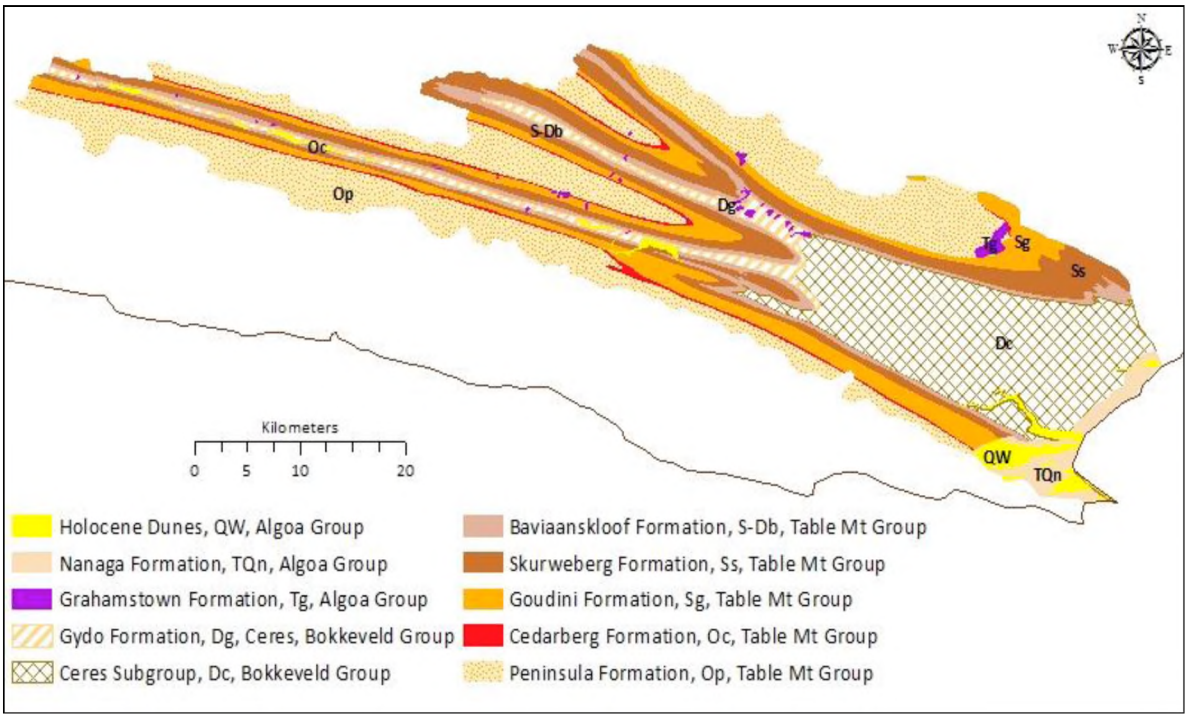

Figure 8: Dominant geology of the Krom River catchment (source: 1:250 000 geological layer)

TOPOGRAPHY AND DRAINAGE

The Krom River forms a trellis drainage pattern within the Langkloof Valley (Figure 7). There are many unnamed and mostly non-perennial tributaries that flow into the Krom River from the surrounding mountain ranges. The two major tributaries of the Krom River are the Diep River and the Geelhoutboom River (Figure 7), which are perennial. The first enters the Krom River below Churchill Dam and the latter below the Impofu Dam. Both these tributaries have their sources in the mountain range north of the Krom River.

The K90A quaternary catchment includes six large tributaries and five minor tributaries that enter the Krom River from the Tsitsikamma Mountains on the wetter southern side. In contrast, seven large and numerous short, for the most part non-perennial, tributaries enter the Krom River from the drier Suuranys Mountains to the north. In the Kompanjiesdrif basin there are four minor non-perennial tributaries stemming from the drier north and two larger tributaries from the south (Table 1).

A number of alluvial fans are evident on the Krom River valley floor where tributaries join the trunk stream. These are thought to exert a fundamental control on the wetlands of the Krom River by limiting the extent of valley-bottom wetlands and possibly influencing their longitudinal slope (Haigh, 2009).

Table 1: Characteristics of the Krom River wetland complex, Kompanjiesdrif basin and the major non-perennial tributaries entering the wetland complex

Wetland/ Major non-perennial tributary	Catchment (km^2)	Size (km^2)	Length (km)	Slope (%)
Krom River wetland complex	~55	~1.4	~6	0.77
Kompanjiesdrif basin wetland	~55	~0.30	~1.8	1.05
First tributary (N)	~3	N/A	~3.5	0.33
Second tributary (N)	~1	N/A	~1.3	17.6
Third tributary (N)	~0.5	N/A	~0.6	15
Forth tributary (N)	~3	N/A	~4	11.5
First tributary (S)	~20	N/A	~7	10.7
Second tributary (S)	~3	N/A	~3	11.7

GEOMORPHOLOGY

Although tributary alluvial fans influence the structure and function of the Krom River wetland basin (Haigh, 2009), the Langkloof valley is structurally controlled. The Krom River flows on a constricted synclinal sliver of the Bokkeveld shale, bordered on both sides by the folded and faulted resistant Table Mountain quartzite of the Tsitsikamma and Suuranys Mountains to the south and north of the valley respectively. The valley has been eroded and shaped by the Krom River (Lubke, 1998).

3.3 CLIMATE AND HYDROLOGY

The Krom River catchment, with its five quaternary catchments (K90A, B, C, D and E), falls within the transition zone between the Western Cape winter rainfall zone and the year round rainfall that characterises the coastal zone of the Eastern Cape. Although rain can take place all through the year (Midgley *et al.,* 1994), it tends to exhibit a bimodal pattern, with high rainfall in spring and autumn. Most of the Krom River catchment receives between 500 and 800 mm of rainfall per year, but the rainfall patterns vary both seasonally and annually, giving rise to extremely variable runoff regimes. The rainfall pattern within the Krom River catchment tends to decrease from west to east and from the coast inland (Figure 9). The mean annual precipitation (MAP) for the entire catchment is slightly more than 600 mm. Mean annual runoff (MAR) for the entire catchment is approximately 75 mm, which makes up about 10 % of the rainfall (Middleton & Bailey, 2008). The mean annual evaporation (MAE) for most of the catchment is approximately 1 600 mm (Figure 9).

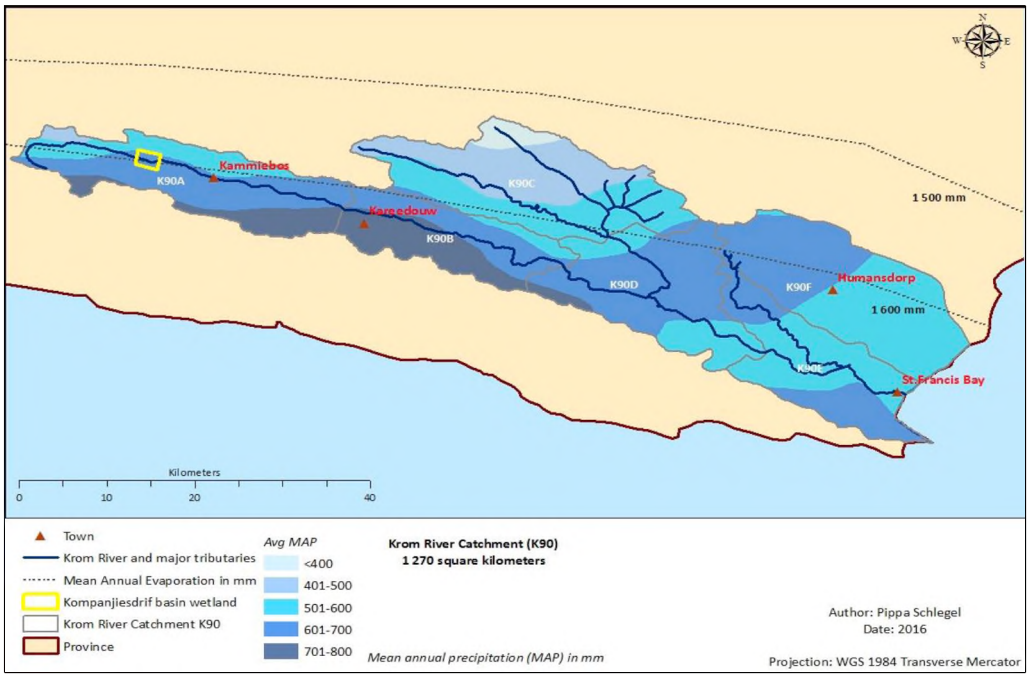

Figure 9: Mean annual precipitation (MAP) map for the Krom River catchment. Dotted lines represent the Mean annual evaporation (MAE) in mm

Analysis of the average rainfall from 1900 to 1996 of two weather stations (Kareedouw and Hendrikskraal) in the Krom River catchment and one just above the catchment but still in the Langkloof (Joubertina) reveals that during the wettest year (1981) 1 081.8 mm of rain was received at Hendrikskraal (Figure 10). During the driest year (1949) only 285.8 mm was received at Joubertina. The pattern of rainfall within the catchment is such that the town of Hendrikskraal receives the most rainfall, followed by Kareedouw and then Joubertina (Figure 10). This depicts the decreasing trend inland from the coast and from the west to east. May is the wettest month on average with 53 mm while January is the driest with 33 mm of rain.

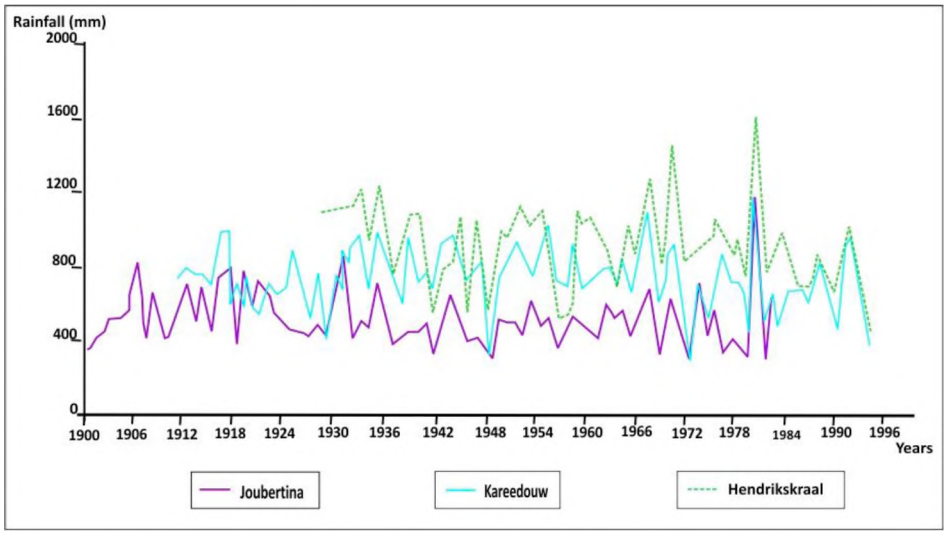

Figure 10: Average annual rainfall (1900 to 1996) at two locations in the Krom River Valley and Joubertina in the Langkloof

3.4 VEGETATION

The Southern part of the Eastern Cape is the eastern most extension of the Cape Floral Region, which has its epicenter in the South-western Cape. The Krom River catchment lies mostly within the fynbos biome (Figure 11), on nutrient-poor soils, with a small section at the bottom of the catchment falling under the Albany Thicket biome that occurs on slightly more nutrient rich soils (Mucina & Rutherford, 2006).

The headwater streams that form the Krom River arise within the Tsitsikamma Sandstone Fynbos on the northern aspect slopes of the Tsitsikamma mountain range, which has a Vulnerable Status and the Kouga Grassy Sandstone Fynbos on the southern aspect slopes of the Suuranys mountain range, which is categorised as Least Threatened. Grassy fynbos typically comprises the usual elements of fynbos, such as ericoids (heaths) restioids and proteoids, although only the re-sprouting proteiods have survived the frequent fire regime imposed by local farmers to encourage fodder grasses such as *Themeda* and *Heteropogon* to flourish. The natural fynbos has been altered and transformed due to agriculture prevailing grazing practices, artificial burning regimes and invasion of black wattle (*Acacia mearnsii*). Wetland vegetation which in the past occupied much of the bottom of the Langkloof valley has suffered a similar fate except, for a few remnant pockets.

Wetland vegetation along the bottom of the valley in the Kompanjiesdrif basin is dominated by palmiet (*Prionium serratum*) with a mixture of herbaceous shrubs, sedges, restios, and rushes along the edges of the wetland. Palmiet is a robust plant that has a tendency to dominate fluvial systems with catchments underlain by quartzite bedrock and is endemic in the Western Cape with isolated pockets stretching into the Eastern Cape as far north as southern KwaZulu-Natal. For many farmers palmiet is viewed as a ‘problem’ plant as it is widely believed to restrict waterways and to promote flooding of arable farming land and infrastructure.

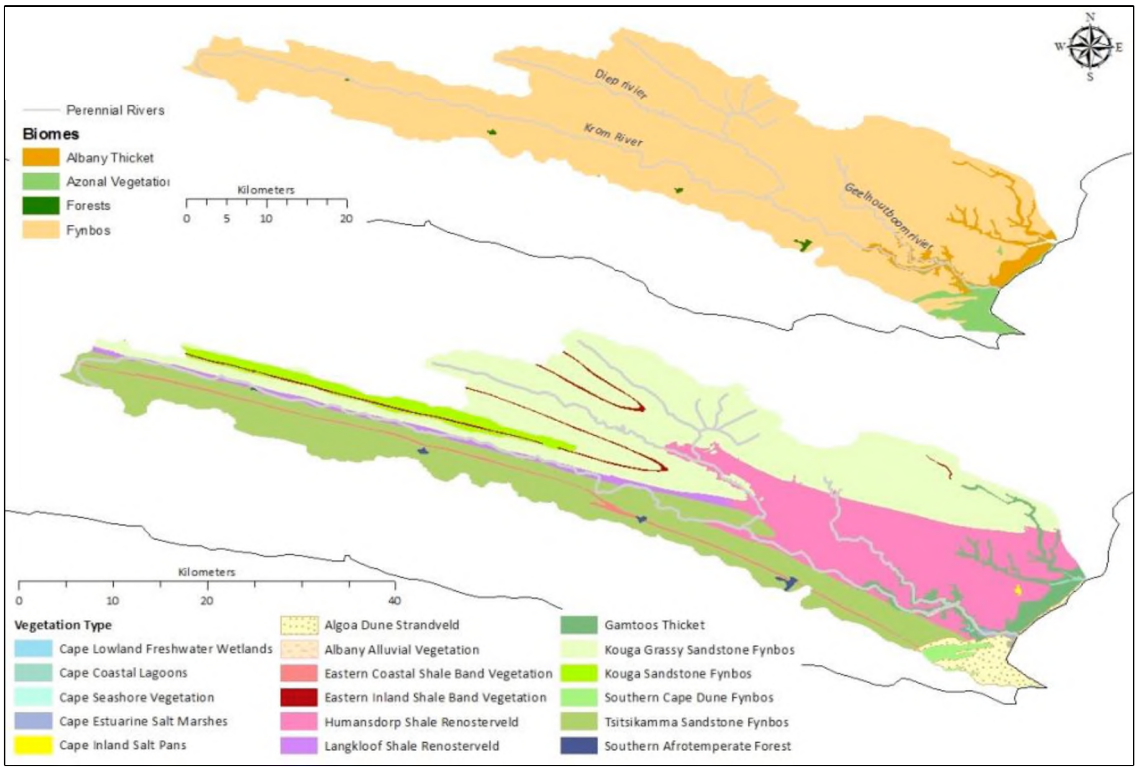

Figure 11: Biomes and vegetation types present in the Krom River catchment, based on information from Mucina &Rutherford (2006)

3.5 SOCIO-ECONOMIC CHARACTERISTICS

The upper Krom River catchment is mostly comprised of privately owned farms. Historically, the land along the Krom River was used for orchards, however only a few farms still practice this. At present, the land is mainly utilised for beef and dairy cattle and sheep farming as well as pastures for growing feed. Natural vegetation can still be found, especially on the steeper regions. The top of the catchment is state-owned with near-pristine natural vegetation, where the primary objective is conservation.

The data is based on the 2011 census data. The nearest town to the Kompanjiesdrif basin is Joubertina, found in the next catchment. Joubertina has a population of ~ 6 000 people. Kareedouw is the only town that falls within the upper catchment of the Krom River. The town was established in 1905 for the surrounding farming community. Kareedouw has a population ~ 5 000.

CHAPTER FOUR: MATERIALS AND METHODS

The methods used in this research study are subdivided into three sections: desktop analysis, field methods and modelling methods. The desktop analysis includes an investigation into discharge, rainfall and output analysis from CAESAR-Lisflood and HEC-RAS software. Field methods include field observations, topographical surveys, topographical mapping and vegetation sampling. Modelling methods comprises the input parameters needed for the simulation and the calibration process.

4.1 DESKTOP ANALYSIS

In order to achieve the objectives the data required was:

- Geo-referenced orthophotographs at 1:10 000 scale with 10 meter contour lines, obtained from the National Geo-spatial Information agency, Cape Town
- Geographical Information Systems (GIS) shapefiles, obtained from the Geography Department, Rhodes University
- Geological maps, obtained from the Geography Department, Rhodes University, sourced from the National Geo-spatial Information agency, Cape Town
- Flow data, obtained from the Department of Water and Sanitation
- Rainfall data, obtained from the South African Weather Service

In order to plot the longitudinal profile of the Krom River from the headwaters to the point at which the river widens and enters the Churchill Dam, orthophotographs with 10 meter contour lines were used. The longitudinal profiles of all the major tributaries entering the Krom River were plotted on the longitudinal profile. This was done in order to explore the characteristics of the Krom River longitudinal profile and depositional features associated with the tributaries.

The wetland and catchment boundaries were also mapped and digitised in ArcMap 10.3 (WGS84 projection) using the available 5, 10 and 20 m contour intervals together with 2009. These orthophotographs were deemed suitable with a resolution of 50 cm for the research study site.

Geological maps at a scale of 1:250 000 were appraised for any recorded lithological and structural characteristics of the study area.

Flow data for the period of 1970 to 2016, collected by the Department of Water and Sanitation (DWS, 2015) at flow gauge K90 below Churchill Dam was analysed. This data is limited as anecdotal reports of the guaging weir located on the Krom River below Churchill Dam and other rivers in the

area suggest that at times flows are suspected to exceed the ability of the available instruments to record them and thus go unrecorded. In addition, the effectiveness of the dam at catching smaller to medium sized floods means that these will be estimated.

The Kompanjiesdrif basin makes up the upper most 15 % of the Churchill Dam catchment. A non-linear method for calculating peak discharges, the Rational Method, was used to scale the flow data of the Churchill Dam catchment to the catchment of the Kompanjiesdrif basin. The method for the calculation of the Rational Method was followed using the South African National Roads Agency Limited, Drainage Manual (SANRAL, 2006). Firstly a land use map was created in order to calculate the runoff coefficient (Figure 12). These peak discharges were used as an input parameter in CAESAR-Lisflood and HEC-RAS.

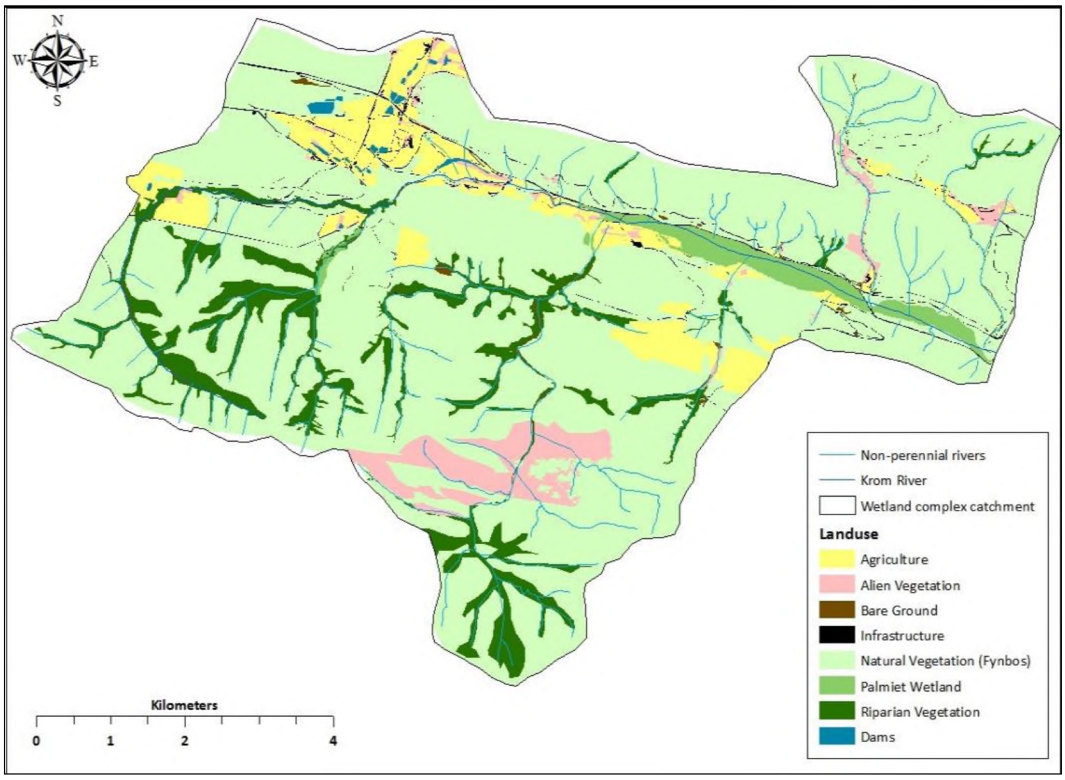

Figure 12: Land use map of the Kompanjiesdrif basin catchment, data sourced from Rebelo (2012)

4.2 FIELD DATA COLLECTION

The CAESAR-Lisflood and HEC-RAS software requires elevation data that suitably represents the true ground surface (Wilson & Atkinson, 2003). Whereas, HEC-RAS requires cross-sectional data, CAESAR-Lisflood, a higher accuracy Digital Terrain Model (DTM) is desirable since the DTM errors will largely dictate the errors in the model results (Farr *et al.,* 2007). In order to create a suitable resolution Digital Terrain Model of the Kompanjiesdrif basin, detailed topographic surveys were carried out

using a Geomax Zenith 10/20 Differential Geo Positioning System (DGPS). Nine transects were undertaken at locations down the length of the basin (Figure 13). Both the relative elevation of the land surface and the water level were recorded along these cross-sections in order to map changes in morphology down the entire length of the basin. The surveys were also needed to investigate the role of alluvial fans encroaching onto the wetland, which are fed by tributaries originating in the adjacent Tsitsikamma and Suuranys mountain ranges. These transects were located within the existing wetland and are numbered starting from the head of the wetland to the toe of the wetland, as presented in Figure 13. In order to reconstruct the wetland surface prior to gully formation, a further ten transects were conducted. These were located below the toe of the wetland, but did not include the large gully that has formed there. The gully was excluded as this research was interested in hydraulic features of flow that might initiate erosion. In some places of complexity and topographic significance, extra survey points were taken to supplement the data (Figure 13). This information was then stored in ArcMap 10.3 and further supplemented by the 10 meter contour lines in the terrain adjacent to the wetland. In total 3 410 points were surveyed of the wetland and the immediately surrounding floodplain.

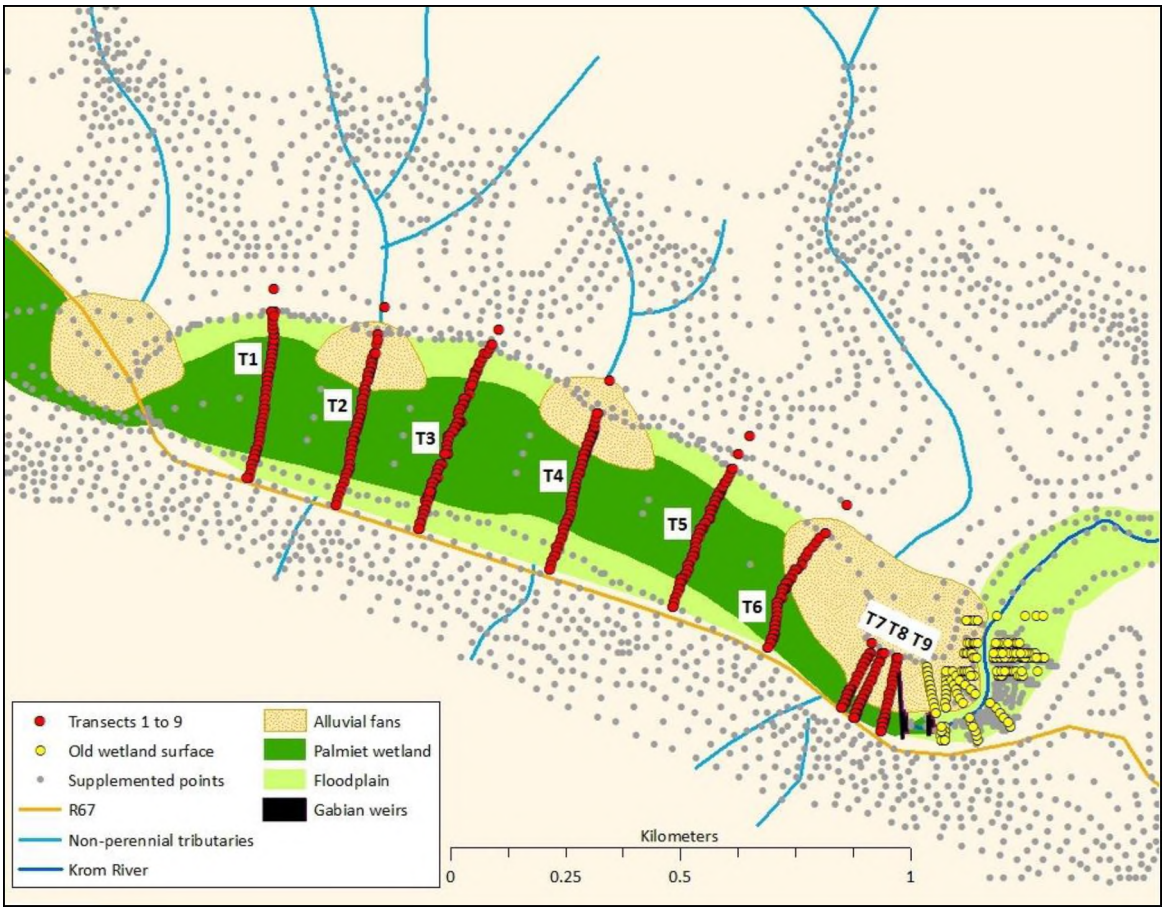

Figure 13: Location of topographic surveys and supplemental data points in the Kompanjiesdrif basin

The hydraulic properties of the wetland surface were measured by systematic random sampling along the topographical survey lines using 2 by 2 meter quadrats. This method was applied as described by Kent & Coker (1992) for measuring herbaceous vegetation. Stem density, height, and stem diameter were recorded, for all species found, from 60 quadrats in the field survey. This data was used to indicate an estimated roughness value that could be used within the modelling software. Photo A in Figure 14 below is an example of a typical palmiet (*Prionium serratum*) plant. Photo B in Figure 14 is an example of a 2 by 2 meter quadrate survey of the vegetation sample. As is evident by the photo palmiet is the dominant species found within the wetland.

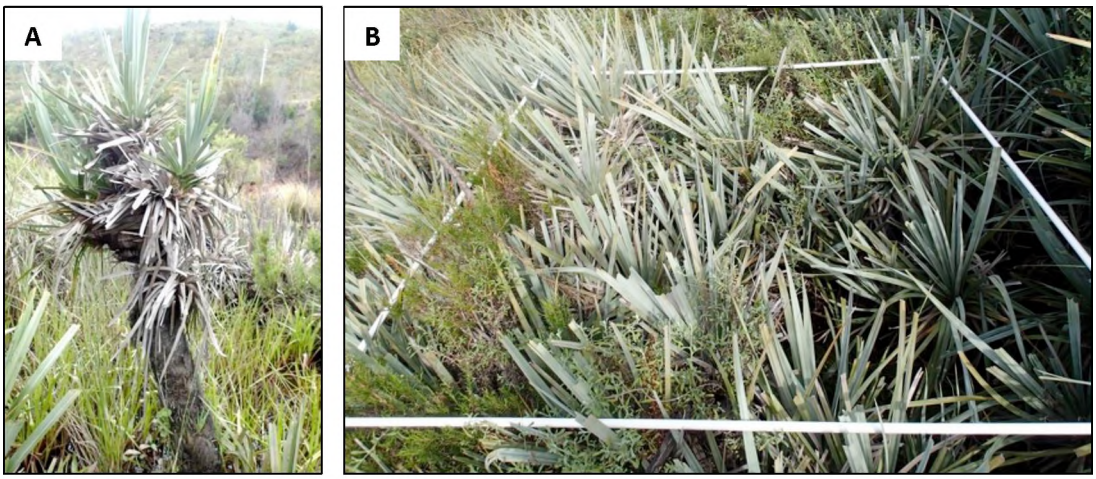

Figure 14: Vegetation surveys. Photo A is of a typical palmiet (*Prionium serratum*) plant. Photo B is an example of a 2 by 2 meter quadrate survey conducted in the field

The flood extent of the wetland was measured using a DGPS in May 2015, October 2015, November 2015 and June 2016. Discharge was measured using a Marsh-McBirney Flo-Mate 2000 in conjunction with the flood extent measurements in order to connect a particular flood extent with its relating discharge. The calibration process used these results in order to calibrate the model results. This was done by taking a known discharge and changing the roughness parameters in the model until the best fit inundation map was created that was most suited to the measured data (Di Baldassarre *et al.*, 2010).

Soil samples from the study area were collected for the characterisation of soil properties. Twelve sample sites along two cross-sectional transects (left bank to right bank) were chosen in close proximity to the point of loss of confinement of the valley where there was a valley floor depositional feature (as shown in Figure 15). This was done in order to gain an understanding of the characteristics of the sediment properties such as particle size, as this gives an indication of stream competence and stream capacity. Transect 1 was situated closest to the point of loss of confinement (Figure 15). Transect 2 was located approximately 50 m downstream of Transect 1.

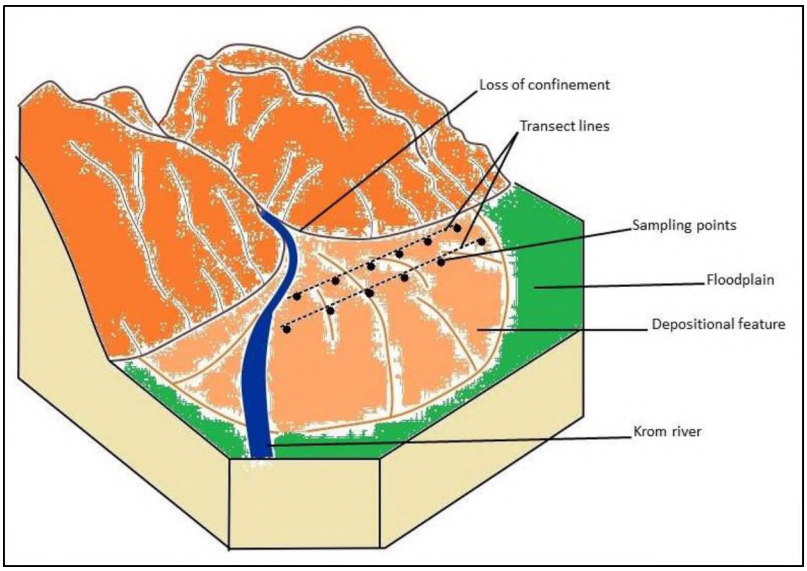

Figure 15: Schematic illustrating the location of Transects 1 and 2 in relation to the point of loss of confinement

Sediment/soil particles are usually sorted on the basis of their diameter, and can be classified using scales such as Wentworth-Udden (Wentworth, 1922), shown in Table 2. The distribution of particle size determines the texture of the sediment - whether it is predominantly sandy, silty or clayey. The procedure of determining the proportion of soil particles in each of these classes is a particle size analysis. The proportion of gravel and larger particles was determined by first grinding the soil to disaggregate it and then passing it through a 2 mm sieve. What remains in the sieve was weighed and its proportion calculated as a percentage of the whole sample. The proportion of the coarse, medium and fine sand are likewise determined by sieving using stacked sieves of different sizes, thus separating them from the clay and silt fractions of the soil.

Table 2: Sediment classes determined by sediment sizes

Class (Wentworth)	Diameter (mm)		Class (Wentworth)	Diameter (mm)
Very large boulder	4096-2048		Coarse sand	1-0.5
Large boulder	2048-1024		Medium sand	0.5-0.25
Medium boulder	1024-512		Fine sand	0.25-0.125
Small boulder	512-256		Very fine sand	0.125-0.0625
Large cobble	256-128		Coarse silt	0.0625-0.0312
Small cobble	128-64		Medium silt	0.0312-0.0156
Very coarse gravel	64-32		Fine silt	0.0156-0.0078
Coarse gravel	32-16		Very fine silt	0.0078-0.0039
Medium gravel	16-8		Coarse clay	0.0039-0.0020
Fine gravel	8-4		Medium clay	0.0020-0.0010
Very fine gravel	4-2		Fine clay	0.0010-0.0005
Very coarse sand	2-1		Very fine clay	0.0005-0.00024

Hjulstrom's Diagram was used to investigate the relationship between velocity and sediment movements in the basin. In the diagram shown in Figure 16, the upper curve represents the minimum stream velocity required to erode sediments of varying sizes from the stream bed. The middle curve represents the minimum velocity required to continue to transport sediments of varying sizes. This curve has an unexpected shape has it describes the work (energy) needed to lift a particle off the bed of the river. The exact velocity at which erosion will occur is dependent on both sediment and water characteristics. The lower curve shows settling velocity at which particles settle out of suspension and deposit on the bed of the stream. It reveals that once a particle is in suspension, the velocity at which particles settle is dependent upon particle size alone, being higher for larger grains and lower for smaller particles.

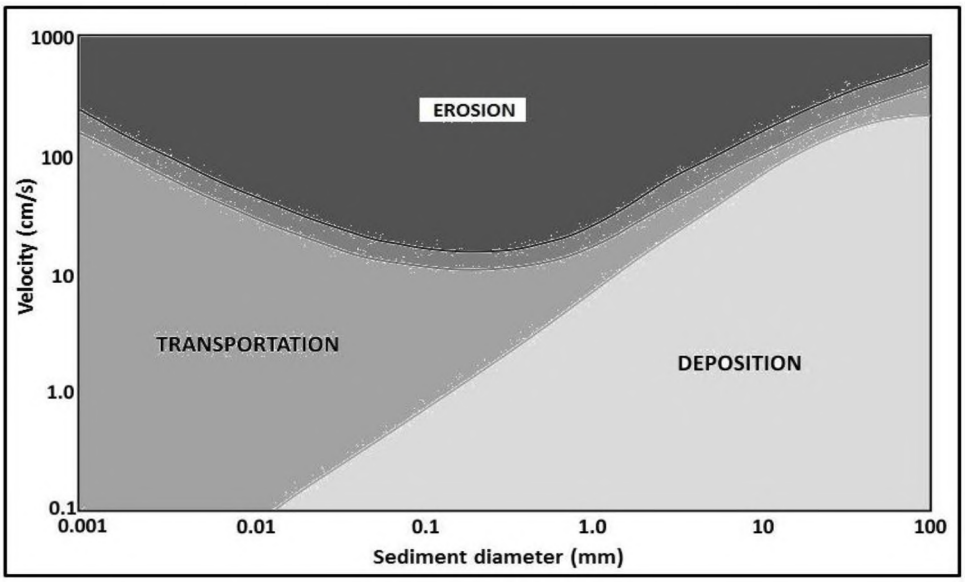

Figure 16: Hjulström's diagram illustrating the relationship between erosion, transportation and deposition to sediment grain size and velocity, adapted from Hjulström (1935)

4.3 MODELLING METHODS

Two types of modelling software were used. The first was HEC-RAS (Hydrologic Engineering Centre-River Analysis System), which is a one-dimensional model intended for hydraulic analysis of river channels. The second was CAESAR-Lisflood which is a two-dimensional hydrodynamic model that was run in reach mode. Measured discharges and their related wetted extent were used for calibration and validation processes. Simulations were then created for a range of discharges in order to understand the effect of discharge on flood extent, velocity, and stream power and bed shear stress within the wetland.

4.3.1 REASONS FOR SELECTING THE MODELLING SOFTWARE

HEC-RAS

HEC-RAS software has been used for more than twenty years. It has been peer reviewed and calibrated. Upgrades and revision of software capabilities are created and produced continuously. The software is freely available for download from the HEC-RAS website and is supported by the U.S Army Corps of Engineers. It is fairly easy to set up and simulations are fast. As a result many models can be run in succession. HEC-RAS 5.0.1 was selected for these reasons.

CAESAR-LISFLOOD

The user interface of CAESAR-Lisflood is relatively easy to learn, and the code is very well supported by online resources. The model has been tested in a multitude of research programs, and CAESAR-Lisflood is available as open source software. There are several advantages to using this code over more complex two-dimensional or three-dimensional hydrodynamic codes, as it is easier to learn and faster to run. This means that more simulations can be run for a better understanding of uncertainty and the software can evaluate problems at both landscape and river-reach scales.

4.3.2 HYDRAULIC MODEL BUILDING

There are two key methods for specifying the inputs to build a model in HEC-RAS and CAESAR-Lisflood. The first is to do a physical survey of the study site, and collect data manually to define the river and floodplain geometry. The other way is to use geospatial datasets like Digital Elevation Models (DEM) and develop the geometric data in ArcGIS. DEMs are freely available to be downloaded online and can be processed relatively easily to extract the geometric data. However, these freely available DEMs usually have a coarse resolution and for this reason are not suitable for areas of low relief or wetlands covered with thick vegetation. Data was collected from manual field surveys for this research. In HEC-RAS the topographical survey lines across the wetland (perpendicular to the flow) were used as the input parameter to represent the land surface (Figure 13). For the two-dimensional model CAESAR-Lisflood the topographical data points conducted in the field were imported into Arc Map 10.3. A suitable DTM was created using the *'topo to raster'* function. DTMs of varying cell sizes were created in order understand the effects of cell size (and hence resolution) on the model computation time and the effects on the output. After running the model, both software programs HEC-RAS and CAESAR-Lisflood, generate results for water depth, water velocity and velocity vectors, which are either in an existing digital exchange format (CAESAR-Lisflood) or can be exported into a digital exchange format (HEC-RAS). Most hydrodynamic and

hydraulic modelling software follows the three-step framework of pre-processing, processing and post-processing data, as depicted by Figure 17.

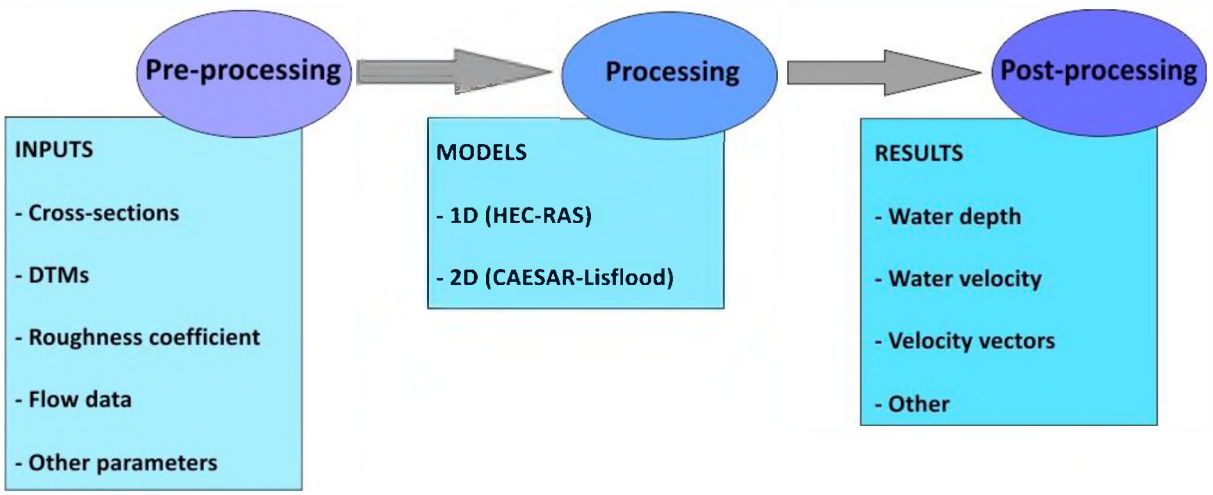

Figure 17: Schematic showing the processes taken in hydrodynamic and hydraulic analysis using modelling software

4.3.3 CAESAR-LISFLOOD

TOOL DESCRIPTION

CAESAR-Lisflood, as discussed previously, is the product of the integration of the Lisflood-FP 2D hydrodynamic flow model (Bates *et al.,* 2010) and the CAESAR geomorphic model (van de Wiel *et al.,* 2007; Coulthard *et al.,* 2013). This has created a hydrodynamic landscape evolution model which is able to simulate processes at either the catchment or reach scale. Only the reach scale mode was used in this research. For both scales the model involves the specification of several input parameters. These include elevation, grain sizes and rainfall (catchment mode), or a flow input (reach mode). The initial topography of the landscape drives fluvial processes that determine the spatial distributions of these processes that occur at a specified time step. CAESAR-Lisflood can produce a number of calculations within a simulation and these may be chosen by the user. These are saved in a text format that can be converted easily to be read in ArcGIS.

CAESAR-LISFLOOD PARAMETERS

The input parameters for CAESAR-Lisflood at the reach scale are:

- A Digital Terrain Model data file, which was derived from topographical surveys carried out in the field combined with 10 meter contour data of slopes adjacent to the wetland. This resulted in a suitable resolution DTM of the wetland. Different cell sizes of the DTM were explored in order to understand the effect of varying cell sizes on the results of the model.

- Under the numerical tab (Figure 18) within the software: max number of iterations, the minimum time step, the maximum time step and maximum run duration were specified.
- Under the hydrology tab (Figure 18) the discharge data file is specified, the inputs from this file were spread across a number of cells within the DTM to more accurately represent the input of flow to the wetland.
- In the flow model tab, the input/output difference and minimum discharge for depth calculation were indicated following the advice from the manual.

It must be noted that there are many input parameters within CAESAR-Lisflood that can be defined/modified according to the users' needs or to suit different circumstances. All the parameters explained above are inputs that were adjusted for this research. The remaining input parameters were set up according to the user manual and were not varied for this study.

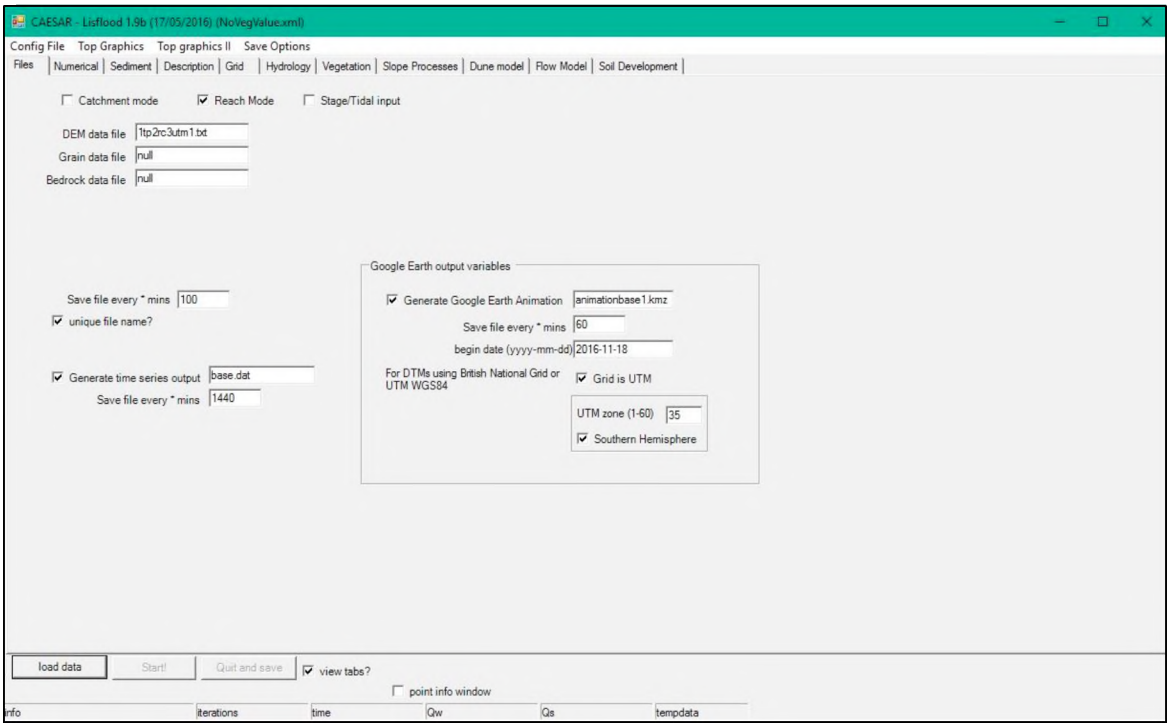

Figure 18: The start-up page of CAESAR-Lisflood

4.3.4 HEC-RAS

TOOL DESCRIPTION

HEC-RAS was established and is distributed by the United States Army Corps of Engineers. It is an open source hydraulic analysis model. The software includes a graphical user interface, separate hydraulic analysis components, data storage and management capabilities, and graphics and reporting services. HEC-RAS is a one-dimensional program that has four river analysis components.

These are steady flow simulations, unsteady flow simulations, sediment transport computations and water quality analysis. Furthermore, the software comprises a number of hydraulic design features that can be used once water surface profiles are calculated.

HEC-RAS PARAMETERS

HEC-RAS uses a number of input parameters for hydraulic analysis of the stream channel geometry and water flow. These parameters are used to establish a series of cross-sections along the stream. In each cross-section, the locations of the stream banks are identified and used to divide into segments, the left floodplain, main channel, and right floodplain (Figure 19). HEC-RAS subdivides the cross-sections in this manner, to account for variances in hydraulic parameters. This subdivision allows control over parameters of the channel and floodplain, such as roughness values.

At each cross-section, HEC-RAS uses several input parameters to describe channel and floodplain geometry, elevation, and relative location along the stream (Figure 19):

- River station (cross-section) number, starting at the most upstream section.
- Lateral and elevation coordinates for each (dry, unflooded) terrain point.
- Left and right bank station locations.
- Reach lengths between the left floodplain, stream centerline, and right floodplain of adjacent cross-sections. The three reach lengths represent the average flow path through each segment of the cross-section pair. The three reach lengths between adjacent cross-sections may differ in magnitude due to bends in the stream.
- Manning's roughness coefficients.
- Channel contraction and expansion coefficients.
- Geometric description of any hydraulic structures, such as bridges, culverts, and weirs.
- Geographic coordinates can be entered for the topographic points and stream line.

After defining the stream geometry, flow values for each reach within the river system are entered. One can choose from either a steady flow or unsteady flow analysis. In this research steady flow analysis was used. Steady flow describes conditions in which, if discharge is constant, depth and velocity at a given channel location does not change with time. Gradually varied flow is characterised by minor changes in water depth and velocity from cross-section to cross-section. The primary procedure used by HEC-RAS to compute water surface profiles assumes a steady, gradually varied flow scenario, and is called the direct step method. The channel geometric description and flow rate values are the primary model inputs for the hydraulic simulations.

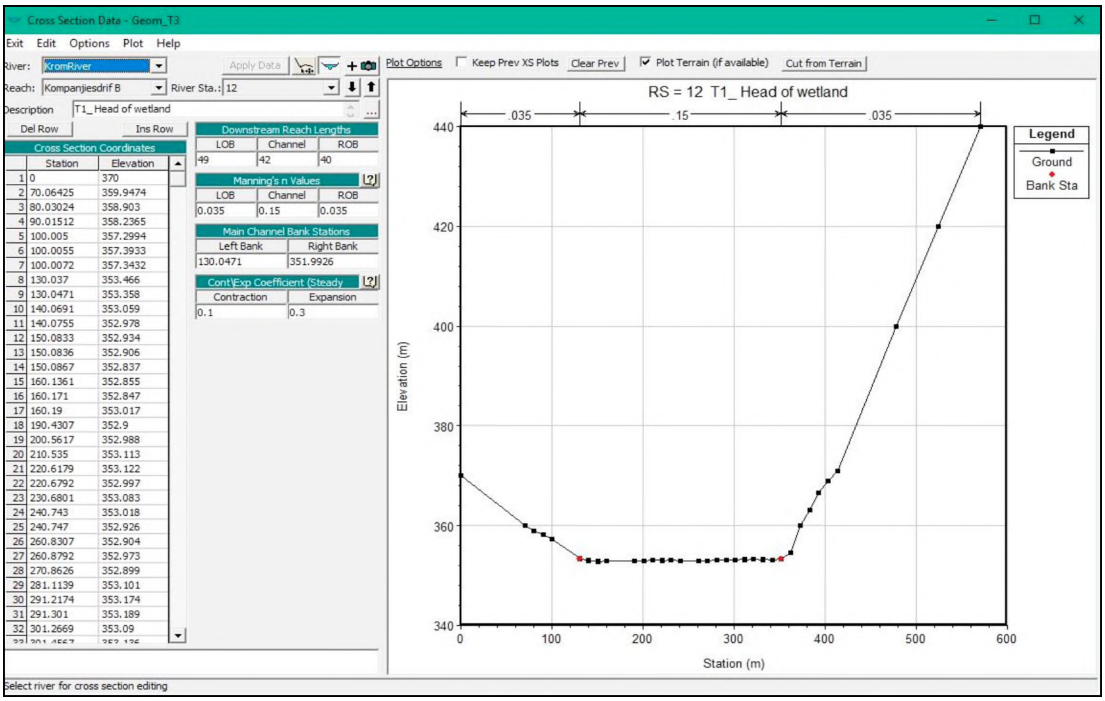

Figure 19: HEC-RAS set-up

4.3.5 CAESAR-LISFLOOD MODELLING

THE SENSITIVITY OF THE MODEL

In order to understand the sensitivity of CAESAR-Lisflood a number of models were run changing certain parameters, such as Manning's roughness coefficient and cell resolution of the Digital Terrain Model. This is important because reduced complexity models, like CAESAR-Lisflood, are inherently sensitive to cell size and roughness coefficient.

ROUGHNESS COEFFICIENT

In the consideration of varying roughness coefficients, a number of models were run in which all parameters were kept constant, except the roughness coefficient. In these simulations, section 5.2, a cell size of 20 by 20 meters was used in order to speed up the simulation time. A discharge of 55 $m^3.s^{-1}$ was used in all simulations. Peak discharges that could occur within the Kompanjiesdrif basin were calculated. It is important to note when a flood of 55 $m^3.s^{-1}$ is spread over a relatively flat, rough surface, the depth-averaged velocities are not likely to be high. Likewise, in reality there are flow paths that are much smaller than the grid cell size (in this case 20 x 20 meters) that will have much higher velocities; however these velocities are smoothed out as they are averaged across the cell area.

Roughness coefficient values affect the water surface profile, velocity and velocity distribution of the simulation. Wide ranges of Manning's n values were used to represent a number of possible water surface elevations, and simulated velocities within the range of uncertainty associated with estimated n values. The Manning's roughness coefficients considered in this study were 0.035, 0.055, 0.075, 0.095, 0.115, 0.135 and 0.155. These ranges of roughness coefficients are considered to be within range for a natural wetland (Table 3). For each run, the effects of various Manning's roughness coefficients on water depths and velocities were analysed, while keeping the other input parameters constant.

Table 3: Manning's roughness coefficient 'n' for natural channels (Chow, 1959)

Manning's n roughness coefficient			
Type of channel and description	**Minimum**	**Normal**	**Maximum**
Natural streams			
Main channels			
A. clean, straight, full stage, no rifts or deep pools	0.025	0.03	0.033
B. same as above, but more stones and weeds	0.03	0.035	0.04
C. clean, winding, some pools and shoals	0.033	0.04	0.045
D. same as above, but some weeds and stones	0.035	0.045	0.05
E. same as above, lower stages, more ineffective slope and sections	0.04	0.048	0.055
F. same as "d" with more stones	0.045	0.05	0.06
G. sluggish reaches, weedy, deep pools	0.05	0.07	0.08
H. very weedy reaches, deep pools, or floodway's with heavy stand of timber and underbrush	0.075	0.1	0.15

CELL SIZE

Grid cell resolution (cell size) is an important aspect that needs to be understood within hydrodynamic simulations. Results such as water depth and velocities are inherently linked to the topographic data of the Digital Terrain Model (DTM) that the model is built on. The raster cell size (resolution), therefore, affects the simulation results (water depth, velocities and velocity distributions). Another aspect to consider is that the overall file size of each grid dataset is directly related to the size of the grid cells selected. For example, the decision to use a 1 meter resolution grid as opposed to a 3 meter resolution grid will approximately increase the file size on disk by a factor of 9 (nine, 1 x 1 meter grid cells can fit within one 3 x 3 meter grid cell). This affects simulation time and is assumed to have little benefit in improving the accuracy of the simulation results.

Three cell resolutions were used to analyse the sensitivity of the simulations to cell size. The cell sizes selected were 5 x 5 meter, 10 x 10 meter and 20 x 20 meter resolutions. Water depth, velocities and velocity distributions were analysed for each of the cell sizes to determine the uncertainty and stability associated with the DTM resolution. Results were also compared with the simulation time of each run of the model in order to choose a DTM resolution to be used in further analysis. For each run, the effects of various cell resolutions on water depths, velocities, velocity distributions and simulation time were analysed while keeping the other input parameters constant. A smaller cell size needed a greater amount of pre-processing as any sinks or lumps (inconsistencies) within the DTM would have an effect on the simulated results.

4.3.6 HEC-RAS MODELLING

THE SENSITIVITY OF THE MODEL: ROUGHNESS COEFFICIENT

In order to understand the sensitivity of HEC-RAS a number of models were run, changing Manning's roughness coefficient. This is important because HEC-RAS, a one-dimensional hydraulic analysis model, uses the Manning's equation to compute flows and water levels. In this application, roughness coefficients did not vary horizontally across individual cross-sections or down the length of the wetland. However, separate simulations were run where the Manning's input parameter was varied. The Manning's roughness coefficients considered in this study were 0.035, 0.055, 0.075, 0.095, 0.115, and 0.155 respectively, and matched the values used in the CAESAR-Lisflood simulations, all these simulation results can be found in section 5.2. The results are presented for one cross-section with the same input parameters such as slope (0.14 %) and discharge (55 $m^3.s^{-1}$). Independent variables, such as top width, maximum depth, average velocity, stream power and shear stress are affected by the roughness coefficient in hydraulic analysis. A statistical analysis was conducted between the roughness coefficient and the independent variables in order to understand the sensitivity of HEC-RAS to varying roughness coefficient values.

4.3.7 EFFECTS OF VALLEY CONFINMENT

In order to understand what happens to surface water hydraulic characteristics (water depth, wetted extent, velocity and velocity distribution) from a wide to a narrow valley as discharge increases, simulations were performed whereby models were run varying only discharge while all other input parameters were kept constant. In these simulations a cell size of 20 x 20 meter and a Manning's roughness coefficient of 0.035 were used in order to speed up the simulation time. Discharges used in this analysis were 5, 30, 50, 70, 90, 100, 150, 200, 250 and 300 $m^3.s^{-1}$. In the HEC-

RAS software cross-sectional data and the same parameters as CAESAR-Lisflood were used as input. The analysis of the simulations concentrated on the velocity distribution and water depth at the contact where the large alluvial fan enters the system at the toe of the wetland, as depicted by the black circle in the Figure 20. In order to explore the differences between a simplified two-dimensional model and a one-dimensional hydraulic analysis model, both software packages, CAESAR-Lisflood and HEC-RAS, were used.

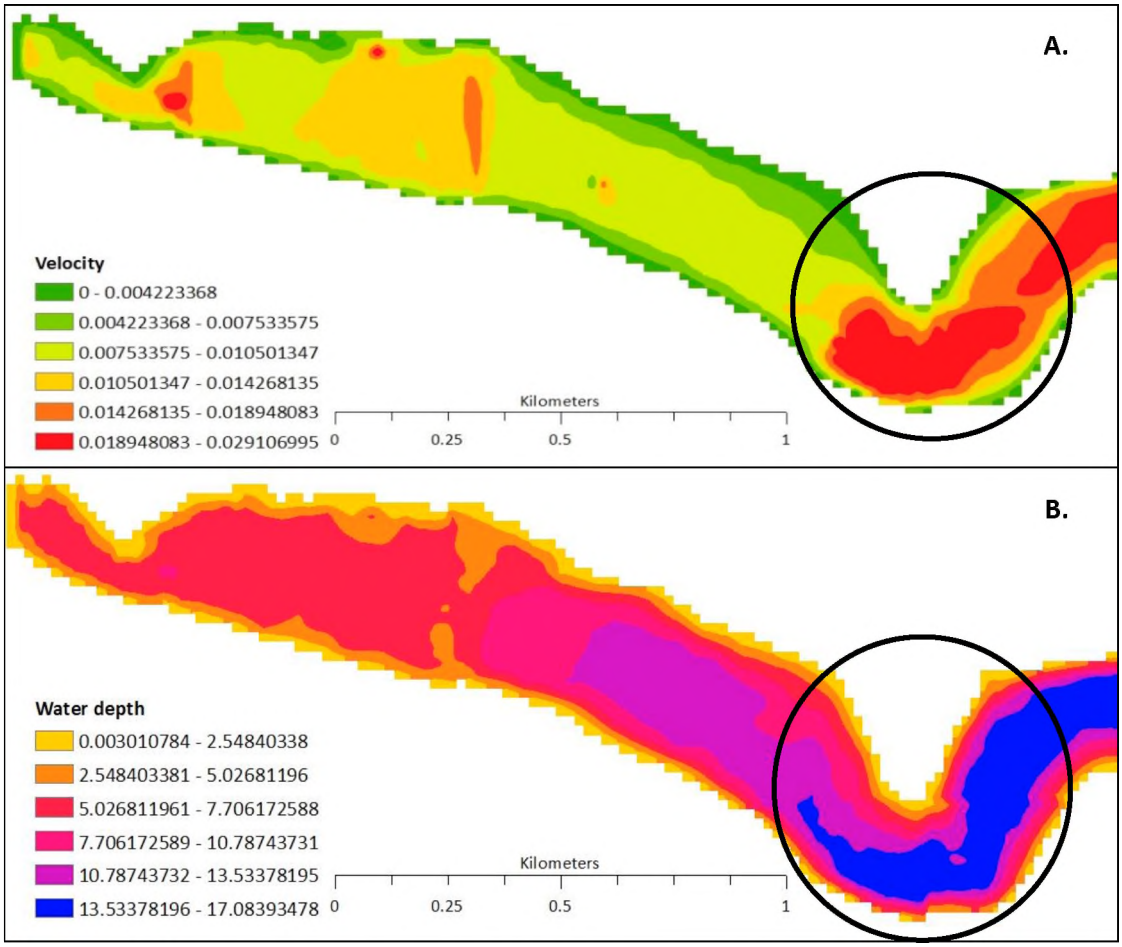

Figure 20: Black circles indicating the area of concentrated changes in hydraulic features due to an alluvial fan encroaching on the wetland

4.3.8 SLOPE VERSUS WIDTH

In order to obtain a relationship between width (confinement), water depth, velocity (as a function of slope), and discharge simulations using HEC-RAS were run through six cross-sections. Three examples of broad cross-sections (Transect 1, 2 and 3) and three examples of narrow cross-sections (Transect 4, 5 and 6) were used. The input parameters included the range of discharges described in the section above and a constant Manning's roughness value of 0.035. Simulations were run in

which the longitudinal slopes were varied. A study conducted on reaches within the Krom River system found slopes ranging from 0.15 to 5 % (Hermon, 2014). Thus, in this analysis the slopes that were used were 0.15, 0.25, 0.5, 1, 2, 3, 4 and 5 %.

4.3.9 CALIBRATION APPROACH

The goal of this research was to understand the changes in key hydraulic properties (flow velocity, water depth and stream power) of a wetland that has been confined by a large impinging tributary alluvial fan when discharges of different magnitude were simulated. This was done in order to understand the initiation of erosional gullies within the wetland. This was accomplished in HEC-RAS by setting up a hydraulic model which is able to simulate the hydraulic responses with varying discharge along cross-sections down the length of the wetland with reasonable accuracy. In CAESAR-Lisflood this was executed by setting up hydrodynamic simulations so as to understand the hydraulic responses with varying discharge magnitudes down the length of the wetland in two-dimensions. In order to calibrate the results of the simulations different discharges were measured in the field and this was connected to a measured wetted extent. The key parameter that was varied in the calibration process was the roughness coefficient, known as Manning's 'n'. However other parameters can also be varied such as boundary conditions. In this study only Manning's 'n' values were generalised across the wetland (the "channel") and floodplain surfaces. Generalised values make the calibration process easier and quicker. Changes were made to the channel 'n' values until a known water surface or wetted extent was reached. However, the changes to the 'n' values must represent (or near enough) a natural system. It is pertinent to remember that modelling in CAESAR-Lisflood is not suited to replicate exact values that would be found in the natural environment, or to determine point velocity values. Since this study evaluates relative values for a given flow regime, this software was deemed adequate.

CHAPTER FIVE: RESULTS

This chapter is presented in two sections. The first assesses the characteristics of the Krom River and the Kompanjiesdrif basin in particular. It also explores parameters that formed part of the model simulations. The second component analyses the results from the simulation runs with CAESAR-Lisflood and HEC-RAS, in relation to the hydraulic features that are associated with gully initiation within the wetland.

5.1 INPUT PARAMETERS

5.1.1 LONGITUDINAL CHARACTERISTICS OF THE KROM RIVER AND KOMPANJIESDRIF BASIN

Figure 21 A shows the longitudinal profile of the Krom River beginning at an elevation of approximately 1 060 m.a.s.l and terminating at the head of the Churchill Dam at 160 m.a.s.l. The Krom River had a longitudinal form that was approximately logarithmic, with steep headwaters and with a slope that gradually declined in a downstream direction. There was distinct steepening of the slope at approximately 6 000 to 9 000 m from the top of the profile (4.3 %), which may be related to the underlying lithologies as the Baviaanskloof, Skurweberg and Goudini Formations, which are quartzitic sandstones, are known to be relatively erosion-resistant (Figure 21 B).

A number of tributaries entered the Krom River, from both the north and the south banks, approximately 10 000 m downstream of the head of the Krom River (Figure 21 A). These originated within the surrounding quartzitic sandstone mountain ranges and were non-perennial tributaries.

From approximately 10 000 m along the profile in Figure 21 A, the slope of the Krom River was remarkably uniform, with a slightly steeper upper zone from approximately 10 000 m to 20 000 m along the profile (0.82 %), and a more gently sloping lower zone downstream of approximately 20 000 m to the head of the Churchill Dam (0.44 %). The Kompanjiesdrif basin occurs in the upper of these zones, covering a distance from approximately 14 000 m to 16 000 m along the profile.

There were a small number of locally elevated zones along the profile that were co-incidental with the confluence of tributary streams with the Krom River, most notably at about 32 000 m from the head of the Krom River. These are likely to reflect depositional features such as tributary alluvial fans impinging on the Krom River (Figure 21 A).

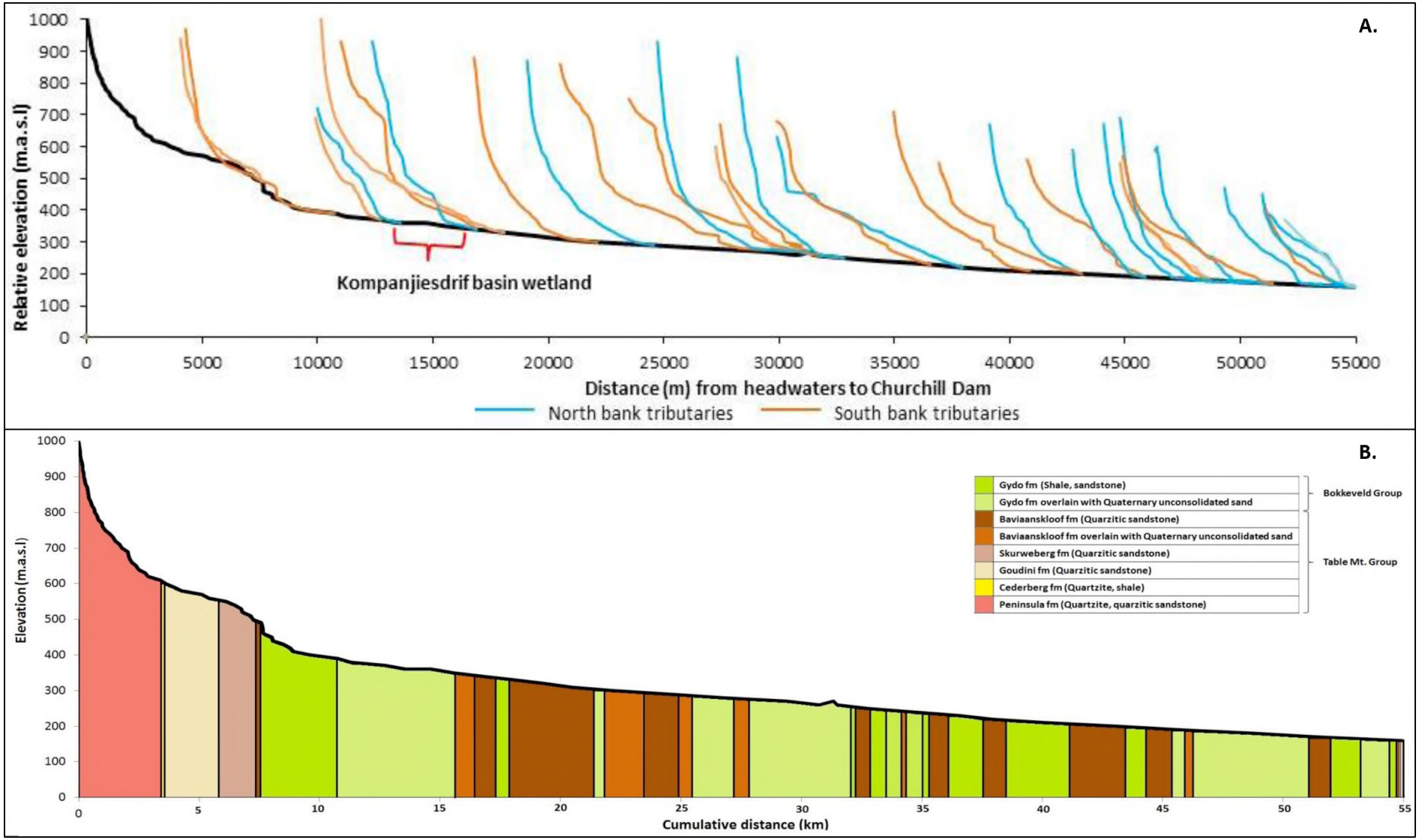

Figure 21: Longitudinal profile of the Krom River, from the headwaters to Churchill Dam, with major tributaries (A) superimposed on the major geological formations (B)

According to Ellery *et al.* (2009), a wetland's vulnerability to erosion is linked to the relationship between the slope of the wetland and the wetland size. It was discovered that wetlands with steep slopes for their size were incised, whereas the opposite was true for wetlands with shallow slopes for their size. Therefore, it is crucial to consider the longitudinal slope in relation to a wetlands size in order to understand whether or not a certain wetland has an inherent propensity to erode. In Figure 22 below, it can be seen that the Krom River wetland complex (0.77 %) falls in the vulnerable region of the vulnerability graph.

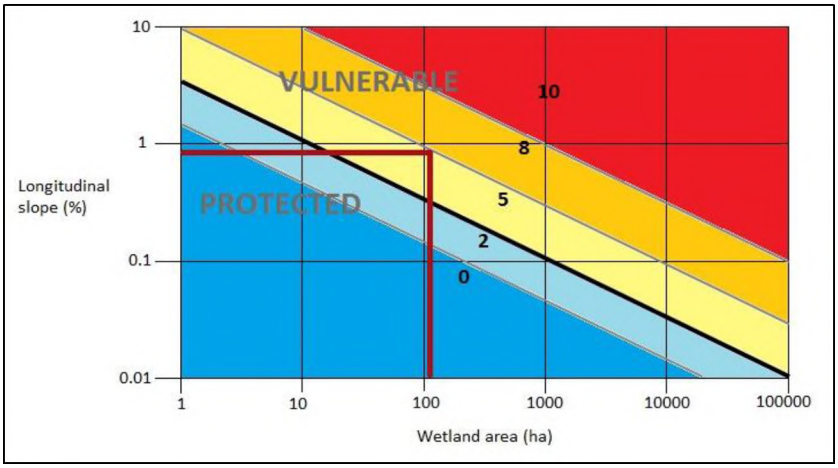

Figure 22: Wetland vulnerability to erosion graph depicting the Krom River wetland complex (red line, Ellery *et al*. 2009)

The Krom River wetland complex is an un-channeled valley bottom palmiet wetland covering an approximate length of 6 km with a longitudinal slope of 0.77 %. The tributaries entering the wetland are illustrated in Figure 23, and show that there was generally a substantial reduction in width of the wetland where large tributary alluvial fans entered the trunk valley. The Kompanjiesdrif basin formed the lower 1.8 km of the wetland and had a slope of 1.05 %, which represents a considerable increase compared to the whole Krom River wetland complex (Figure 24). Examination of the slope of the Krom River wetland complex showed it to be relatively uniform with minor irregularities along its length. These were associated with the introduction of sediment onto the valley floor by tributary alluvial fans that impinged on the trunk valley at a high angle (~90 degrees). This has resulted in the longitudinal slope on the trunk valley to be lowered in an upstream direction by the introduction of tributary alluvial fan sediment and was increased in a downstream direction (Figure 24).

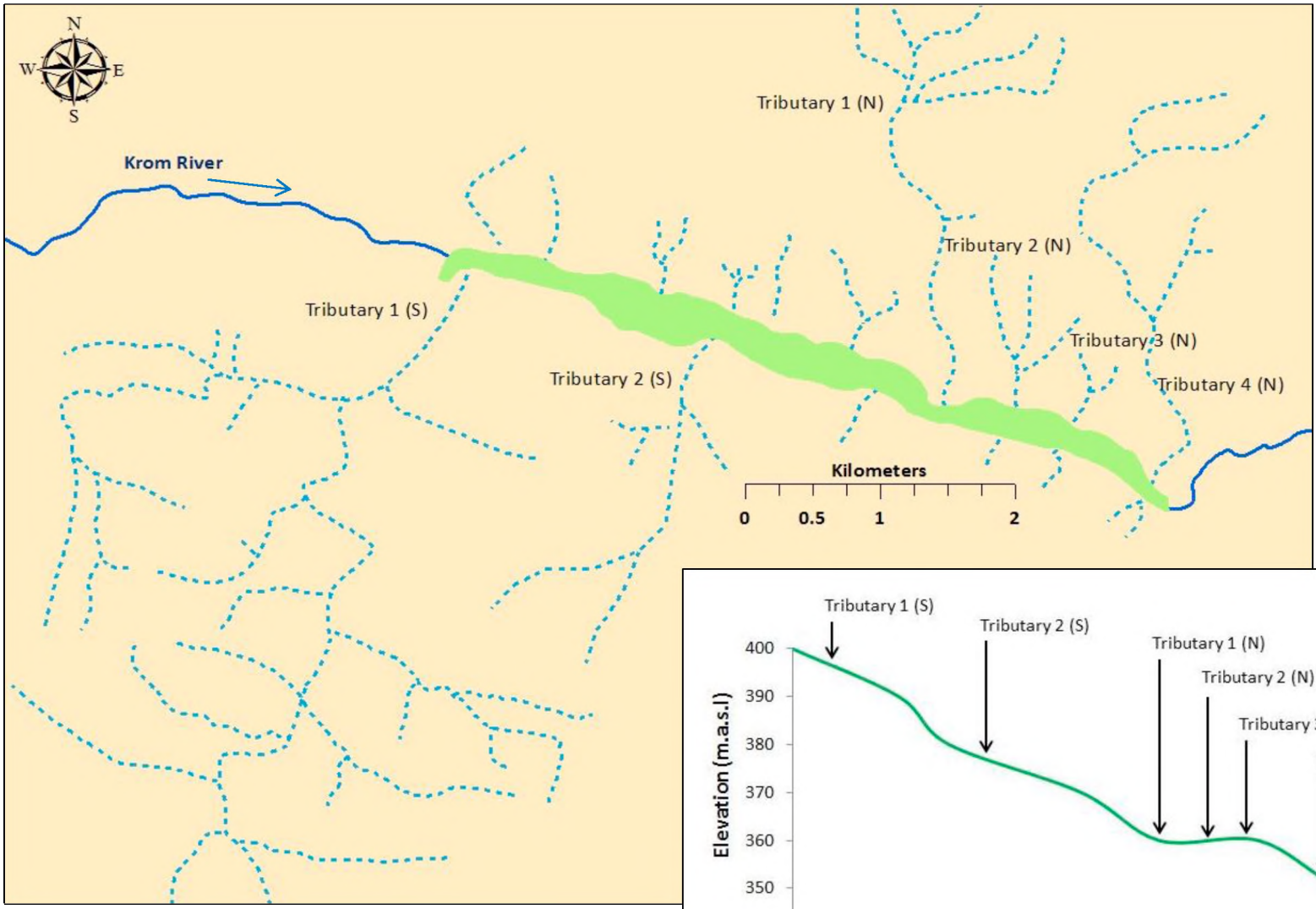

Figure 23: Tributary locations of the Krom River wetland complex

Figure 24: Longitudinal profile of the Krom River wetland complex with the associated major tributaries from the south (right bank) and north (left bank). This data was obtained from orthophotographs with a 5 m contour interval

5.1.2 CROSS-SECTIONAL CHARACTERISTICS OF THE KOMPANJIESDRIF BASIN

The un-channeled palmiet wetland occupied most of the valley bottom (Figure 25). The valley widened considerably downstream of where the regional road (R67) crossed the Krom River wetland complex at the head of the Kompanjiesdrif basin. The floor of the valley was near-horizontal in cross-section with local relief of less than 1 m over a distance of approximately 250 m. On the left (north) bank the adjacent land surface sloped gently upwards away from the wetland until reaching the foot hills of the Suuranys Mountain range. The land surface to the north of the valley-bottom comprised alluvial fans that were found where tributary streams impinged on the valley floor. The land surface to the south of the floodplain sloped steeply away from the valley bottom to the Tsitsikamma Mountain range. Transects 1 to 6 were positioned, roughly alternating with the peaks and troughs of the alluvial fans encroaching on the valley floor from the north (Figure 25). Transects 7 to 9 were positioned in an area where the valley was confined significantly by a large impinging alluvial fan at the toe of the wetland. Local relief within the wetland was minor and there was a gentle slope downwards from the left (north) to the right (south) of the wetland.

Transects presented in Figure 25 show that at the head of the wetland, the valley floor was approximately 250 m wide (T 1), and continued to widen to 345 m (T 3). Approximately 1 km downstream of the head of the wetland, at T 4, the valley narrowed to 230 m, and varied slightly for the next 500 m. At T 6 the effects of the large impinging alluvial fan became evident. At the toe of the wetland (T 7, T 8 and T 9) the wetland was confined to tens rather than hundreds of meters.

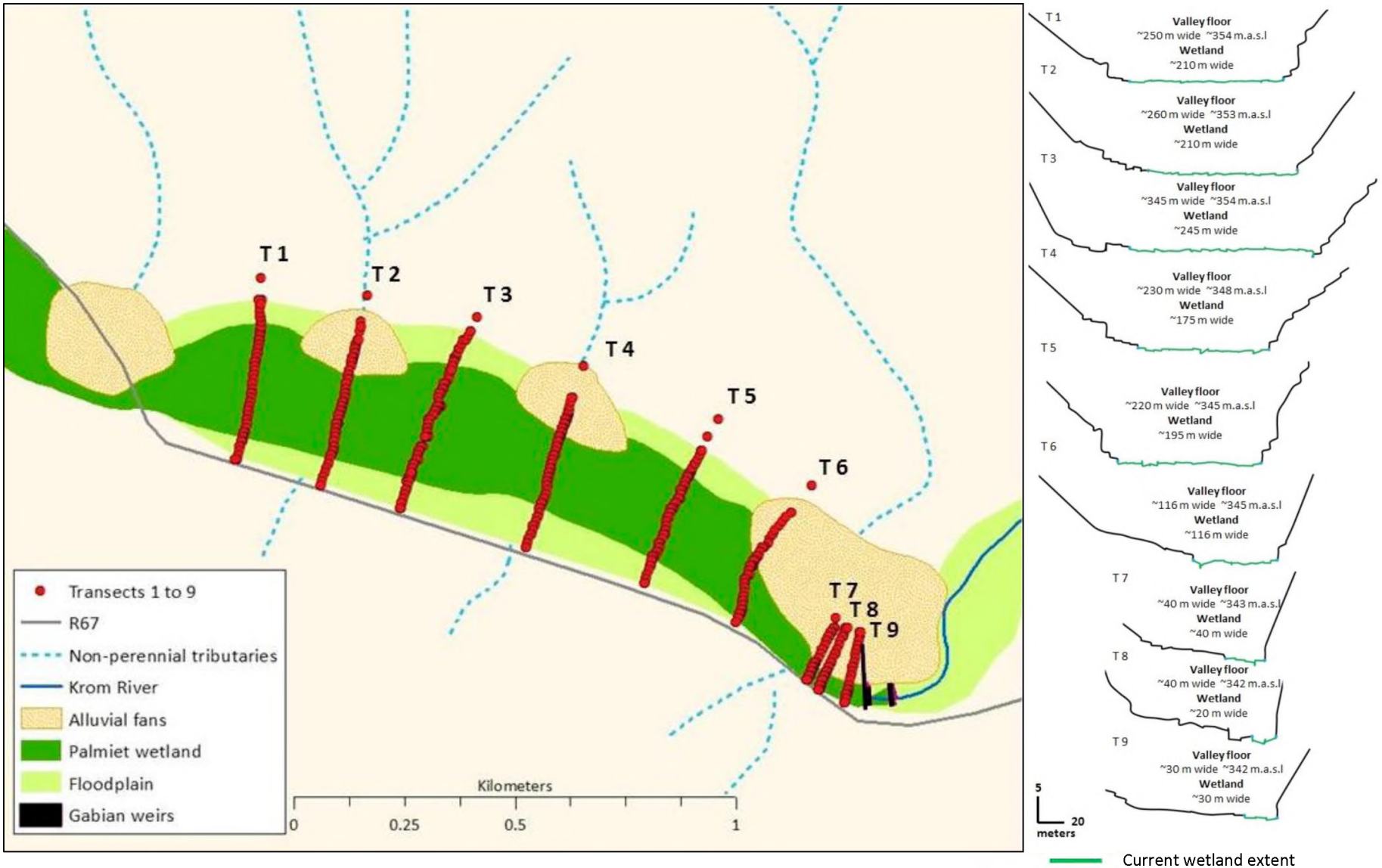

Figure 25: Cross-sectional locations and characteristics of the Kompanjiesdrif basin

5.1.3 VEGETATION SURVEYS

Results from the vegetation surveys are shown in Figure 26. Palmiet (*Prionium serratum*), a tall, rigid and single stemmed plant with palm-like growth form, was dominant in most of the plots and covering almost 50 % of the wetland. The second most dominant species found was *Miscanthus capensis*, a tall tufted, robust grass. The rest of the wetland was made up of a combination of various other functional groups of herbaceous plants as shown in Figure 26.

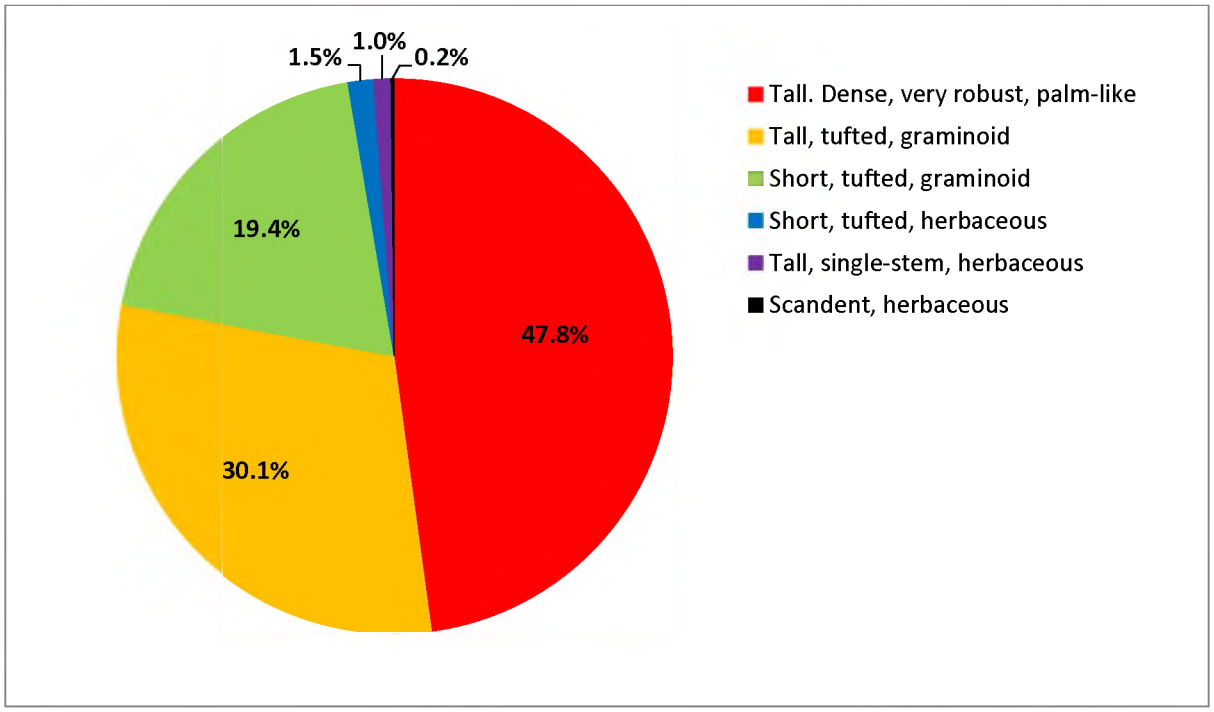

Figure 26: Percentage cover of the Kompanjiesdrif basin of different functional groups of plant

5.1.4 VALLEY FILL PARTICLE SIZE DISTRIBUTION

The results of sediment samples taken along Transects 1 and 2 are shown in Figure 27 and Figure 28 respectively.

In Transect 1 Sediment Samples 1.1 to 1.6 (Figure 27), running from the left to the right bank, showed that 40 % to 60 % of each sample had a particle size ranging from 0.25-0.5 mm (medium sand). In addition to medium sand, coarse sand (0.5-1 mm) and very coarse sand and gravels (>2 mm), made up a larger proportion of the sample at the center of the depositional feature (Sediment Sample 1.2 and 1.3). Fining of sediment occurred progressively outward towards each bank. These sediment samples were mostly composed of fine sand (0.125-0.25 mm) ranging from 20 % to 40 % and less than 10 % very fine sand (0.0625-0.125 mm) and silt and clay (<0.0625 mm; Figure 27).

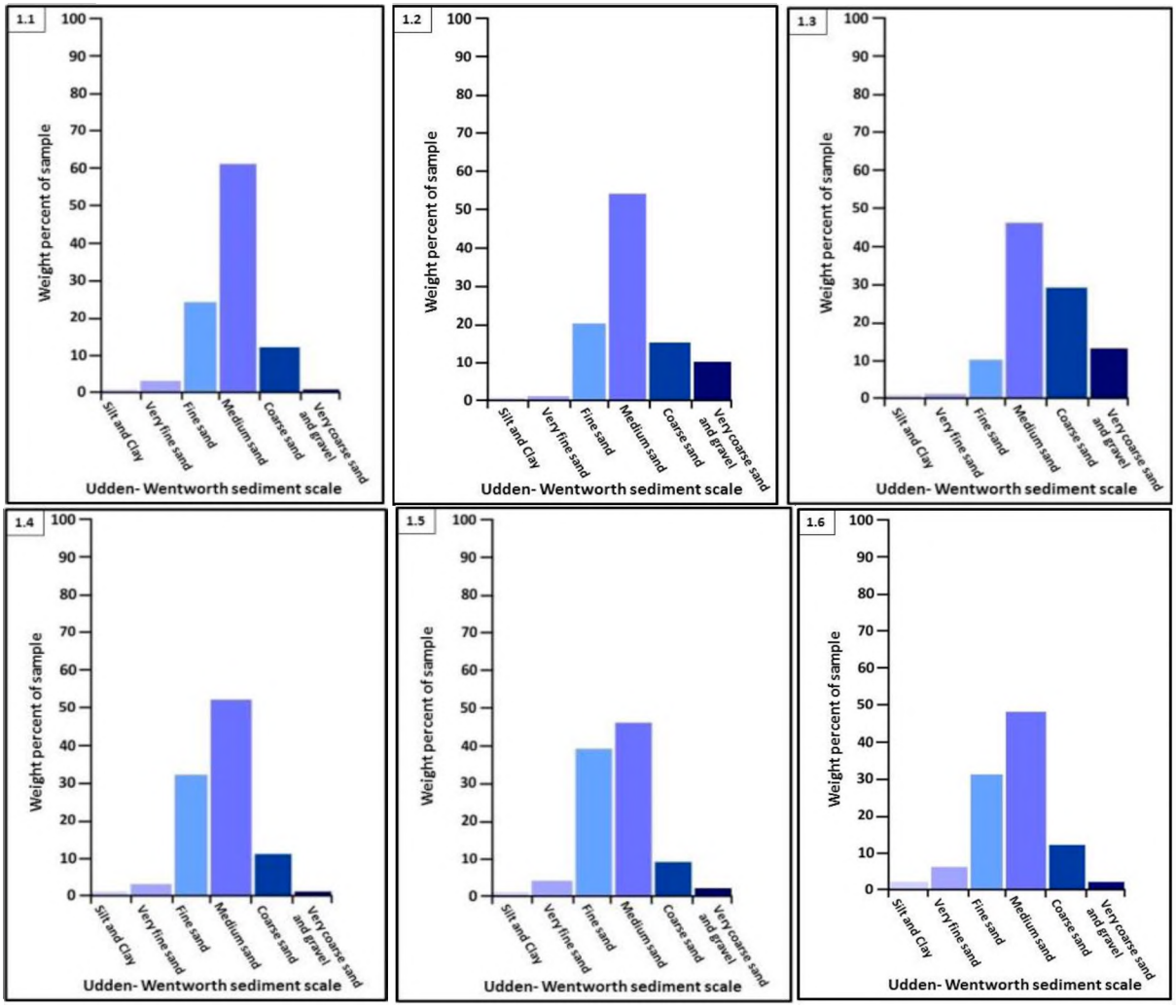

Figure 27: Variation in size class distribution of sediment samples from Transect 1. Samples are at different depths in cores taken in order from left to right bank

Variation in particle size distribution of valley-fill sediments with depth along Transect 2, approximately 50 m downstream from Transect 1, is shown in Figure 28. Similar to Transect 1, medium sand accounts for the greatest percentage (>30 %) of the samples taken in Transect 2. Fine sand accounts for between 20 and 55 % of the Sediment Samples 2.1 to 2.5. Sediment Sample 2.6 showed that less than 10 % of the sample was fine sand and there was a larger proportion of coarse sand and very coarse and gravels (33 and 28 % respectively).

According to Hjulstrom's diagram (Figure 16), velocities of >0.005 $m.s^{-1}$ are needed to entrain and transport the sediment grain sizes found at the study site. Erosion may be initiated when velocities reach above 0.2 $m.s^{-1}$.

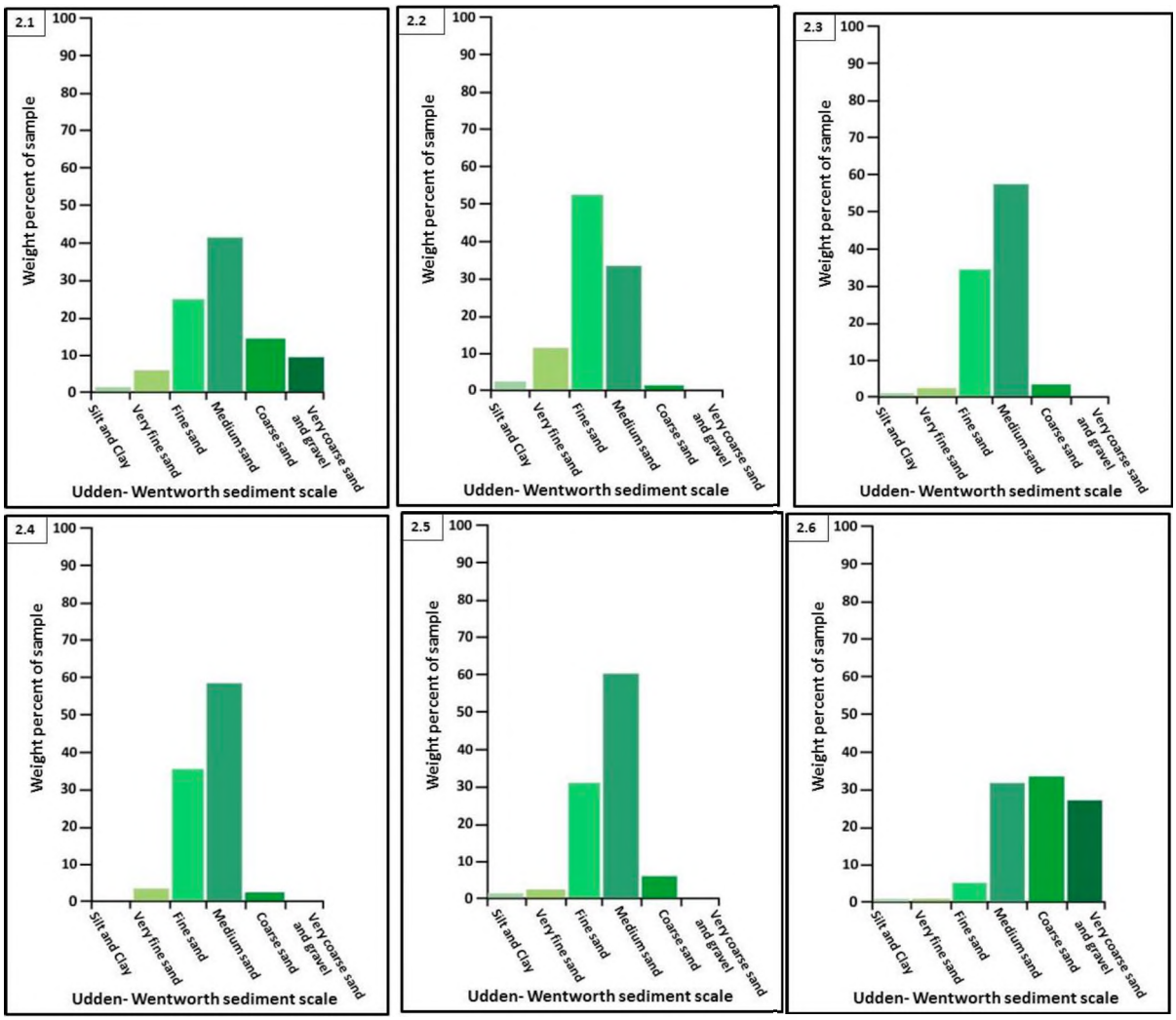

Figure 28: Variation in size class distribution of sediment samples from Transect 2. Samples are at different depths in cores taken in order from left to right bank

5.1.5 FLOW DYNAMICS

This section presents results of the analysis of the flow data for the Krom River Catchment at gauging station K90H001 provided by the Department of Water and Sanitation. This is followed by a site specific analysis for the Kompanjiesdrif basin.

The highest discharge reported over the period from 1955 to 2016 at the gauging station located below Churchill Dam was 617.9 $m^3.s^{-1}$ which occurred in 2006. The mean value for the data set was 0.855 $m^3.s^{-1}$. Median flow from the daily discharges (1970 to 2016) recorded was 0.05 $m^3.s^{-1}$ and the 90th percentile was 0.837 $m^3.s^{-1}$. Very high flows were relatively uncommon such that discharges in the Krom River generally fall below 1 $m^3.s^{-1}$. Peak discharges of over a 100 $m^3.s^{-1}$ occurred for the years of 1981, 1983, 1992, 1996, 2003, 2006, 2007, 2011 and 2012. The data suggests that large

flows of over 100 $m^3.s^{-1}$ are becoming increasingly frequent within the known record, however, this is too short a period to infer long term patterns.

In the Kompanjiesdrif basin peak discharges were calculated for different return periods. The peak discharges calculated for the catchment increased with increasing return periods implying that large flood events are less frequent than smaller ones. The Kompanjiesdrif basin was characterised by both steep, impermeable regions as well as flat, permeable regions, such that the runoff is provided for impermeable and permeable catchment lithologies and soils (Table 4).

Table 4: Peak discharges for different return periods using the Rational Method

Return period (year)	Peak flow ($m^3.s^{-1}$) for steep and impermeable catchment	Peak flow ($m^3.s^{-1}$) for flat and permeable catchment
2	74	52
5	112	79
10	145	112
20	196	148
50	258	225
100	344	344

5.2 MODEL RESULTS

5.2.1 EXPLORING THE SENSITIVITY OF CAESAR-LISFLOOD AND HEC-RAS

VARYING ROUGHNESS COEFFICIENT: CAESAR-LISFLOOD

The simulations shown in Figure 29 illustrate that there were relatively small changes in water depth with varied roughness coefficients for a given flood event size (55 $m^3.s^{-1}$). The highest simulated water depth was 8.3 m which occurred with a Manning's roughness value of 0.055 (Figure 29 B).

Calculated wetted extent for the simulation with a low Manning's roughness value of 0.035 was 0.6304 km^2 and the wetted extent for the simulation with a high Manning's roughness value of 0.155 was 0.6313 km^2. The difference in wetted extent between simulations with the highest and lowest Manning's roughness values was 0.0009 km^2, which again was relatively minor.

Varying Manning's roughness values resulted in relatively small variations in velocity gradients (Figure 31). The range of velocities found in the simulations was from 0 $m.s^{-1}$ to ~ 0.02 $m.s^{-1}$.

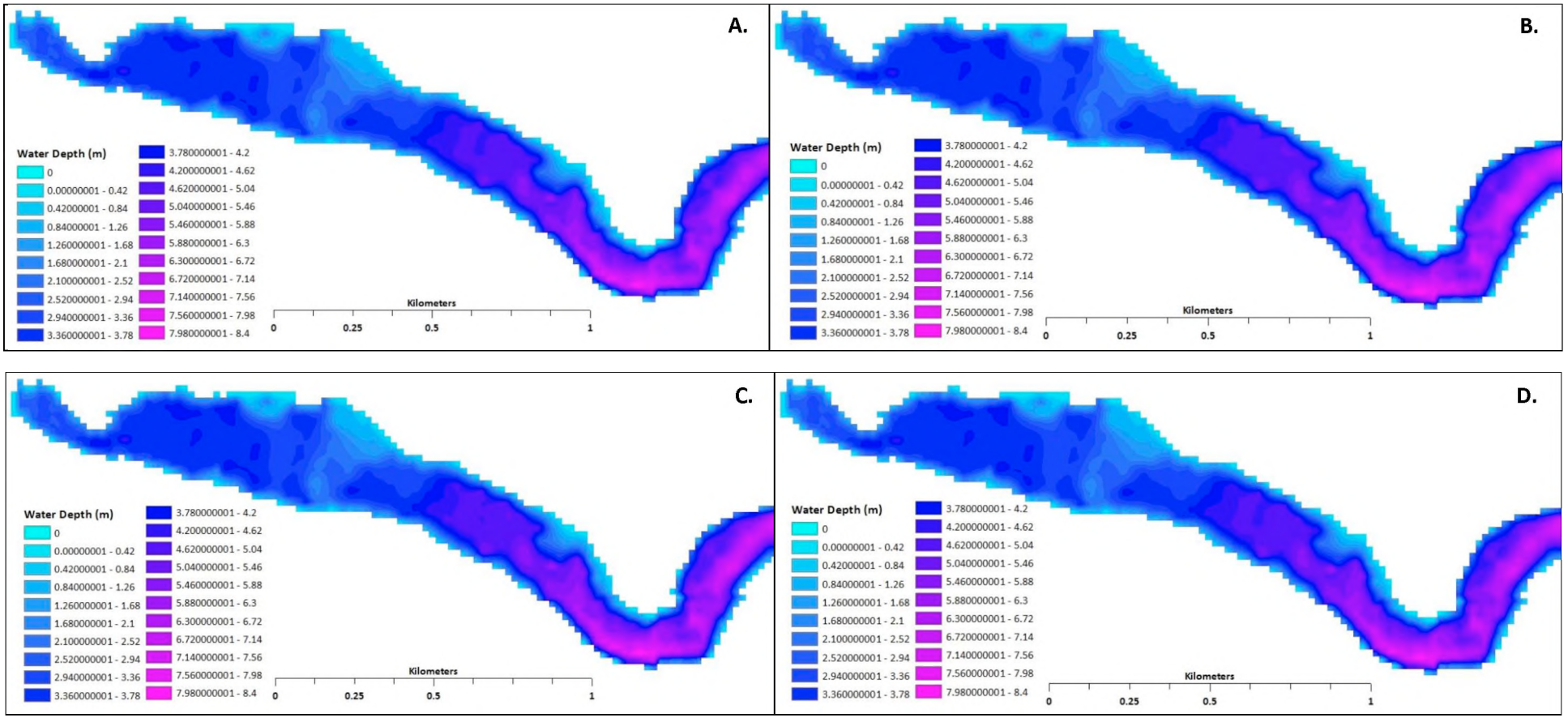
A.
B.
C.
D.
Water Depth (m)
0
0.00000001 - 0.42
0.42000001 - 0.84
0.84000001 - 1.26
1.260000001 - 1.68
1.680000001 - 2.1
2.100000001 - 2.52
2.520000001 - 2.94
2.940000001 - 3.36
3.360000001 - 3.78
3.780000001 - 4.2
4.200000001 - 4.62
4.620000001 - 5.04
5.040000001 - 5.46
5.460000001 - 5.88
5.880000001 - 6.3
6.300000001 - 6.72
6.720000001 - 7.14
7.140000001 - 7.56
7.560000001 - 7.98
7.980000001 - 8.4
Kilometers
0
0.25
0.5
1

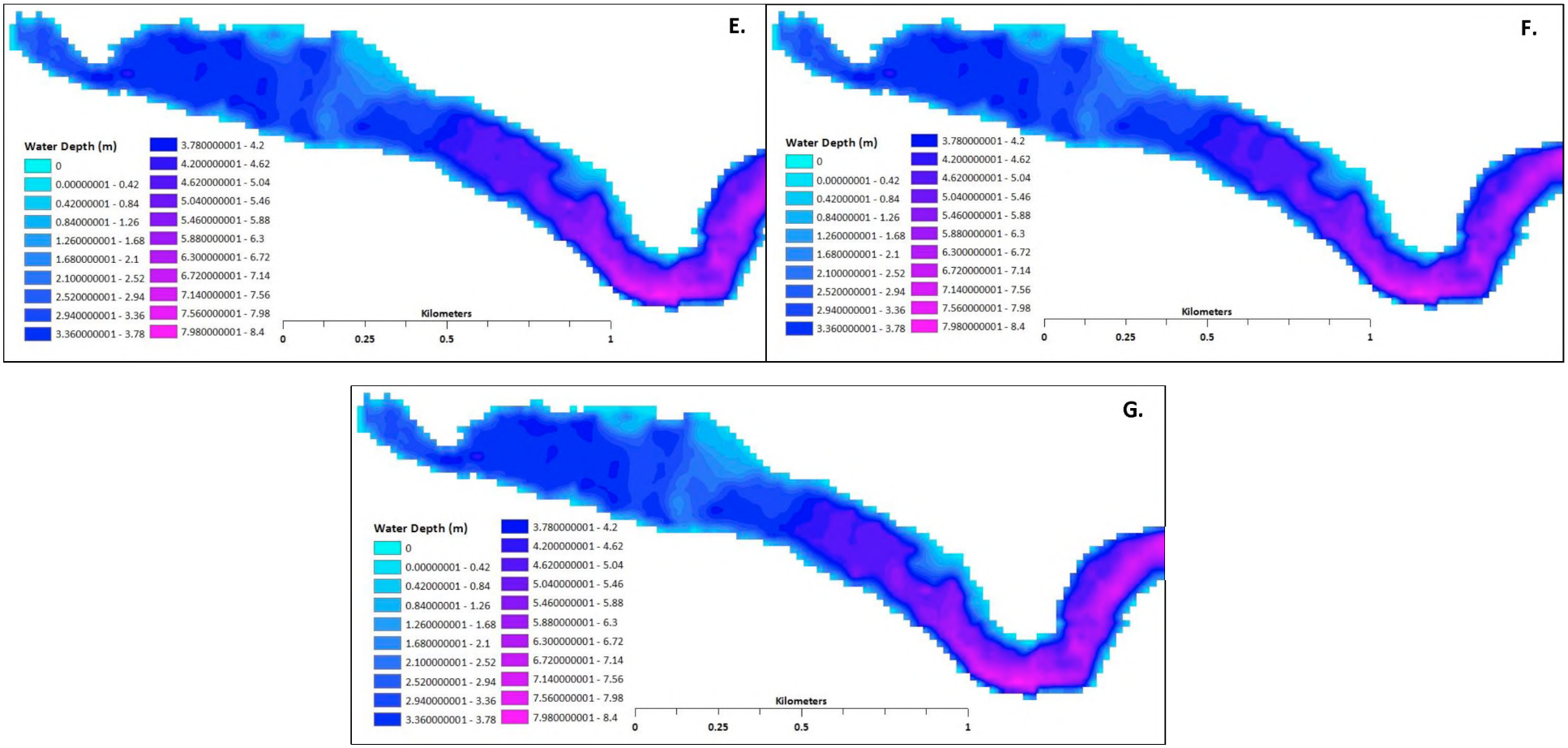

Figure 29: CAESAR-Lisflood simulation of water depth in relation to varying roughness coefficients with 'n' values of 0.035 (A), 0.055 (B), 0.075 (C), 0.095 (D), 0.115 (E), 0.135 (F), and 0.155 (G)

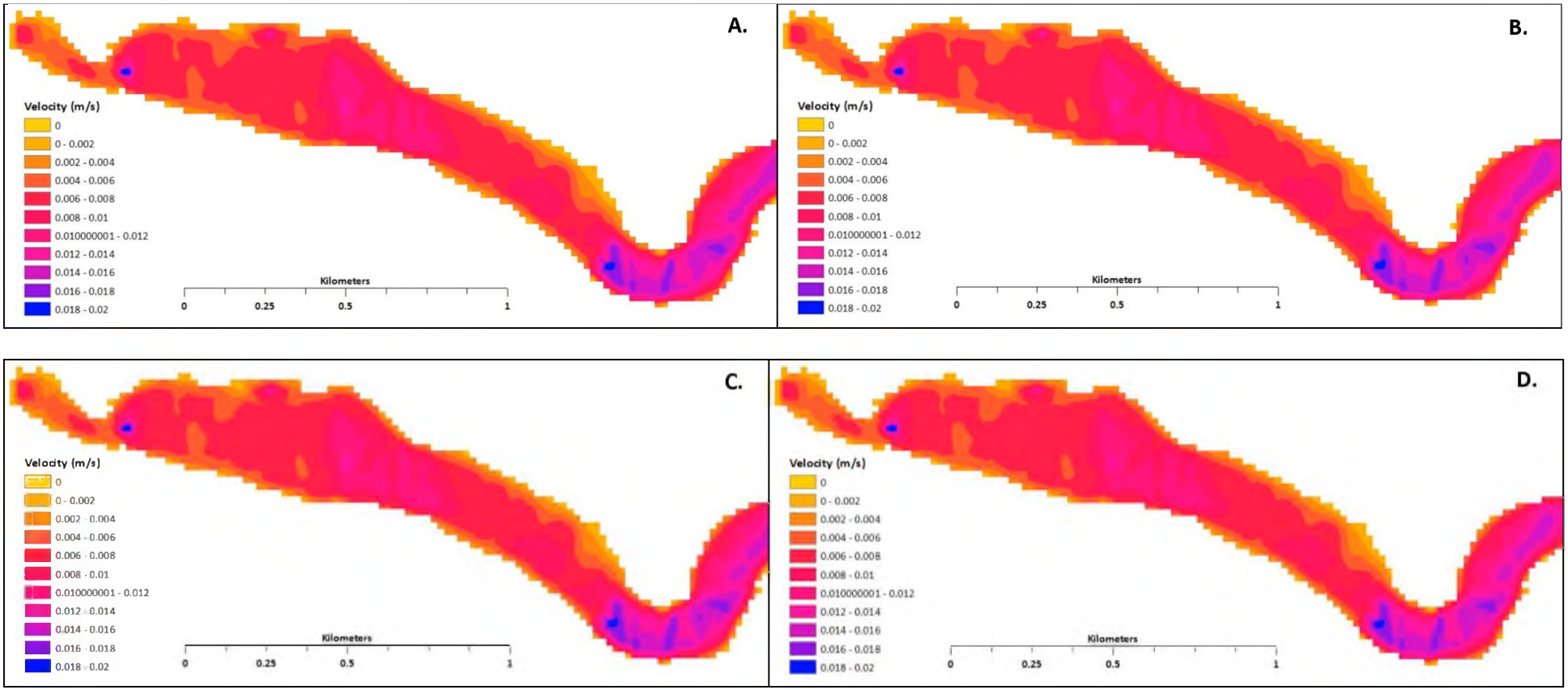
A.
B.
C.
D.
Velocity (m/s)
0
0 - 0.002
0.002 - 0.004
0.004 - 0.006
0.006 - 0.008
0.008 - 0.01
0.010000001 - 0.012
0.012 - 0.014
0.014 - 0.016
0.016 - 0.018
0.018 - 0.02
Kilometers
0
0.25
0.5
1

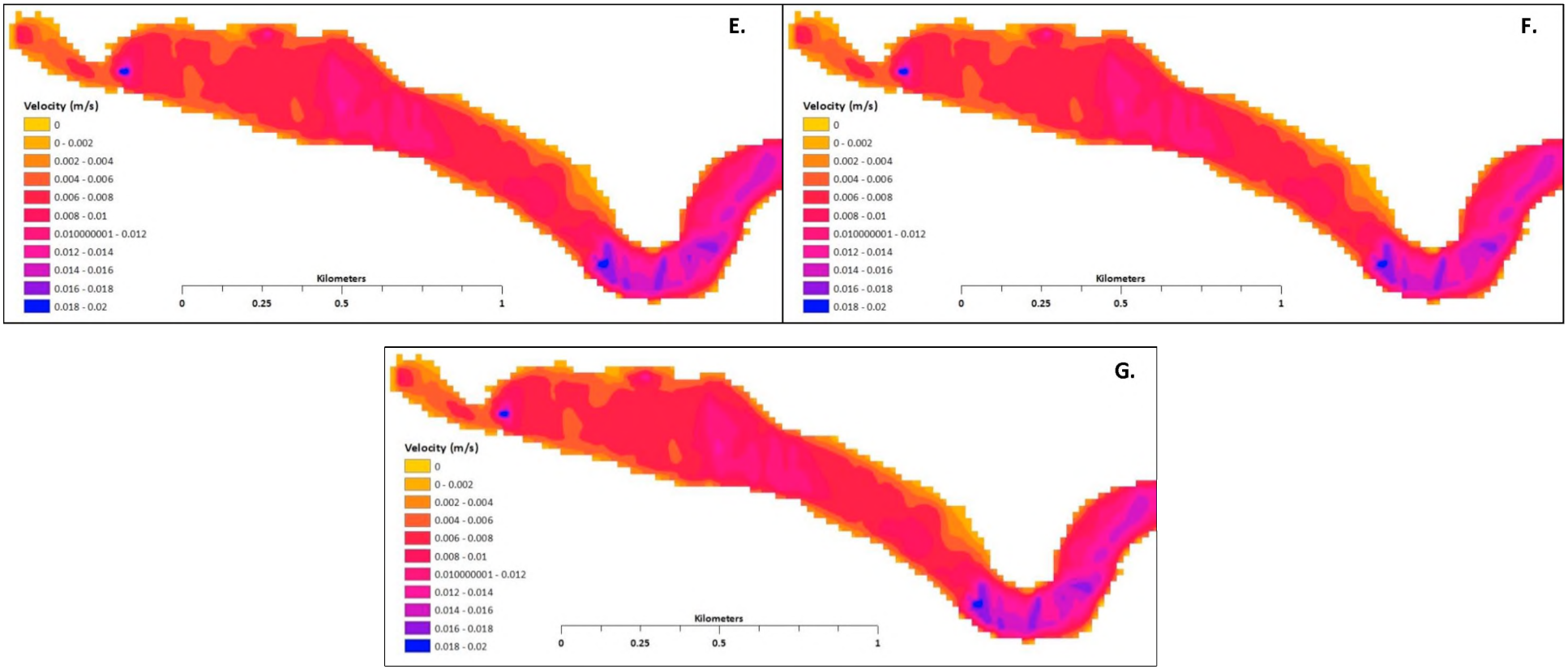

Figure 30: CAESAR-Lisflood simulation of velocity in relation to varying roughness coefficients with 'n' values of 0.035 (A), 0.055 (B), 0.075 (C), 0.095 (D), 0.115 (E), 0.135 (F), and 0.155 (G)

VARYING CELL SIZE: CAESAR-LISFLOOD

For each simulation it was found that the length of time to run each simulation of water depth, velocity and velocity distribution varied greatly with variation in cell size. Furthermore, the resulting average water depth and velocity varied with cell size such that the smaller the cell size the higher both the average velocity and water depth. This was because CAESAR-Lisflood averaged the velocity and water depth over the area covered by the cell. A smaller area took into account more of the values that are found within it. However, simulation time was greatly increased by a smaller cell size, for example one simulation took 36 hours for a DTM with a cell size of 5 m compared to a simulation time of 6 hours for cell size of 10 m and 1.5 hours for cell size of 20 m.

VARYING ROUGHNESS COEFFICIENTS: HEC-RAS

This section presents the analysis for one cross-section (Transect 6) where the Manning's roughness coefficient was changed while all the other parameters were kept constant. The Manning's roughness coefficients used for this analysis were 0.055, 0.075, 0.095, 0.115, 0.135 and 0.155.

Table 5 provides a summary of the simulation results from varying roughness values in HEC-RAS. The data presented shows the width of the cross-section increases with increasing roughness, as does the maximum water depth. However, average velocity and average stream power decline with increasing roughness. Average shear stress increases with increasing roughness.

Based on the analyses presented, significant positive relationships were found between the roughness coefficient and the independent variables, top width, maximum depth and average shear stress (Table 6). Significant negative relationships were evident between the roughness coefficient and the independent variables, average velocity and average stream power.

Table 5: Summary of the simulation results from varying roughness values in HEC-RAS

Transect Number 6						
Roughness coefficient	**Total discharge ($m^3.s^{-1}$)**	**Top width (m)**	**Maximum depth (m)**	**Average velocity ($m^3.s^{-1}$)**	**Average stream power (N.m.s)**	**Average shear stress ($N.m^{-2}$)**
0.055	55	39.25	0.93	2.43	489.61	203.85
0.075	55	42.19	1.05	1.99	478.22	243.25
0.095	55	44.59	1.15	1.72	479.43	282.36
0.115	55	47.15	1.26	1.49	444.50	302.00
0.135	55	49.44	1.36	1.33	419.78	320.96
0.155	55	51.79	1.44	1.21	398.03	334.77
Average	55	45.74	1.2	1.7	451.6	281.2

Table 6: Correlation coefficient and statistical significance of independent variables (channel geometry and hydraulic characteristics) and roughness coefficient (Manning's 'n' value)

Transect Number 6		
Independent variable	**Correlation to roughness coefficient**	**Statistical significance**
Top width (m)	r=0.99	p<0.05
Maximum channel depth (m)	r=0.99	p<0.05
Average velocity ($m.s^{-1}$)	r=-0.97	p<0.05
Average stream power (N.m.s)	r=-0.96	p<0.05
Average shear stress ($N.m^{-2}$)	r=0.97	p<0.05

5.2.2 HYDRAULIC CHARACTERISTICS: CAESAR-LISFLOOD SIMULATIONS

THE EFFECTS OF VARYING DISCHARGE ON WATER DEPTH AND WETTED EXTENT

Figure 31 shows that there was a general trend that as discharge increased there was a corresponding increase in wetted extent and in mean water depth down the length of the wetland.

For example, the largest increase in wetted extent occurred at a discharge of 80 $m^3.s^{-1}$ whereby the wetted extent increased from 0.69 km^2 (at 70 $m^3.s^{-1}$) to 0.81 km^2 (at 80 $m^3.s^{-1}$, Figure 31). The greatest increase in mean water depth also occurred at this discharge whereby it increased from 4.62 m to 7.44 m, Figure 32.

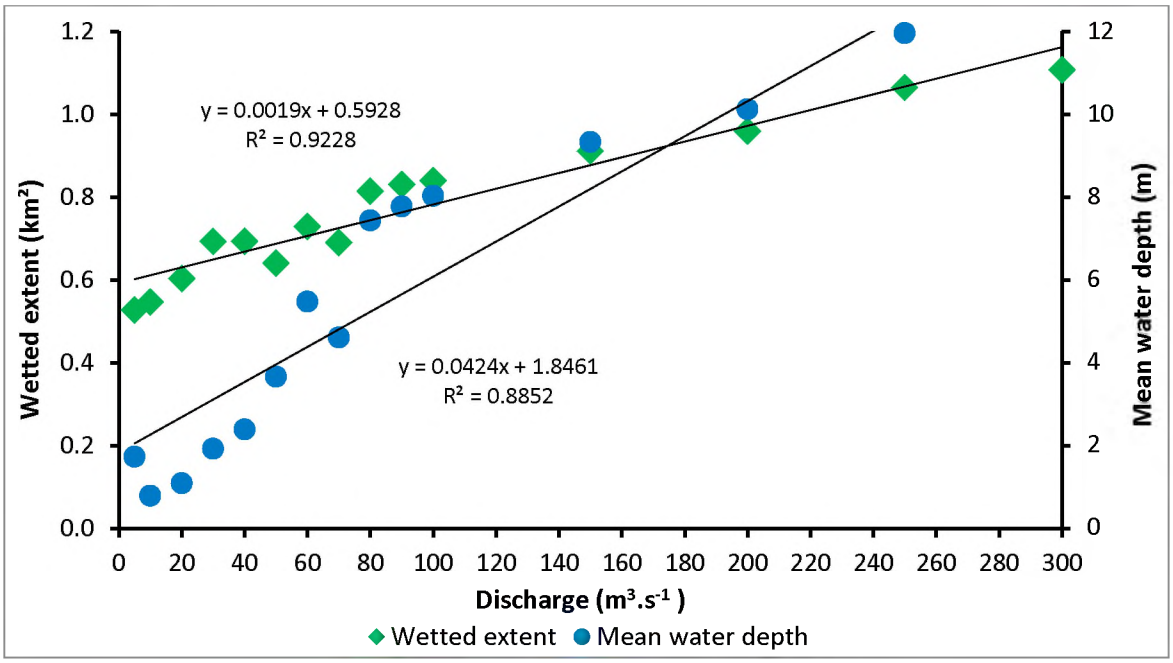

Figure 321: Graph depicting the relationship between wetted extent and mean water depth as discharge is increased

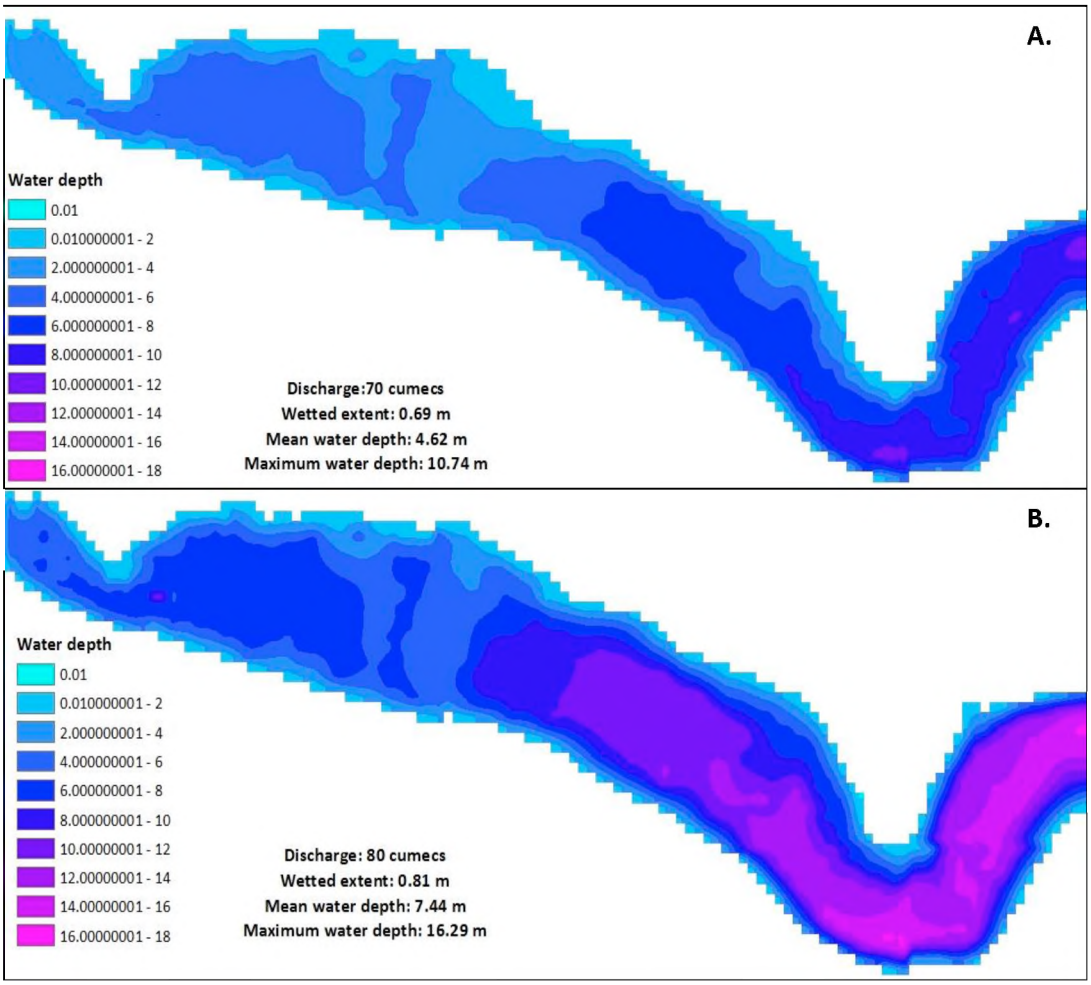

Figure 332: Simulation results showing the greatest difference in wetted extent and water depth between a discharge of 70 $m^3.s^{-1}$ (A) and 80 $m^3.s^{-1}$ (B)

Figure 33 illustrates that there was a general trend as discharge increased there was a corresponding increase in velocity values. Velocity is highly influenced by discharge, cross-sectional form (wetted extent) and water depth; such that the greatest increase in velocity values occurred between a discharge of 70 $m^3.s^{-1}$ (0.022 $m.s^{-1}$) and 80 $m^3.s^{-1}$ (0.029 $m.s^{-1}$, Figure 34).

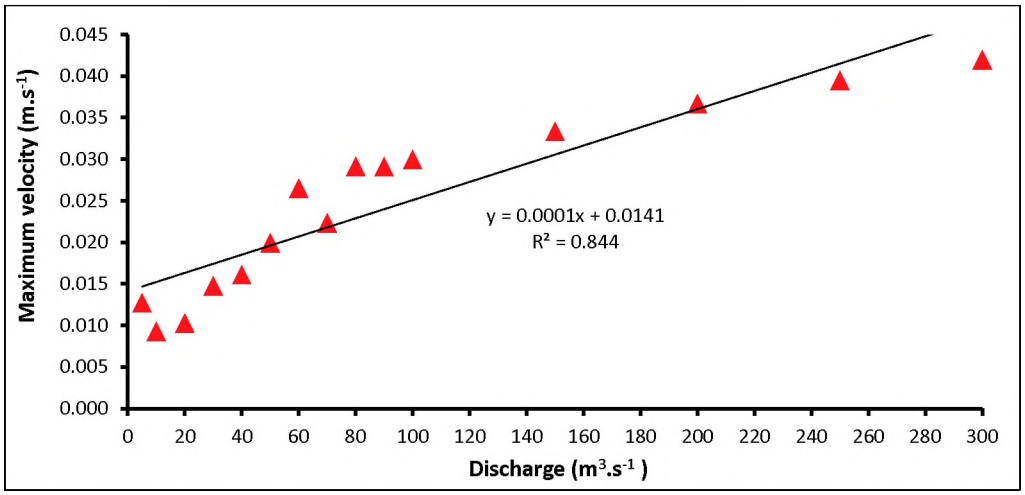

Figure 343: The relationship between discharge and modelled maximum velocity

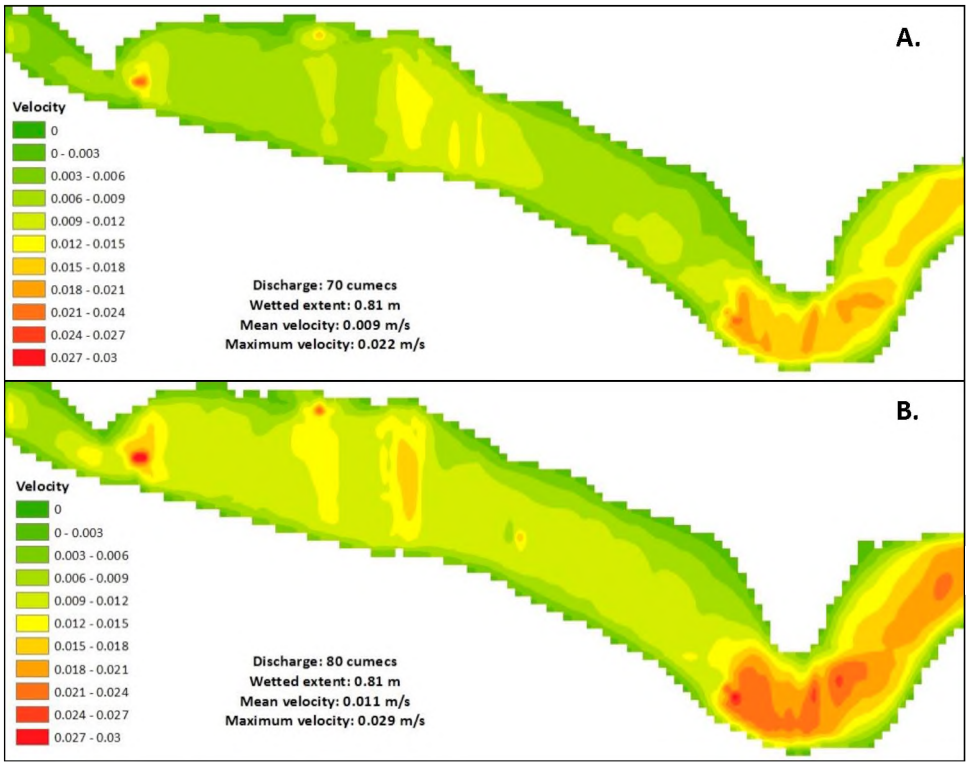

Figure 354: Simulation results showing the greatest difference in velocity between a discharge of 70 $m^3.s^{-1}$ (A) and 80 $m^3.s^{-1}$ (B)

An interesting observation was that from the point of loss of confinement near the head of the wetland there was a small area in the centre of the wetland with very high velocity, and with values decreasing downstream and laterally from the localised zone of high velocity. This corresponds to a zone of high water depth immediately upstream of the zone of high velocity (Figure 35).

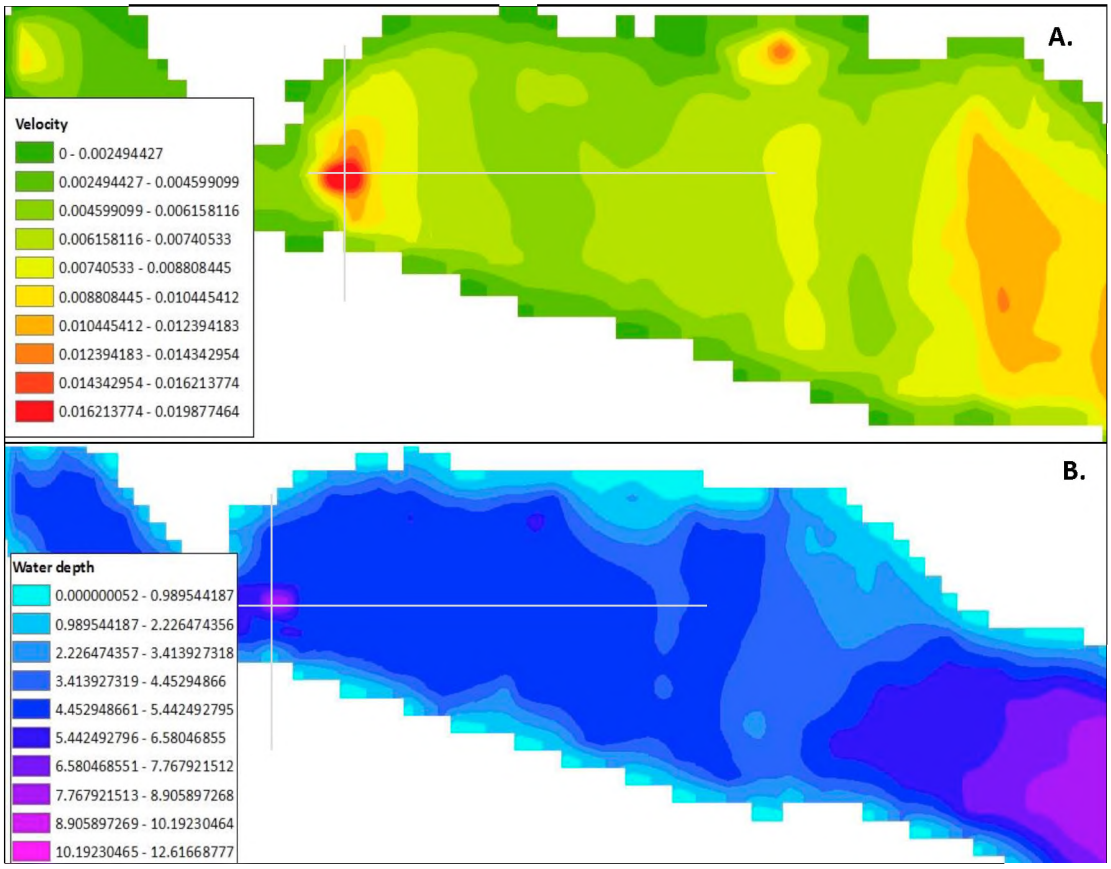

Figure 365: Simulation results illustrating the zone of high velocity and water depth values decreasing downstream and laterally from this point depicted by cross-hair lines

5.2.3 EFFECTS OF VALLEY CONFINEMENT

VARYING DISCHARGE: CAESAR-LISFLOOD

Results of simulations run at different discharges are presented in this section. This provides insight into the way that flooding is accommodated by the valley, and where flows are concentrated in relation to valley form in the Kompanjiesdrif basin.

Figure 36 illustrates that at the point of confinement there was a distinct increase in water depth and velocity. Confinement of the valley as a result of impingement by a large left-bank alluvial fan resulted in an increase in velocity and water depth occurring on the right bank. An increase in

discharge resulted in a greater increase of both water depth and velocity. The effects of this were concentrated where the valley was confined. For example, at a discharge of 30 $m^3.s^{-1}$ (Figure 36 B), the water depth in the confined section was between 4 m and 7 m and the velocity was between 0.01 $m.s^{-1}$ and 0.015 $m.s^{-1}$. At a flood with a discharge of 300 $m^3.s^{-1}$ (Figure 36 J), stream competence and capacity increased significantly. Velocities at the site, given this discharge, were between 0.02 and 0.05 $m.s^{-1}$, and water depths were between 19 m and 26 m.

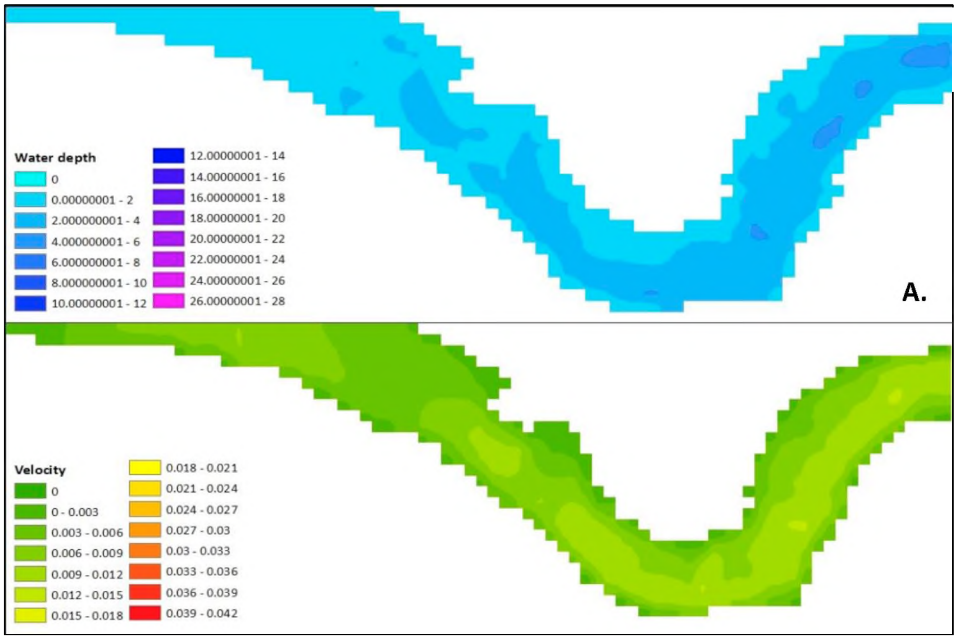

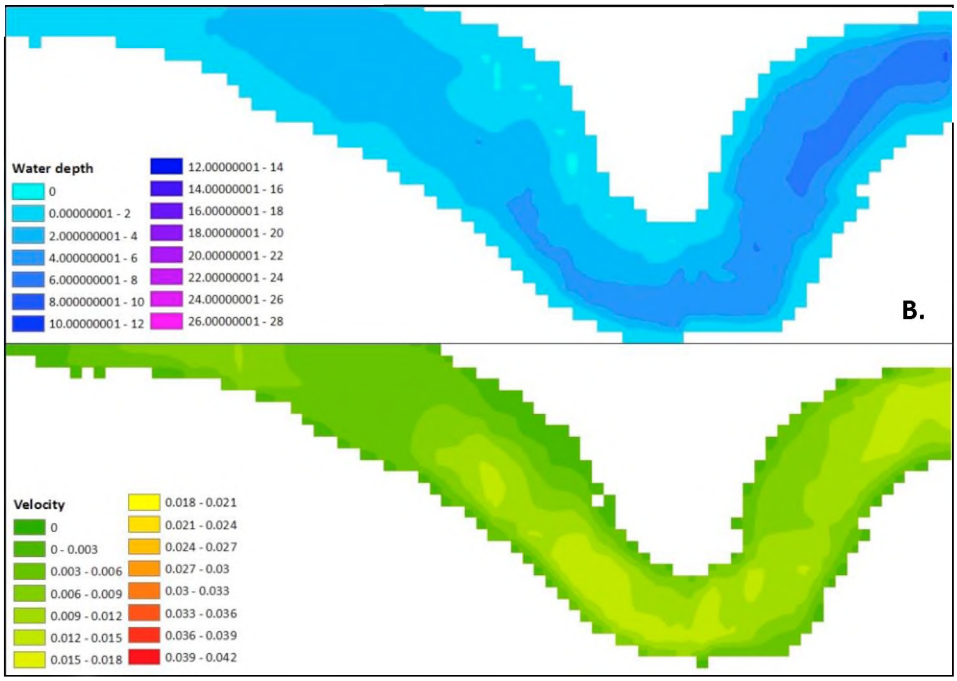

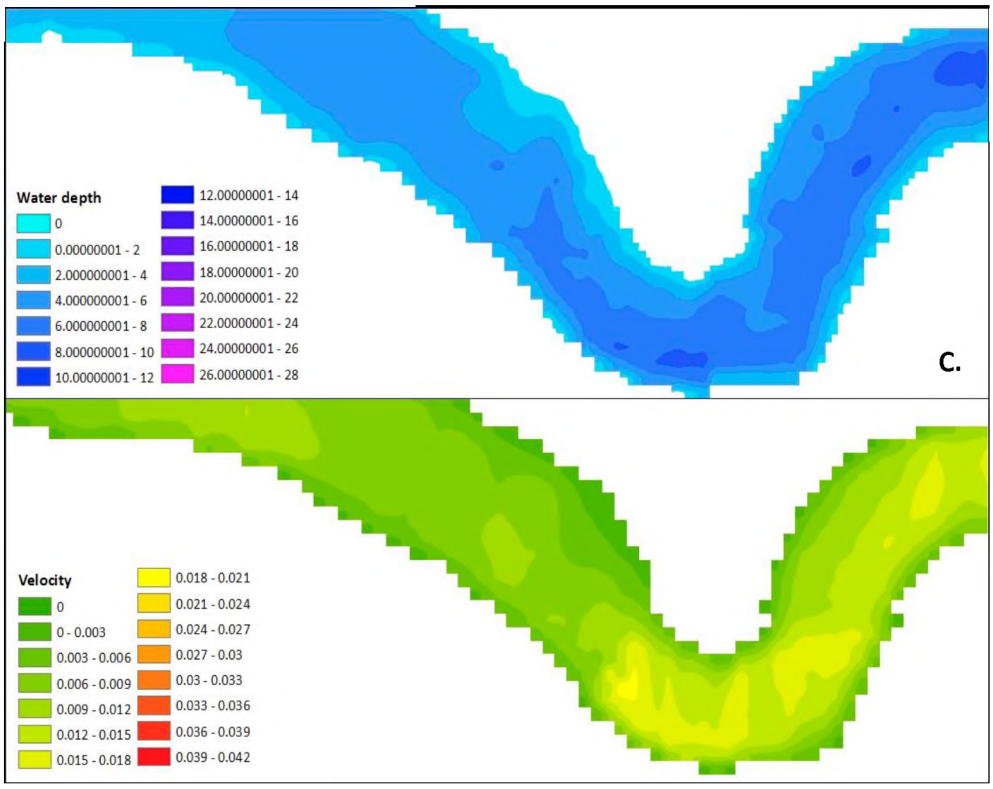
Water depth
0
0.00000001 - 2
2.000000001 - 4
4.000000001 - 6
6.000000001 - 8
8.000000001 - 10
10.00000001 - 12
12.00000001 - 14
14.00000001 - 16
16.00000001 - 18
18.00000001 - 20
20.00000001 - 22
22.00000001 - 24
24.00000001 - 26
26.00000001 - 28
C.
Velocity
0
0 - 0.003
0.003 - 0.006
0.006 - 0.009
0.009 - 0.012
0.012 - 0.015
0.015 - 0.018
0.018 - 0.021
0.021 - 0.024
0.024 - 0.027
0.027 - 0.03
0.03 - 0.033
0.033 - 0.036
0.036 - 0.039
0.039 - 0.042

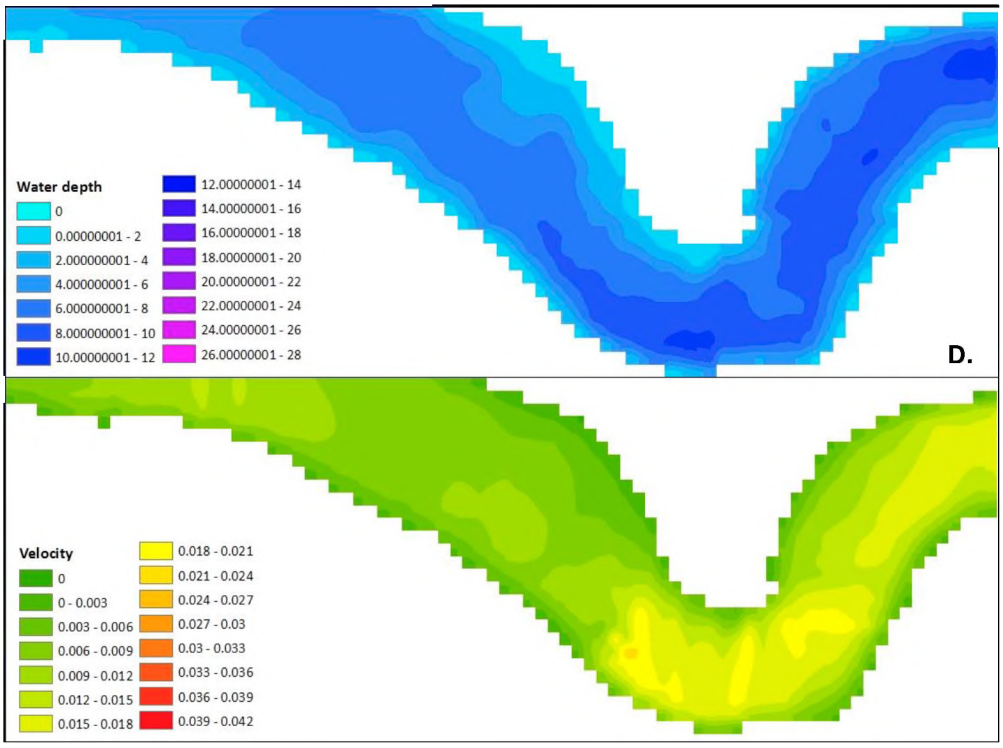
Water depth
0
0.00000001 - 2
2.000000001 - 4
4.000000001 - 6
6.000000001 - 8
8.000000001 - 10
10.00000001 - 12
12.00000001 - 14
14.00000001 - 16
16.00000001 - 18
18.00000001 - 20
20.00000001 - 22
22.00000001 - 24
24.00000001 - 26
26.00000001 - 28
D.
Velocity
0
0 - 0.003
0.003 - 0.006
0.006 - 0.009
0.009 - 0.012
0.012 - 0.015
0.015 - 0.018
0.018 - 0.021
0.021 - 0.024
0.024 - 0.027
0.027 - 0.03
0.03 - 0.033
0.033 - 0.036
0.036 - 0.039
0.039 - 0.042

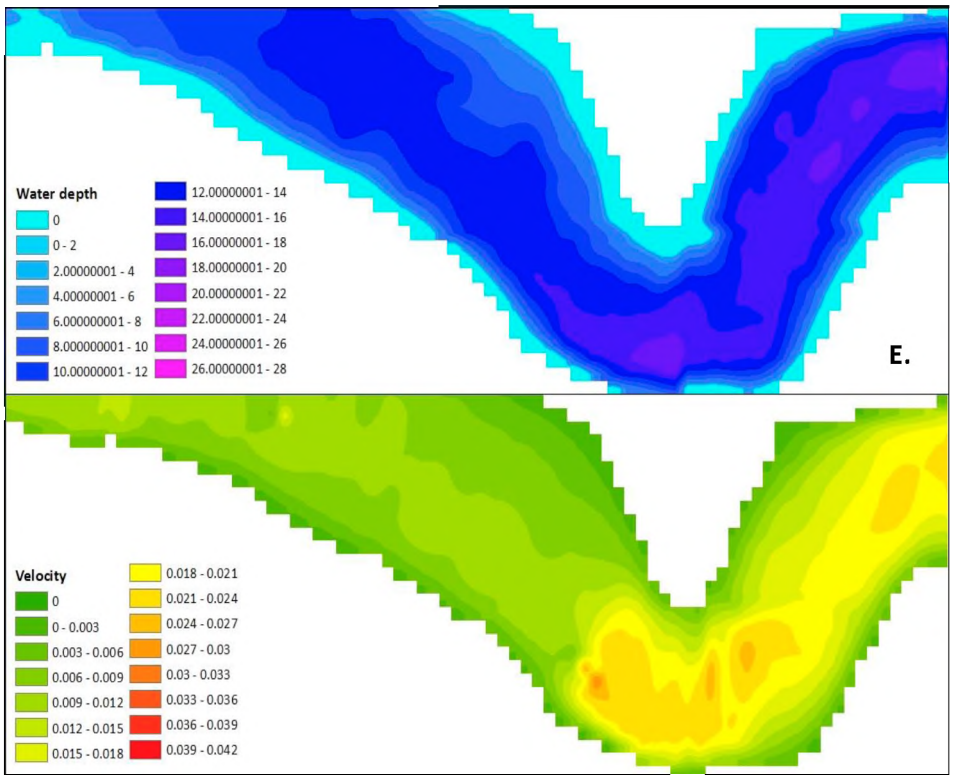
Water depth
0
0 - 2
2.00000001 - 4
4.00000001 - 6
6.000000001 - 8
8.000000001 - 10
10.00000001 - 12
12.00000001 - 14
14.00000001 - 16
16.00000001 - 18
18.00000001 - 20
20.00000001 - 22
22.00000001 - 24
24.00000001 - 26
26.00000001 - 28
E.
Velocity
0
0 - 0.003
0.003 - 0.006
0.006 - 0.009
0.009 - 0.012
0.012 - 0.015
0.015 - 0.018
0.018 - 0.021
0.021 - 0.024
0.024 - 0.027
0.027 - 0.03
0.03 - 0.033
0.033 - 0.036
0.036 - 0.039
0.039 - 0.042

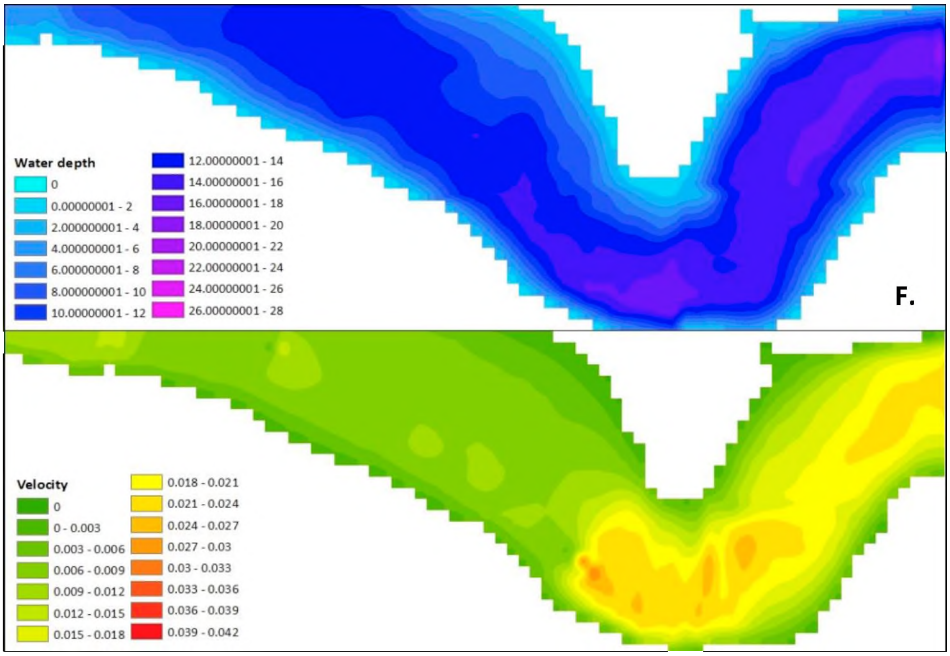
Water depth
0
0.00000001 - 2
2.000000001 - 4
4.000000001 - 6
6.000000001 - 8
8.000000001 - 10
10.00000001 - 12
12.00000001 - 14
14.00000001 - 16
16.00000001 - 18
18.00000001 - 20
20.00000001 - 22
22.00000001 - 24
24.00000001 - 26
26.00000001 - 28
F.
Velocity
0
0 - 0.003
0.003 - 0.006
0.006 - 0.009
0.009 - 0.012
0.012 - 0.015
0.015 - 0.018
0.018 - 0.021
0.021 - 0.024
0.024 - 0.027
0.027 - 0.03
0.03 - 0.033
0.033 - 0.036
0.036 - 0.039
0.039 - 0.042

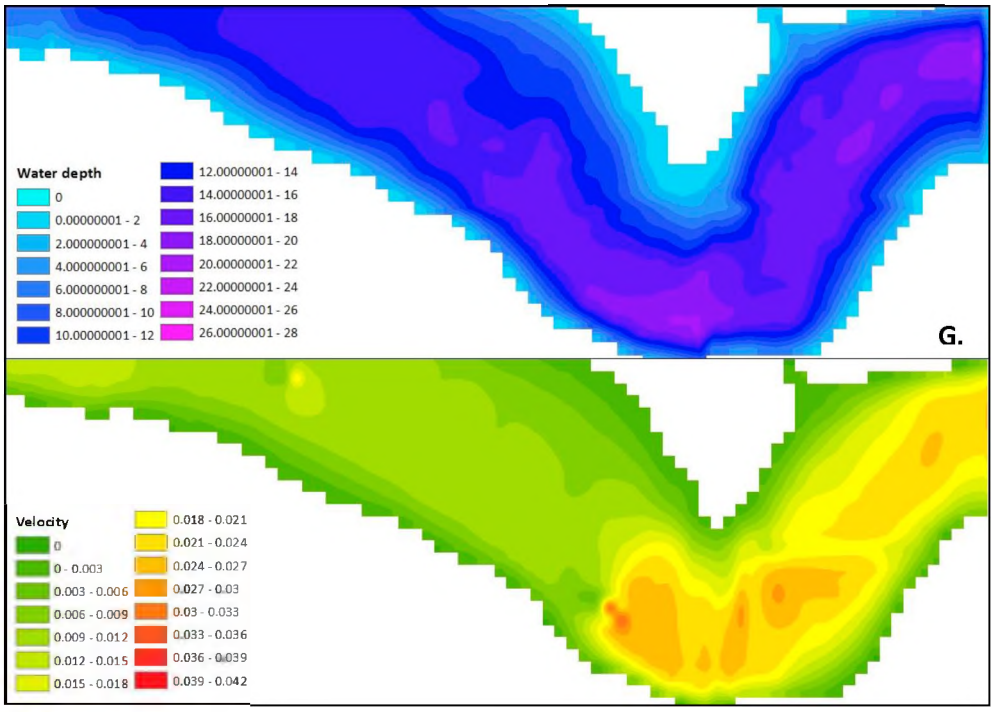
Water depth
0
0.00000001 - 2
2.000000001 - 4
4.000000001 - 6
6.000000001 - 8
8.000000001 - 10
10.00000001 - 12
12.00000001 - 14
14.00000001 - 16
16.00000001 - 18
18.00000001 - 20
20.00000001 - 22
22.00000001 - 24
24.00000001 - 26
26.00000001 - 28
G.
Velocity
0
0 - 0.003
0.003 - 0.006
0.006 - 0.009
0.009 - 0.012
0.012 - 0.015
0.015 - 0.018
0.018 - 0.021
0.021 - 0.024
0.024 - 0.027
0.027 - 0.03
0.03 - 0.033
0.033 - 0.036
0.036 - 0.039
0.039 - 0.042

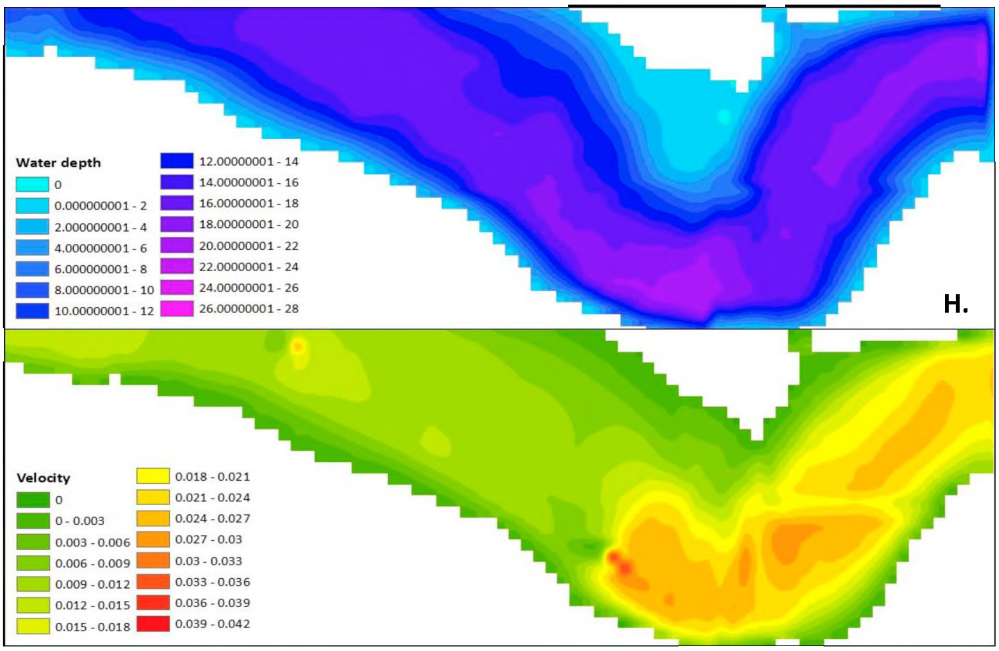
Water depth
0
0.000000001 - 2
2.000000001 - 4
4.000000001 - 6
6.000000001 - 8
8.000000001 - 10
10.00000001 - 12
12.00000001 - 14
14.00000001 - 16
16.00000001 - 18
18.00000001 - 20
20.00000001 - 22
22.00000001 - 24
24.00000001 - 26
26.00000001 - 28
H.
Velocity
0
0 - 0.003
0.003 - 0.006
0.006 - 0.009
0.009 - 0.012
0.012 - 0.015
0.015 - 0.018
0.018 - 0.021
0.021 - 0.024
0.024 - 0.027
0.027 - 0.03
0.03 - 0.033
0.033 - 0.036
0.036 - 0.039
0.039 - 0.042

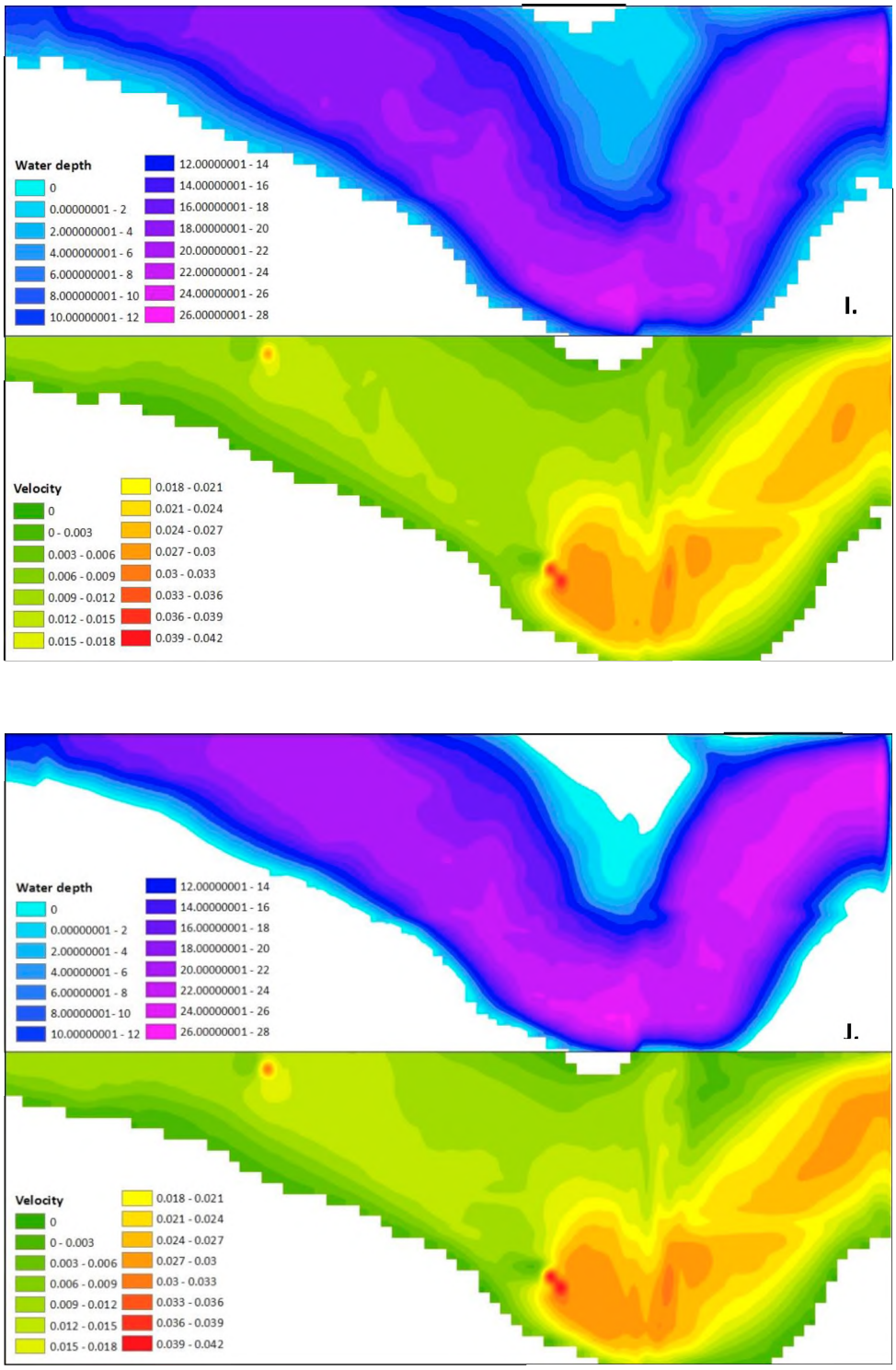

Figure 376: Simulation results of water depths and velocities within the confined section at varying discharges of 5 (A), 30 (B), 50 (C), 70 (D), 90 (E), 100 (F), 150 (G), 200 (H), 250 (I), 300 $m^3.s^{-1}$ (J)

VARYING DISCHARGE: HEC-RAS

In this section steady flow analysis data for two transects were presented; one broad transect (Transect 1) at the head of the wetland and one narrow transect (Transect 7) at the point of confinement at the toe of the basin.

Figure 37 shows that the depth of flooding and the velocity of water at a low discharge of 5 $m^3.s^{-1}$ are low, but greater in the confined section at the toe of the basin than in the broad section near the upper end of the basin. At a greater discharge of 300 $m^3.s^{-1}$, both the depth of inundation and the average velocity are greater than at low flows and also greater in the narrow confined section at the toe of the basin than the broad zone of the valley near the head of the basin.

Figure 38 illustrates that as discharge was increased at the point of confinement (Transect 7) there was a distinct increase in water depth, velocity, stream power and shear stress compared to the broad reach (Transect 1). For example, at a discharge of 30 $m^3.s^{-1}$ (Figure 38) the water depth at Transect 1 was approximately 0.44 m and the velocity was 0.60 $m.s^{-1}$ and at the confined section (Transect 7), the water depth was approximately 0.69 m and the velocity was 2.09 $m.s^{-1}$. During a large flood of 300 $m^3.s^{-1}$ water depth was increased from 1.13 m in Transect 1 to 2.1 m in Transect 7 (Figure 38). Correspondingly average velocity, stream power and shear stress increased significantly.

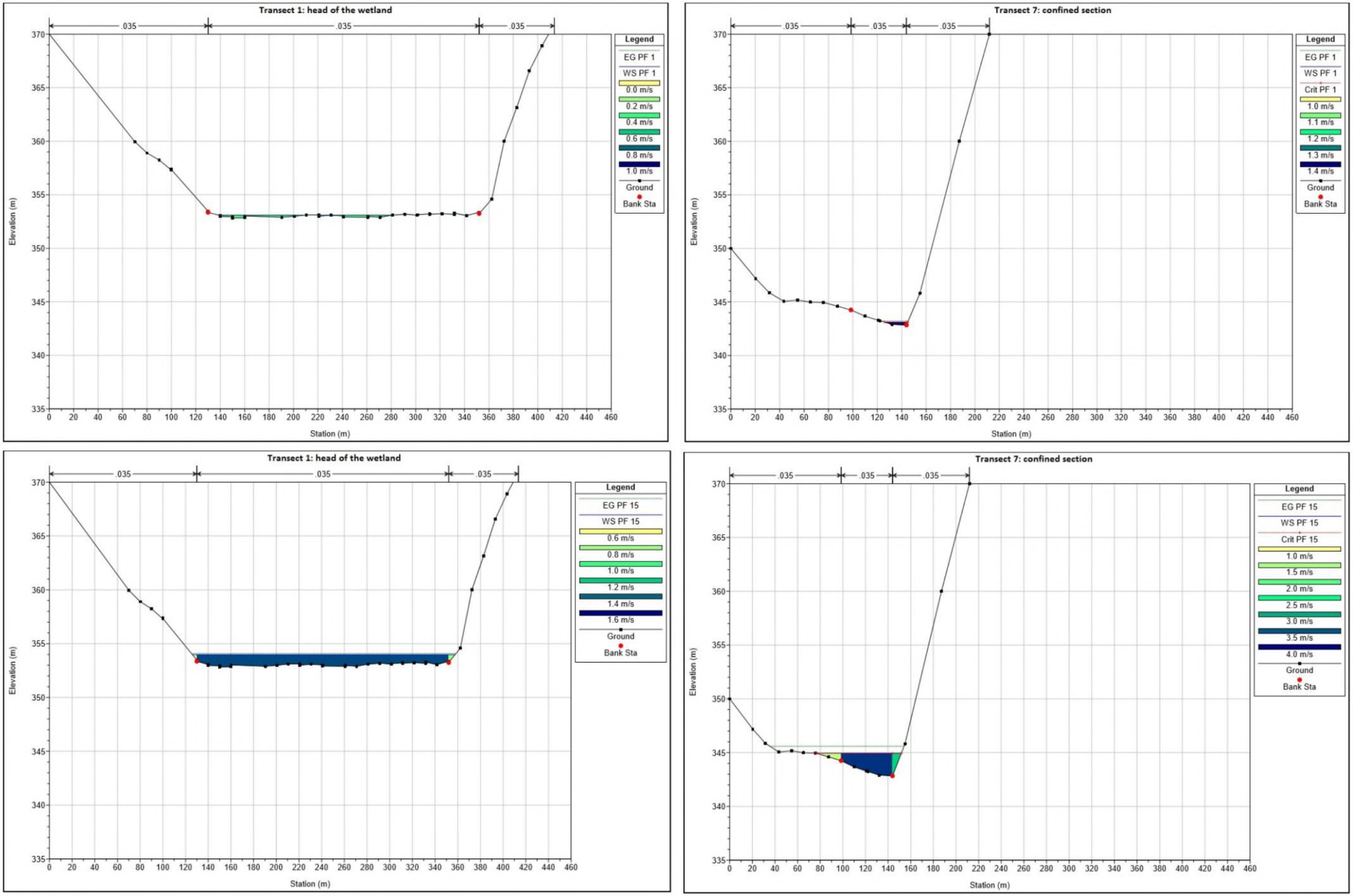

Figure 387: HEC-RAS simulation results showing water depth and velocities at the wide section (I) compared with the narrow section (II), at different discharges of 5 $m^3.s^{-1}$ (A) and 300 $m^3.s^{-1}$ (B)

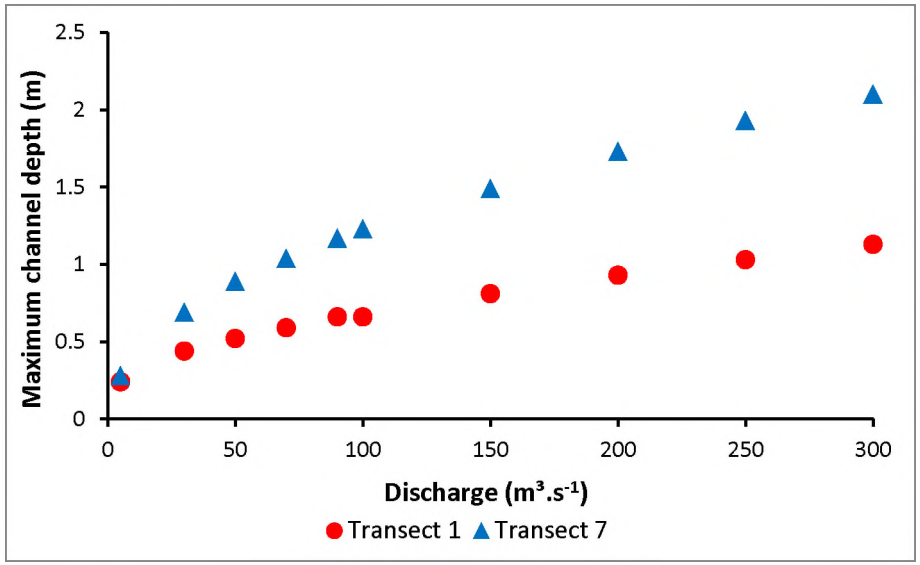

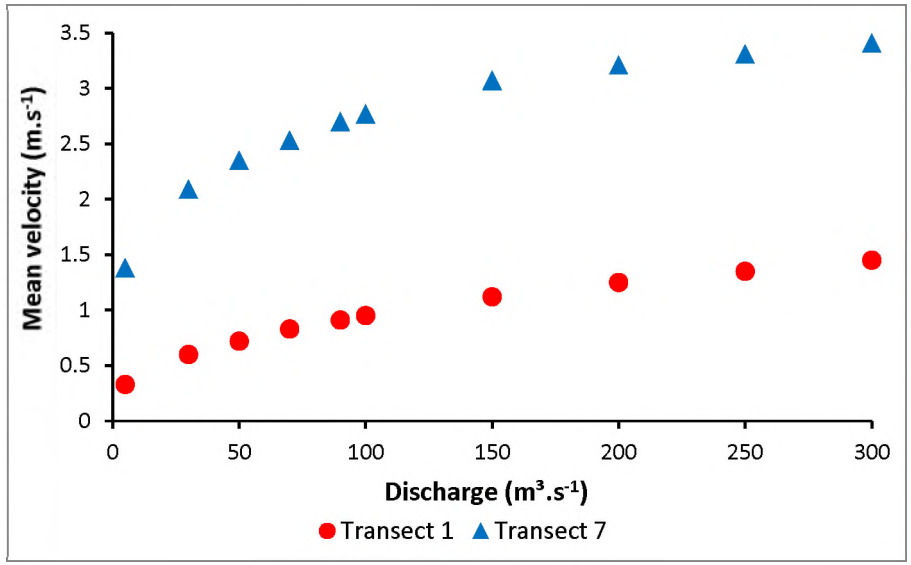

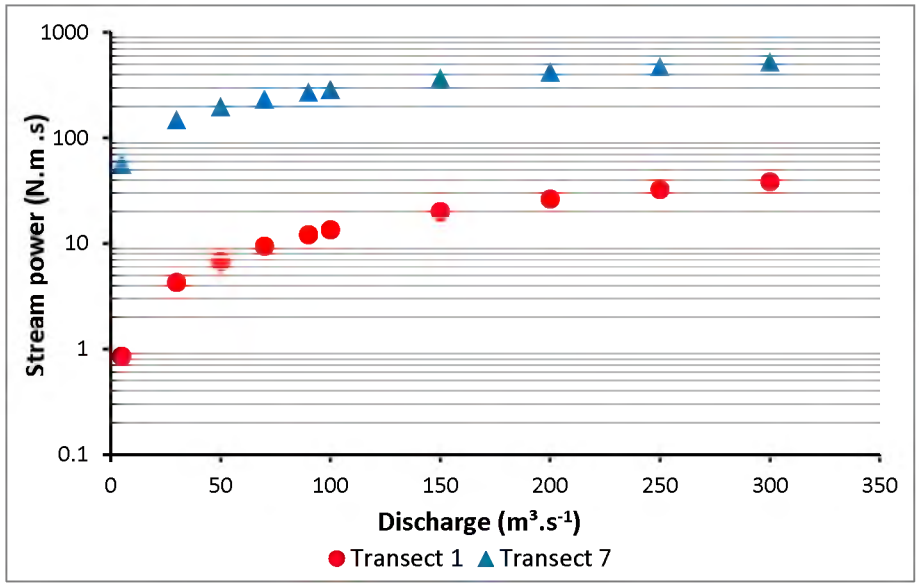

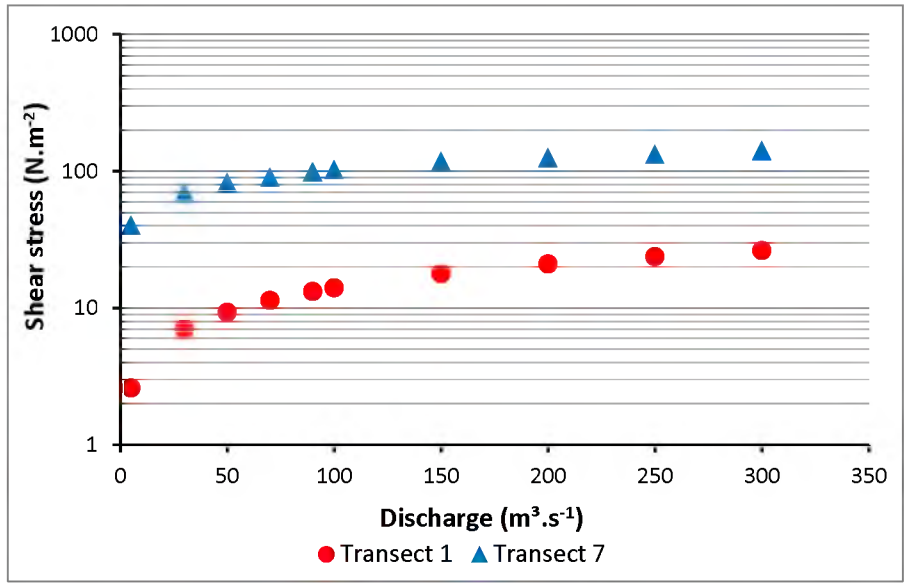

Figure 398: Graphs depicting hydraulic characteristics at varying discharges comparing unconfined (Transect 1) and confined (Transect 7) reaches from HEC-RAS simulations

5.2.4 SLOPE VERSUS WIDTH

This section explores variation in flooded valley width, depth and current velocity in response to variation in discharge as determined from a number of simulations run in HEC-RAS.

The results show that width increased by a factor of two, mean depth increased by a factor of three, and mean velocity increased by a factor of three with increasing discharge (Figure 39).

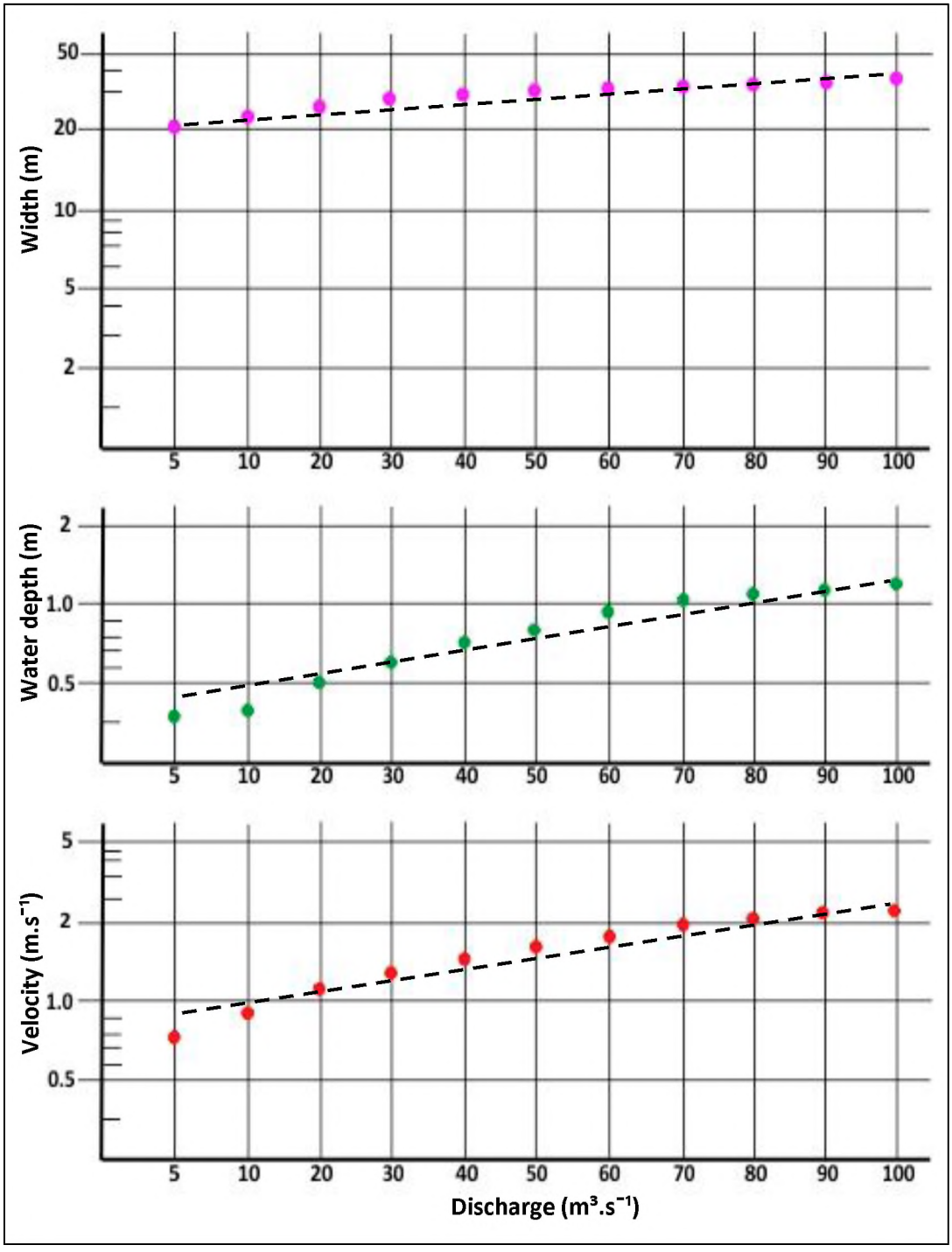

Figure 39: Relationship between of width (A), depth (B) and velocity (C) to variation in discharge

5.2.5 CALIBRATION

It was determined that both CAESAR-Lisflood and HEC-RAS simulation results were a good representation of the Kompanjiesdrif basin with a discharge of 55 $m^3.s^{-1}$ discharge and a Manning's roughness coefficient of 0.035. However, this could not be validated for higher discharges as no flows greater than this were recorded over the study period.

CHAPTER SIX: DISCUSSION

Although gully erosion is a worldwide phenomenon and is fairly well established in the research sphere not much focus has been put on the natural causes of erosion and its effect to the wider geomorphological history and characteristics of an area. Many studies have attributed gully formation as either being caused or accelerated by anthropogenic changes within the catchment. However, this does not take into account climate change, natural geomorphic thresholds, and instabilities that may be inherent to the system; or the long term (thousands rather than tens or hundreds of years) evolution of the system. In addition, gullies are found to be present in almost all landscape settings, from those heavily modified by humans to environments that are near pristine. These facts highlight the need for research and a better understanding of the natural features that may initiate gully formation. This research highlights the role of intrinsic geomorphological factors and their effect on flow hydraulics in the creation of conditions that may naturally initiate gully formation.

The southern African landscape lends itself to the study of the natural mechanisms of gully erosion and landscape evolution. The effects of geomorphic evolution and landscape characteristics on river systems, and the wetlands present on those river systems, are evident in the region. Due to southern Africa's highly elevated landscape following major uplift events 20 and 5 Million years Before Present, erosion is happening at a subcontinental scale. The unique landscape of South Africa, coupled with the low average precipitation and high evapotranspiration rates, make geomorphological considerations highly pertinent. Due to South Africa being characterised as semi-arid with a negative water balance, most large wetlands form part of fluvial systems. In terms of understanding wetland origin, formation, persistence and demise one must explore the intimate relationship to larger scale processes (i.e. geomorphological evolution of the sub-continent), with the micro-scale processes that occur within the wetland (i.e. erosion and deposition), as well as the intermediate process occurring within the drainage basin.

There are many models that exist explaining the formation and dynamics of wetlands in southern Africa. This research contributes to a model of wetland formation that is broadly related to the model proposed by Tooth *et al.* (2002; 2004). Tooth *et al.* (2002) proposed that conditions conducive to valley bottom wetland formation are linked to local resistant lithologies creating a local base level upstream of which a meandering stream laterally planes the less resistant lithology. These two features result in valley widening and a decreasing regional longitudinal slope, allowing favourable conditions for wetland creation. However, in the Kompanjiesdrif basin wetland there is no evidence of a meandering stream or a local resistant lithology such as a dolerite dyke or sill that forms a local

base level below which erosion is not possible. Nevertheless, the valley of the Kompanjiesdrif basin has been laterally planed to produce a relatively wide valley that is near horizontal in cross-section and has a very gentle longitudinal slope, which has allowed for the formation of an un-channelled valley bottom wetland.

In the Kompanjiesdrif basin gullies are prominent features that have been observed to coincide with a number of tributary alluvial fans entering the trunk valley, and in so doing, they confine the lateral extent of the valley floor (the wetland) and locally increase the longitudinal slope. The importance of the concept of geomorphic thresholds is relevant when exploring changes occurring within a system at the local scale (Schumm, 1979). This raises the notion that gullies within the system may be an important natural feature that is integral to landscape evolution. The key issue relates to processes that may lead to the formation of a broad near planar valley in cross-section, with a very low longitudinal slope. This study presents an alternative mechanism for the formation of broad, flat valleys with a low longitudinal slope.

Trunk-tributary relationships are typically described in terms of the influence that the tributary has on the trunk systems behaviour (Garden, 2008). In the Kompanjiesdrif basin, and other similar geomorphic landscapes, steep, sediment-laden tributaries deposit large amounts of sediment on the trunk valley in the form of broad alluvial fans. This plays an important role in the formation, behaviour and processes occurring in the trunk system. In the Kompanjiesdrif basin it is postulated that large amounts of sediment supplied by the tributaries partially blocked flow and caused the formation of backwater lakes upstream. Over time accumulation of organic and clastic sediment steepened the slope at the impeding reaches of the alluvial fans. This resulted in periods of erosion occurring at different reaches followed by more sedimentation thereby creating broad, flat basins. The argument presented here is that gully formation over geological time has created a broad, flat valley with a gentle longitudinal slope that is favourable for the formation of large un-channelled valley bottom wetlands. This study highlights the role of intrinsic geomorphological and hydraulic factors in controlling gully initiation in the Kompanjiesdrif basin, given that gully erosion has been shown to be initiated spontaneously as a consequence of natural processes related to tributary-trunk interactions that lead to the crossing of geomorphic thresholds. This was accomplished using CAESAR-Lisflood, a two-dimensional hydrodynamic model, and a one-dimensional hydraulic analysis model, HEC-RAS.

Overall, the results from this research show that the variation in key hydraulic features (i.e. discharge, velocity, water depth and stream power) are crucial in the spatial variations of gully initiation. In addition, the patterns of variation in hydraulic features is strongly influenced by the

presence of alluvial fan deposits that both reduce the width of the wetland and increase the slope downstream of the node of tributary fan deposition (Figure 40), as observed in the Kompanjiesdrif basin in the present study.

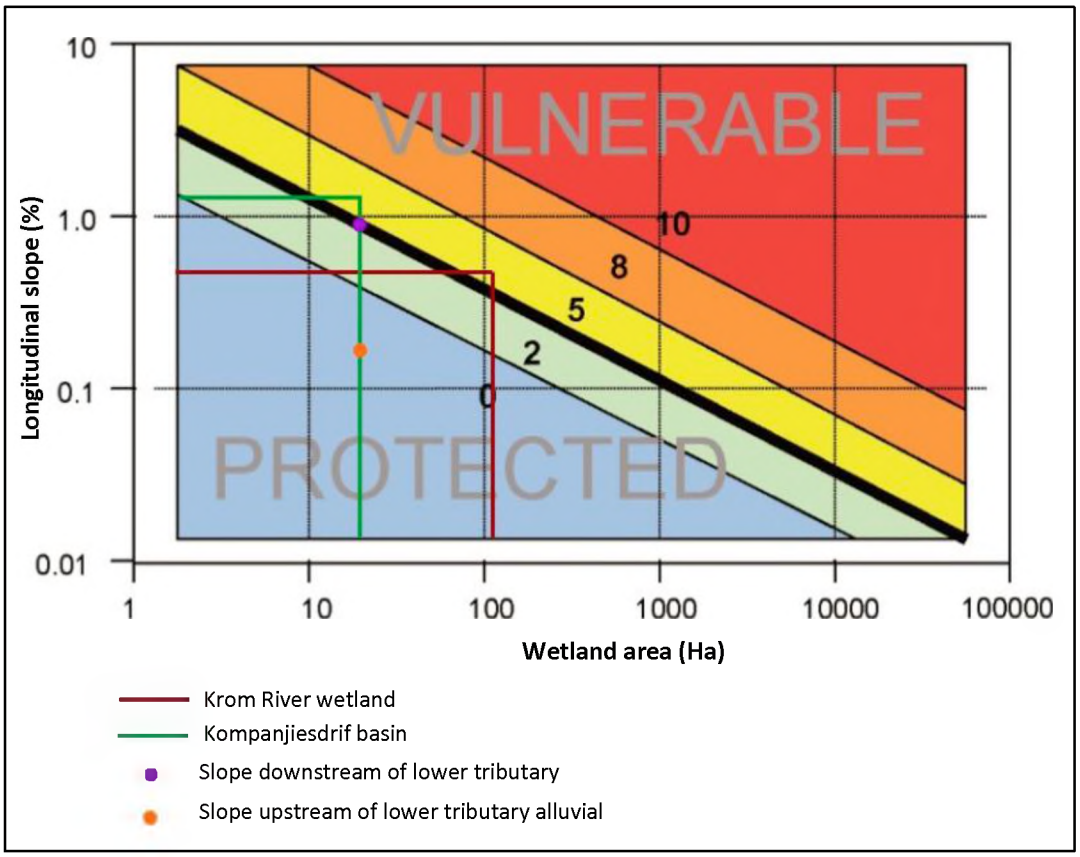

Figure 40: Wetland vulnerability to erosion graph depicting the Krom River wetland complex, Kompanjiesdrif basin, the slope downstream and upstream of the lower tributary alluvial fan, (Ellery *et al*., 2009)

Channel geometry, basin features and characteristics of stream flow are inherently linked. The structural control that alluvial fans have on the Kompanjiesdrif basin wetland plays an important role on the distribution of velocity and water depth within the wetland which ultimately leads to erosion. Using Hjulstrom's diagram the overall modelled results show that the most common sediment particle size (fine to medium sand) found in the basin can be lifted, transported and therefore eroded by velocities greater than 0.03 $m.s^{-1}$ (Figure 41). Figure 42 shows zones of potential erosion according to Hjulstrom's critical erosion velocity curve. According to the modelled results the most crucial of these zones occurs where the valley is pinched by an alluvial fan which has significantly reduced the width of the valley and increased the slope in the downstream direction.

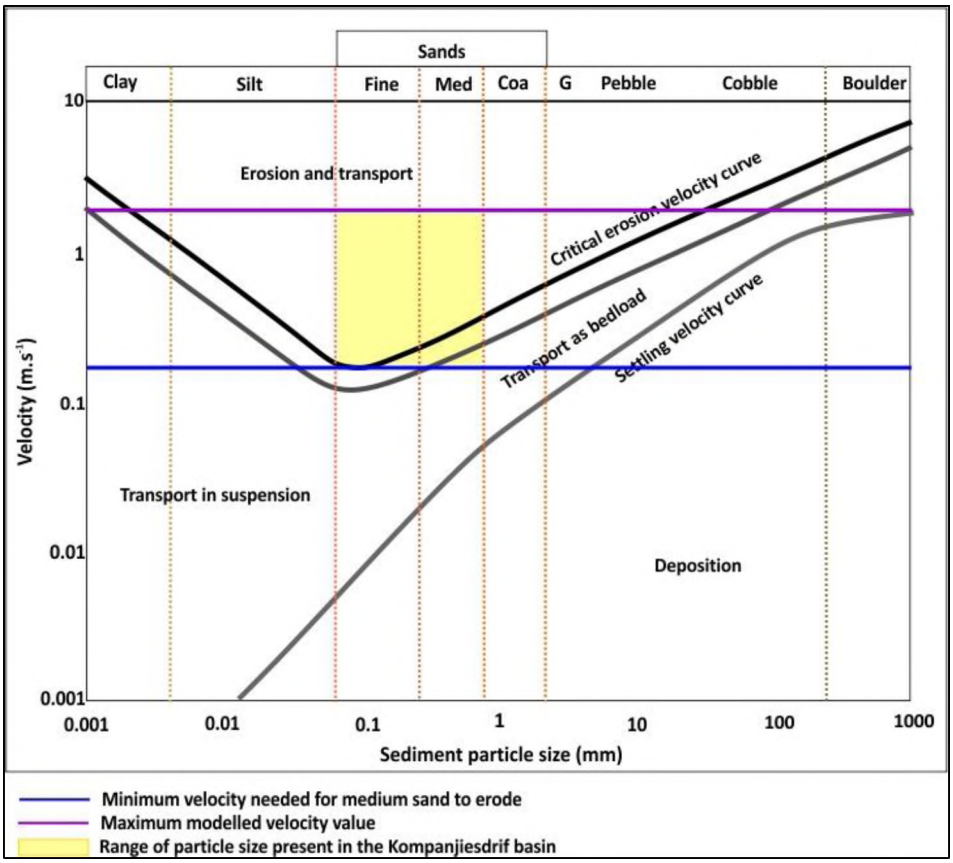

Figure 41: Hjulstrom's diagram illustrating the minimum velocity (blue line) required for medium sand to be eroded and the maximum modelled velocity (purple line)

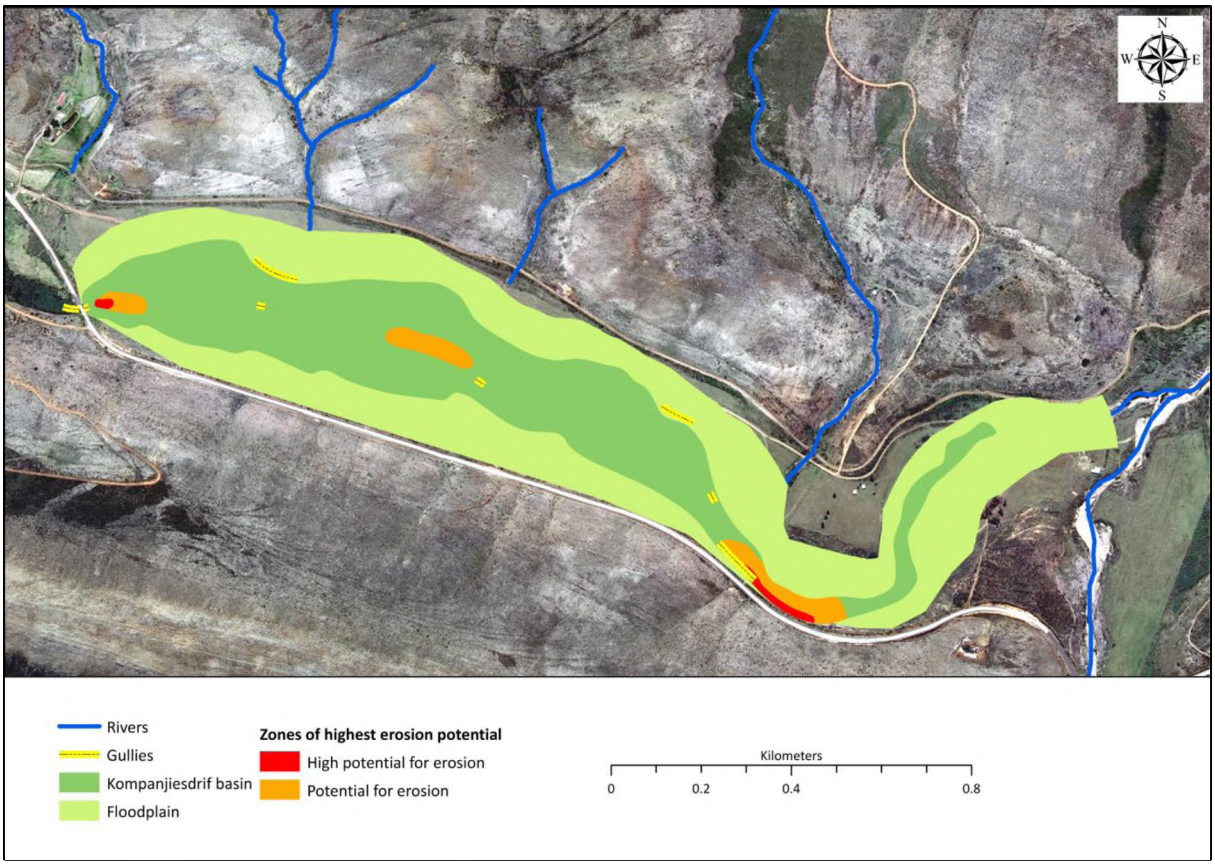

Figure 42: Zones of potential erosion in the Kompanjiesdrif basin in relation to location of current gullies

The first stage of the conceptual model (Figure 43 A) relates to the presence of a broad near-flat valley (in cross-section) with a gentle longitudinal slope. The first process in gully initiation is the delivery of sediment at the toe of the wetland basin to the valley floor by a large tributary alluvial fan (Figure 43 B). This sediment deposit, from a large, steep tributary stream pinches the valley floor and significantly decreases the width of the wetland (from approximately 350 to 50 meters). From the study it is clear that a reduction in cross-sectional width results in increased water depth, leading to increased velocity for a given discharge in the confined section. Eventually the retarding effects of vegetation is overwhelmed as the flood waters flatten the vegetation, initiating erosion (Figure 43 C; Schumm, 1973; Patton & Schumm, 1975; Schumm, 1979; Wohl, 2013).

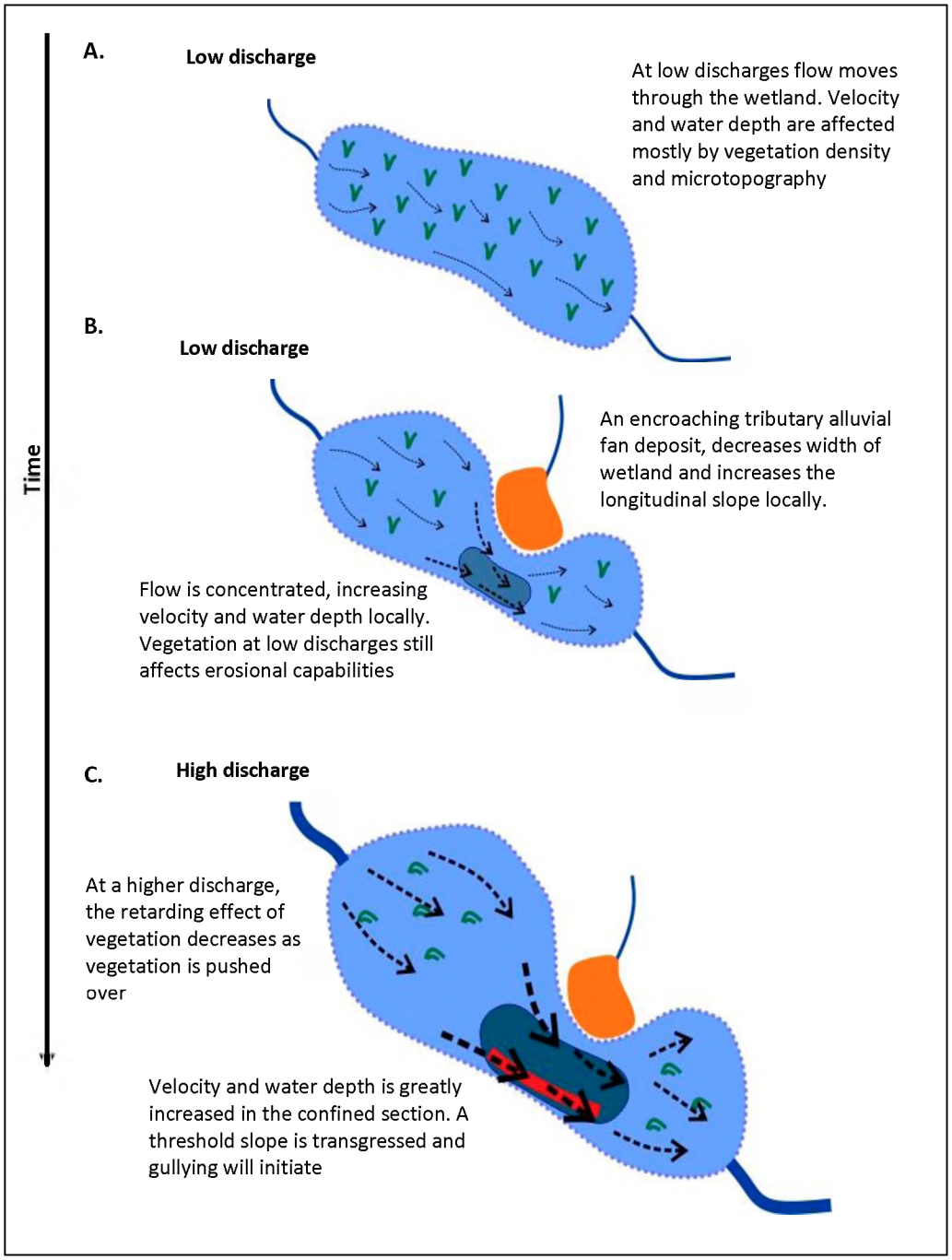

Figure 43: Conceptual model of how gully erosion may be initiated due of width reduction and localised slope steepening

6.1 CONCLUSION

This research has shown that in some wetland landscapes a dominant geomorphological control exists that gives rise to a particular wetland structure and function, a valley-bottom wetland. An example of a geomorphic feature that gives rise to a particular wetland structure is a large tributary alluvial fan that encroaches on the trunk stream, giving rise to an un-channelled valley-bottom wetland. Ongoing encroachment of a tributary alluvial fan has a significant effect on hydraulic features of the surface water flow. A steepening of the longitudinal slope of the trunk stream occurs downstream of the node of deposition. Together with narrowing of the trunk valley associated with encroachment of the tributary alluvial fan, gully erosion is initiated as a result of intrinsic factors that lead to the crossing of a geomorphic threshold. Gully formation in the Krom River controls wetland form in that the valley is widened and longitudinal slope is reduced, thus creating an ideal environment for wetland development. As a consequence gully erosion in this area is a natural phenomenon and is a feature of landscape evolution.

6.2 LIMITATIONS AND FUTURE WORK

A limitation to this research was the calibration process. Future work on hydraulic analysis and hydrodynamic modelling using one-dimensional and two-dimensional programs should use higher measured velocities, water depth and wetted extent in order to calibrate and validate the models more accurately.

Future work should also consider a broader range of cell size resolutions in CAESAR-Lisflood. Due to the lack of computing capabilities used to perform the CAESAR-Lisflood simulations, very high cell resolutions could not be examined extensively.

Future work should examine the role of residual water and groundwater discharges in determining water levels and inundation extents within the wetland system. CAESAR-Lisflood and HEC-RAS work on the assumption that the water depth and inundation extent is due, exclusively, to surface water spread. Working with a combined ground water and surface water modelling program could render interesting results.

To further evaluate the effects of landscape characteristics such as the influence of alluvial fans on wetland structure and function, a greater number of study areas should be evaluated.

REFERENCE LIST

Avni, Y. 2005. Gully incision as a key factor in desertification in an arid environment, the Negev highlands, Israel. *Catena*, 63, pp.185–220.

Baker, C., Thompson, J.R. & Simpson, M. 2009. Hydrological dynamics I: Surface waters, flood and sediment dynamics. In: Maltby, E. & Barker, T. (Eds.), *The Wetland Handbook*. Chichester: Wiley-Blackwell, pp. 120–168.

Bates, P.D. & De Roo, A.P.J. 2000. A simple raster-based model for flood inundation simulation. *Journal of Hydrology*, 236 (1), pp.54–77.

Bates, P.D., Horritt, M.S., Hunter, N.M., Mason, D. & Cobby, D. 2005. Numerical modelling of floodplain flow. In: *Computational Fluid Dynamics: Applications in Environmental Hydraulics*. Chichester: John Wiley and Sons, Ltd, pp. 271–297.

Bates, P.D., Horritt, M.S. & Fewtrell, T.J. 2010. A simple inertial formulation of the shallow water equations for efficient two-dimensional flood inundation modelling. *Journal of Hydrology*, 387 (1), pp.33–45.

Beasley, D.B., Huggins, L.F. & Monke, E.J. 1982. Modelling sediment yields from agricultural watersheds. *Journal of Soil and Water Conservation*, 37(2), pp.113-117.

Beavers, M.A. 1994. *Floodplain determination using HEC-2 and geographic information systems.* Department of Civil Engineering, University of Texas at Austin, Texas (MSc Thesis).

Blackie, J.R. & Eels, C.W.O. 1985. Lumped catchment models. In: Anderson, M.G. and Burt, T.P. (Eds.), *Hydrological Forecasting*. Chichester: Wiley, pp.311-345.

Bork, H. 2004. Soil erosion and its consequences since 1800 AD. *Soil Conservation and Protection for Europe,* pp.11–14.

Brierley, G.J. & Fryirs, K.A. 2005. *Geomorphology and River Management: Applications of the River Styles Framework*. Blackwell Publishing, Oxford, UK.

Brunet, R. 1968. *Les phénomenes de discountinuité en geographie: Centre de Recherches et Documentation Cartographic et Geographique*. Editions du Centre National de la Recherche Scientifique, 7, p. 117

Buckle, C. 1978. *Landforms in Africa,* First edition. Essex, England: Longman Group Limited, pp.249.

Bull, L., and M. Kirkby. 2002. Channel heads and channel extension. In Bull, L., and Kirkby, M. (eds). *Dryland Rivers: Hydrology and Geomorphology of Semi-Arid Channels*. New York: John Wiley, pp. 263–298.

Chow, V. T. 1959. Open-channel flow and its classification. In Davis, H. E. (Ed.), *Open-Channel Hydraulics*. New York: McGraw-Hill Civil Engineering Series, pp. 3–14.

Chow, V. T, Maidment, D.R. & Mays, L.W. 1988. Hydrological processes. In Eliassen, R., King, P. H. & Linsley, R. K. (Eds.) *Applied Hydrology*. New York: McGraw-Hill series in Water Resources, pp. 20–42.

Cooper, A., Murray, R. & McCann, T. 1991. The environmental effects of blanket peat exploitation. University of Ulster.

Coulthard, T.J., Neal, J.C., Bates, P.D., Ramiraz, J., de Almeida, G.A.M. & Hancock, G.R. 2013. Integrating the LISFLOOD-FP 2D hydrodynamic model with the CAESAR model: Implications for modelling landscape evolution. *Earth Surface Processes and Landforms*, 38(15), pp.1897–1906.

Coulthard, T.J. & van de Wiel, M.J., 2013. Numerical modelling in fluvial geomorphology. In: Shroder, J. (Editor in Chief), Wohl, E. (Ed.*), Treatise on Geomorphology*. Academic Press, San Diego, CA, Fluvial Geomorphology, 9, pp.694–710.

Cowan, G. 1995. *Wetlands of South Africa.* South African Wetlands Conservation Programme series. Pretoria: Department of Environmental Affairs and Tourism.

Davis, J.A. and Barmuta, L.A. 1989. An ecologically useful classification of mean and near-bed flows in streams and rivers. *Freshwater Biology*, 21, pp. 271–282.

de Vente, J., Poesen, J. & Verstraeten, G. 2005. The application of semi-quantitative methods and reservoir sedimentation rates for the prediction of basin sediment yield in Spain. *Journal of Hydrology,* 305(1), pp.63–86.

Department of Environmental Affairs and Tourism (DEAT), 2006. *South African Environmental Outlook. A report on the state of the environment*. Department of Environmental Affairs and Tourism, Pretoria.

Department of Water and Sanitation (DWS), 2015. Flow dataset for Krom River station K90H001. Resource Quality Services Directorate, Pretoria.

Di Baldassarre, G.D., Schumann, G., Bates, P.D., Freer, J.E. & Beven, K.J. 2010. Floodplain mapping: a critical discussion of deterministic and probabilistic approaches. *Hydrological Sciences Journal,* 55(3), pp.364–375.

Dollar, L.H., Dollar, E.S.J. & Moolman, J.,2006. Development of an automated desktop procedure for defining macro-reaches for river longitudinal profiles. *Water SA*, 32(3), pp.395–402.

Edwards, R. 2009. *The origin and evolution of Dartmoor vlei in the KwaZulu-Natal Midlands, South Africa*. University of KwaZulu-Natal (MSc thesis).

Eitel, B., Eberle, J. & Kuhn, R. 2002. Holocene environmental change in the Otjiwarongo thornbush savanna (Northern Namibia): evidence from soils and sediments. *Catena*, 47, pp.43–62.

Ellery, W.N., Grenfell, M.C., Grenfell, S.E., Kotze, D.D., McCarthy, T.S., Tooth, S., Grundling, P., Beckedahl, H., le Maitre, D. & Ramsay, L. 2009. *WET-Origins. Controls on the distribution and dynamics of wetlands in South Africa.* In: Breen, C., Dini, J., Ellery, W.N., Mitchell, S. & Uys, M. (Eds.), Wetland Management Series, WRC Report No. TT 334/09.

Ellery, W.N., Grenfell, S.E., Grenfell, M.C., Humphries, M.S., Barnes, K., Dahlberg, A. & Kindness, A. 2012. Peat formation in the context of the development of the Mkuze floodplain on the coastal plain of Maputaland , South Africa. *Geomorphology*, 141–142, pp.11–20.

Everaert, W. 1991. Empirical relations for the sediment transport capacity of interrill flow. *Earth Surface Processes and Landscape*, 16 (6), pp. 513–532.

Farr, T.G., Rosen, P.A., Caro, E., Crippen, R., Duren, R., Hensley, S., Kobrick, M., Paller, M., Rodriguez, E., Roth, L. and Seal, D. 2007. The shuttle radar topography mission. *Reviews of geophysics*, 45(2).

Foster, G. R. and Meyer, L. D. 1972. Transport of soil particles by shallow flow. *Transactions of the. ASAE*, 15 (1), pp. 99–102.

Fryirs, K. & Brierley, G. 1998. The character and age structure of valley fills in Upper Wolumla Creek catchment, South Coast, New South Wales, Australia. *Earth Science Reviews*, 23, pp.271–287.

Fryirs, K.A. & Brierley, G.J. 2010. Antecedent controls on river character and behavior in partly confined valley settings: Upper Hunter River catchment, NSW, Australia. *Geomorphology*, 117, pp.106–120.

Fryirs, K.A. & Brierley, G.J. 2012a. Catchment-scale controls on fluvial geomorphology. In: *Geomorphic analysis of river systems: an approach to reading the landscape*. Chichester, West Sussex: Wiley-Blackwell, pp. 29–41.

Fryirs, K.A. & Brierley, G.J. 2012b. Key concepts in river geomorphology. In: *Geomorphic analysis of river systems: an approach to reading the landscape*. Chichester, West Sussex: Wiley-Blackwell, pp. 9–27.

Garden, S., 2008. *Wetland geomorphology and floodplain dynamics on the hydrologically variable Mfolozi River, KwaZulu-Natal, South Africa.* University of KwaZulu-Natal (MSc thesis).

Gordon, N.D., McMahon, T.A., Finlayson, B.L., Gippel, C.J. & Nathan, R.J. 1992. *Stream Hydrology: An Introduction for Ecologists*, Second Edition. Chichester, West Sussex: John Wiley and Sons, Ltd, pp. 440. ISBN: 978-0-470-845357-4.

Govers, G. 1992. Evaluation of transporting capacity formulae for overland flow. In: Parsons, A. J. & Abrahams, A.D. (Eds.), *Overland Flow Hydraulics and Erosion Mechanics*. London: University College London Press, pp. 243–273.

Grenfell, M.C. 2015. Modelling Geomorphic Systems: fluvial virtual rivers. *Geomorphological Techniques. British Society for Geomorphology*, 4, pp.1–12.

Grenfell, S.E., Ellery, W.N. & Grenfell, M.C. 2010. Sedimentary facies and geomorphic evolution of a blocked-valley lake: Lake Futululu, northern Kwazulu-Natal, South Africa. *Sedimentology,* 57(5), pp.1159–1174.

Haigh, L. 2009. The wetland rehabilitation project in the Kromme River wetlands, Eastern Cape. In: Kotze, G and Ellery, W.N. (eds.). 2009. An evaluation of the rehabilitation outcomes of six wetland sites in South Africa. Wetland Management Series, WRC TT 343/09. Water Research Commission.

Henderson, F.M. 1966. Basic concepts of fluid flow. In Nordby, G. (Ed.), *Open Channel Flow*. New York: McGraw-Hill Civil Engineering Series, pp. 1–18.

Hermon, M. 2016. *The effectiveness of gully restoration in the Kromme River wetland, Eastern Cape.* Rhodes University (Honours Thesis).

Hjulstrőm, F.H. 1935. Studies of the morphological activity of rivers as illustrated by the River Fyris. Uppsala University (A Doctor of Philosophy).

Hoffman, T. & Ashwell, A. 2001. *Nature divided: land degradation in South Africa*. Cape Town: University of Cape Town Press.

Holmes, P.J., Grab, S.W., Knight, J. & Knight, J. 2016. South African geomorphology: current status and new challenges. *South African Geographical Journal*, DOI: 10.1080/03736245.2016.1208581.

Job, N. 2014. *Geomorphic origin and dynamics of deep, peat-filled, valley bottom wetlands dominated by palmiet (Prionium serratum) – a case study based on the Goukou Wetland, Western Cape.* Rhodes University (MSc Thesis).

Joubert, R. & Ellery, W.N. 2013. Controls on the formation of Wakkerstroom Vlei , Mpumalanga province , South Africa. *African Journal of Aquatic Science*, 38 (2), pp.135–151.

Kadlec, R. H. 1990. Overland Flow in Wetlands: Vegetation Resistance. *Journal of Hydraulic Engineering*, 116 (5), pp. 691-705.

Kent, M. & Coker, P. 1992. *Vegetation Description and Data Analysis: A Practical Approach,* First Edition. Chichester, West Sussex: Wiley-Blackwell.

Kirkby, M.J. & Bracken, L.J. 2009. Gully processes and gully dynamics. *Earth Surface Processes and Landforms*, 34, pp.1841–1851.

Kleinhans, M.G. 2010. Sorting out river channel patterns. *Progress in Physical Geography*, 34(3), pp.287–326.

Korup, O., Strom, A.L., & Weidinger, J.T. 2006. Fluvial response to large rock-slope failures: Examples from the Himalayas, the Tien Shan, and the Southern Alps in New Zealand. *Geomorphology,* 78, pp. 3-21.

Kotze, D.C. & Breen, C.M. 1994. *Agricultural Land-Use Impacts on Wetland Functional Values.* WRC Report No. 501/3/94.

Kotze, D.C. & Ellery, W.N. 2009. *WET- OutcomeEvaluate. An evaluation of the rehabilitation outcomes at six wetland sites in South Africa.* In: Breen, C., Dini, J., Ellery, W.N., Mitchell, S. & Uys, M. (Eds.), Wetland Management Series, WRC Report No. TT 343/09.

Langbein, W.B. & Schumm, S.A. 1958. Yield of sediment in relation to mean annual precipitation. *American Geophysical Union Transactions*, 39, pp.1076–1984.

Lane, S.N. 2001. More floods, less rain: changing hydrology in a Yorkshire context. *The Yorkshire and Humber Regional Review*, 11 (3), pp. 18-19.

Lewis, C.A. 2008. *Geomorphology of the Eastern Cape*, Second Edition. Grahamstown: NISC South Africa, pp.188.

Liu, H., Zhang, S., Li, Z., Lu, X. and Yang, Q. 2004. Impacts on wetlands of large-scale land-use changes by agricultural development: the small Sanjiang Plain, China. *AMBIO: A Journal of the Human Environment*, 33(6), pp.306-310.

Lizias, K. & Felix, C. 2013. Wetlands and Urban Growth in Bindura, Zimbabwe. *Greener Journal of Environment Management and Public Safety*, 2 (6), pp. 195-199

Lubke, R. 1998. The coastal environment. In: Lubke, R. & de Moor, I. (Eds), *Field guide to the Eastern and Southern Cape coasts.* Cape Town: University of Cape Town Press, pp. 3–26.

Marker, M.E. & Holmes, P.J. 2005. Landscape evolution and landscape sensitivity: the case of the southern Cape. *South African Journal of Science*, 101 (1-2), pp.53–60.

Marker, M.E. & Holmes, P.J. 2010. The geomorphology of the Coastal Platform in the southern Cape. *South African Geographical Journal*, 92(2), pp.105–116.

Maud, R.R. 2012. Macroscale Geomorphic Evolution. In: Holmes, P. J. & Meadows, M. E. (Eds.), *Southern African Geomorphology: Recent trends and new directions*. Bloemfontein: Sun-Press, pp. 5–23.

McCabe, A.M. & Dardis, G.F. 1989. Sedimentology and depositional setting of late Pleistocene Drumlins, Galway Bay, Western Ireland. *Journal of Sedimentary Research*, 59(6), pp.944–959.

McCarthy, T.S., McIver, J.R. & Cairncross, B. 1986. Carbonate accumulations on islands in the Okavango Delta. *South African Journal of Science*, 82(10), pp.588-591.

McCarthy, T.S. & Hancox, P.J. 2000. Wetlands. In: Partridge, T. C. & Maud, R. R. (Eds.), *The Cenozoic of southern Africa.* Oxford: Oxford University Press.

McCarthy, T.S. & Rubidge, B. 2005. *The story of Earth and Life: A southern African perspective on a 4.6-billion-year journey*. Cape Town: Struik Publishers.

McCarthy, T.S., Arnold, V., Venter, J., & Ellery, W.N. 2007. The collapse of Johannesburg's Klip River wetland. *South African Journal of Science*, 103, pp.391–397.

McCarthy, T.S. 2009. *How on Earth? Answers to the puzzles of our planet,* First Edition. Lucas, M. (Ed.), Cape Town: Struik Nature.

McCartney, M. P. & Acreman, M. C. 2009. Wetlands and Water Resources, In: Maltby, E. and Barker, T. (Eds.), *The Wetlands Handbook.* Oxford, UK: Wiley-Blackwell.

Merten, G.H., Nearing, M.A., & Borges, A.L.O. 2001. Effect of sediment load on soil detachment and deposition in rills. *Soil Science Society of America Journal*, 65(3), pp. 861–868.

Middleton, B.J. and Bailey, A.K. 2008. *Water resources of South Africa, 2005 study (WR2005)*. WRC Report No. TT, 381(08).

Midgley, D., Pitman, W. & Middleton, B. 1994. *Surface water resources of South Africa 1990 Volume lll: Orange-Namaqualand (Appendices)*. WRC Report No. 298/3.1/94.

Mieth, A. & Bork, H. 2005. History, origin and extent of soil erosion on Easter Island (Rapa Nui). *Catena*, 63, pp.244–260.

Mitsch, W.J. & Gosselink, J.G. 2007. *Wetlands*, Forth Edition. New Jersey: John Wiley and Sons, Ltd, pp. 600.

Mucina, L. & Rutherford, M. 2006. *The vegetation of South Africa, Lesotho and Swaziland*. Pretoria: South African National Biodiversity Institute, pp. 807.

Ngetar, N.S. 2011. *Causes of wetland erosion at Craigieburn, Mpumalanga Province, South Africa*. University of KwaZulu-Natal (MSc Thesis).

Nyssen, J., Poesen, J., Veyret-Picot, M., Moeyersons, J., Haile, M., Deckers, J., Dewit, J., Naudts, J., Teka, K. & Govers, G. 2006. Assessment of gully erosion rates through interviews and measurements: a case study from Northern Ethiopia. *Earth Surface Processes and Landforms,* 31(2), pp.167-185.

Partridge, T.C. & Maud, R.R. 1987. Geomorphic evolution of southern Africa since the Mesozoic. *South African Journal of Geology*, 90(2), pp.179–208.

Partridge, T.C. 1988. Of diamonds, dinosaurs and diastrophism; 150 million years of landscape evolution in southern Africa. *South African Journal of Geology*, 101(3), pp. 167-184.

Patton, P.C. & Schumm, S.A. 1975. Gully Erosion, Northwestern Colorado: A threshold phenomenon. *Geology*, 3(2), pp.88–90.

Poesen, J., Nachtergaele, J., Verstraeten, G., and C. Valentin.2003. Gully erosion and environmental change: importance and research needs. *Catena*, **50**, pp. 91–133.

Rebelo, A.J. 2012. *An Ecological and Hydrological Evaluation of the Effects of Restoration on Ecosystem Services in the Kromme River System, South Africa.* Cape Town, Stellenbosch University (MSc Thesis).

Rowntree, K. M. & Wadeson, R. A. 1999. A hierarchical geomorphic model for the classification of selected South African river systems. WRC Report No. 497/1/99.

Rowntree, K.M. 2010. Fluvial Geomorphology. In: Holmes, P. & Meadows, M. E. (Eds.), *Southern African Geomorphology: Recent trends and new directions.* Bloemfontein: Sun-Press, pp. 95–141.

Schumm, S.A. & Hadley, R.F. 1957. Arroyos and the semiarid cycle of erosion. *American Journal of Science*, 255(3), pp.161–174.

Schumm, S.A. & Hadley, R.F. 1961. *Progress in the application of landform analysis in studies of semiarid erosion.* US Geological Survey Circular No. 437, pp.1–18.

Schumm, S.A. 1973. Geomorphic thresholds and complex response of drainage systems. *Fluvial geomorphology*, 6, pp.69-85.

Schumm, S.A. 1979. Geomorphic thresholds: the concept and its applications. *Transactions of the Institute of British Geographers*, 4(4), pp.485–515.

Simon, A.L. 1981. *Practical hydraulics*, Second Edition. USA: John Wiley and Sons, Ltd.

South African National Roads Agency Limited (SANRAL). 2006. *Drainage Manual*. South African National Roads Agency Limited.

Tooth, S. 2000. Process, form and change in dryland rivers: a review of recent research. *Earth-Science Reviews*, 51 (2000), pp. 67–107.

Tooth, S., McCarthy, T.S., Brandt, D., Hancox, P.J. & Morris, R. 2002. Geological controls on the formation of alluvial meanders and floodplain wetlands: the example of the Klip River, Eastern Free State, South Africa. *Earth Surface Processes and Landforms*, 27, pp.797–815

Tooth, S., Brandt, D., Hancox, P.J. & McCarthy, T.S. 2004. Geological controls on alluvial river behaviour: a comparative study of three rivers on the South African Highveld. *Journal of African Earth Sciences*, 38, pp.79–97.

Tooth, S. & McCarthy, T.S. 2007. Wetlands in drylands: geomorphological and sedimentological characteristics, with emphasis on examples from southern Africa. *Progress in Physical Geography*, 31 (1), pp.3–41.

Truswell, J.F. 1977. *The Geological evolution of South Africa*. Cape Town: Purnell, pp. 93-96, 114-159.

Valentin, C., Poesen, J. & Li, Y. 2005. Gully erosion : Impacts, factors and control. *Catena*, 63(2), pp.132–153.

van de Wiel, M.J., Coulthard, T.J., Macklin, M.G. & Lewin, J. 2007. Embedding reach-scale fluvial dynamics within the CAESAR cellular automaton landscape evolution model. *Geomorphology*, 90, pp. 283–301.

Wasson, R.J., Caitcheon, G., Murray, A.S., McCulloch, M. & Quade, J. 2002. Sourcing sediment using multiple tracers in the catchment of Lake Argyle, Northwestern Australia. *Environmental Management*, 29 (5), pp.634–646.

Wentworth, C.K. 1922. A scale of grade and class terms for clastic sediments. *The Journal of Geology*, *30*(5), pp.377-392.

Wilson, M.D. & Atkinson, P.M. 2003. A comparison of remotely sensed elevation data sets for flood inundation modelling. In*: Proceedings of 7th International Conference on Geocomputation*. Southampton: University of Southampton, U.K.

Wohl, E. 2013. The complexity of the real world in the context of the field tradition in geomorphology. *Geomorphology*, 200, pp. 50-58.

Zhang, G., Liu, B., Han, Y., and Zhang, X.C. 2009. Sediment transport and soil detachment on steep slopes: I. Transport capacity estimation. *Soil Science Society of America Journal*, 73(4), pp. 1291–1297.